Synthesis and characterization of metallic nanoparticles with photoactivated surface chemistries

Seyyed Mohammad Hossein Abtahi

Thesis submitted to the faculty of the Virginia Polytechnic Institute and State University in partial fulfillment of the requirements for the degree of

Master of Science

In

Chemical Engineering

Richey Davis, Chair

William Ducker

Steven Martin

12/19/2013

Blacksburg, Virginia

Keywords:

Metallic nanoparticles, gold nanorods, gold nanospheres, silver nanospheres

centrifugal separation, photocleavable oligomer, UV photo activation,

PEG (poly ethylene glycol), surface plasmon resonance, UV-Vis absorbance,

TEM (transmission electron microscopy)

Synthesis and characterization of metallic nanoparticles with photoactivated surface chemistries

Seyyed Mohammad Hossein Abtahi

ABSTRACT

During recent decades metallic nanoparticles have been found very interesting due to their unique characteristics which make them suitable for different applications. In this research, for the very first time, we tried to perform selective surface photo activation chemistry on the targeted facets of nanoparticles while they are in suspension. This technique enabled us to form desired assemblies of nanoparticles.

We focused on elongated shaped gold nanorod due to its unique surface plasmon resonance and probable biomedical applications. In this research we formed a dumbbell shape assembly of nanoparticles in suspension. A probable application for these assemblies can be *in vivo* imaging. Initially, we reproduced gold nanorods using existing techniques in prior papers and optimized them according to our research needs. A low rpm centrifugal separation technique was developed to efficiently separate synthesized gold nanorods from other shapes. Several characterization techniques were utilized to characterize nanoparticles at each step including UV-absorbance, zeta potential, and dynamic light scattering. Different generations of oligomers were synthesized to be used as gold nanorods coating, and each coating was tested and characterized using appropriate techniques. Our two-step coating replacement method using one of these photocleavable oligomers enabled us to achieve, for the very first time, selective UV photo activation of gold nanorod tips. The photo activated tips were then exposed to oppositely charged gold nanospheres to form

dumbbell shape assemblies of gold nanorods and nanospheres. Furthermore, dumbbell shape assembly of nanoparticles was investigated and characterized.

Acknowledgment

Foremost, I would like to express my sincere gratitude to my advisor Prof. Richey M. Davis for the continuous support of my M.Sc. study and research, for his patience, motivation, enthusiasm, and immense knowledge. His guidance helped me in all the time of research and writing of this thesis

Besides my advisor, I would like to thank the rest of my thesis committee: Prof. William Ducker and Prof. Steven Martin, for their encouragement, insightful comments, and hard questions.

My sincere thanks also goes to Dr. Hans Robinson, Dr. Webster L. Santos for their support and co-advising within this collaborative research.

I would like to thank my fellow labmate, Dr. Sharavanan Balasubramaniam for his constructive supports. Hereby, I want to thank Erich See and Xi Guo for their help and collaboration with this research project.

Last but not the least, I would like to thank my parents for supporting me spiritually throughout my life.

Table of Contents

List of Figures

List of Tables

Chapter 1: Introduction and Literature Review

1.1 Nanoparticle Overview - Unique Properties and Applications

A particle in physics can be defined as a tiny object, particularly localized object, that different chemical and physical properties can be attributed to it [1]. Particles can be found in different sizes and shapes. The word 'nano' comes from the Greek word 'nanos'[2], refers to small animal or plant. Nano represents the number 10^{-9}, i.e., one billionth of any unit. 1 nanometer is 10^{-9} meter. In nanotechnology a particle is a unit of material which behaves as a whole regarding chemical and physical properties[1, 2]. Particles can be divided in different categories based on their size. Particles over 2500 nm are called coarse particles while particles with the size range of 100-2500 nm are named fine particles. Coarse particles are totally out of this research interests. Particles in the size range of 1-100 nm are specifically addressed as nanoparticles. Particles over 100 nm up to 1 micron can still be called nanoparticles but mainly when it is said nanoparticles, 1-100 nm is meant[2, 3].

Nanoparticles are very interesting since they possess characteristics which are connections between bulk material and atomic structures. Synthesis and characterization of nanoparticles can be addressed as a bridge between bulk material behaviors and molecular characteristics[4]. Nanoparticles have size and shape dependent properties which make them totally different from bulk materials. Bulk materials have fixed properties regardless of their size but nanoparticles are totally different [2-4]. For example optical properties like refractive index and absorbance of a bulk material is fixed, regardless of its mass or volume. But in nanoparticles optical properties are directly related to the size and shape of that specific nanoparticle. Quantum confinement is an important phenomena in nanotechnology. "Quantum confinement is defined as the changes in the atomic structure as a result of the direct influence of the ultra-small length scale on the energy

band structure"[1]. Usually this size-dependent properties are directly related to surface atoms. Number of atoms on the surface of a nanoparticles is comparable with the number of atoms inside the nanoparticle[3, 5]. Nevertheless, number of surface atoms in a bulk material are negligible in comparison with atoms inside the bulk. Surface area to volume in nanoparticles is huge and usually is in the range of 10^6-10^9.

Such a huge surface area gives nanoparticles unique characteristics such as optical properties and surface plasmon resonance. Gold solution does have a goldish yellow color, but for example a solution of 20 nm gold nanospheres has red ruby color while 200 nm nanospheres has bluish color[6]. High surface area to volume ratio in nanoparticles makes diffusion faster and feasible at lower temperatures. High surface area improves physical and chemical interaction of these particles with surrounding environment which can be a solid, liquid, or even a polymeric matrix. This environment can be human body and nanoparticles can be used as nanocarriers or detecting particles[1, 6]. Nanotechnology has been found more interesting since it challenges the scales in which the viruses and individual cells are. Instead of whole-body bulk-treatment, we can treat just affected cells and tissues without interrupting and poisoning healthy ones. Research into the rational delivery and targeting of pharmaceutical, therapeutic, and diagnostic agents is at the forefront of projects in nanomedicine[7]. These involve the identification of precise targets like specific cells or tissues, and choosing appropriate nanocarriers to achieve the required responses while minimizing the side effects. Tissue engineering and mimicking body organs and tissues using artificial metallic or polymeric scaffolds to replace damaged tissues or organs is another point of interest in nanotechnology field like gene therapy which enables us to remove or replace damaged DNA in cells[8]. Moreover, nanoparticles have found their way in day to day products due to their unique properties. For example titanium dioxide nanoparticles are used in the self-

cleaning products[9]. Zinc oxide nanoparticles do have better UV blocking properties compared to its bulk material and that is the reason why it is used in the sunscreen lotions and textiles[10]. Clay nanoparticles are used to reinforce polymeric matrices[11]. These size-dependent properties of nanoparticles makes them favorable for many applications.

1.2 Gold Nanoparticles

Gold is a chemical element with atomic number of 79. Its standard atomic weight is approximately 197 gr/mol. Gold does have a dense and soft structure with a yellowish-goldish color. Gold as a bulk material is known for thousands years (before 3000 BC) and usually is extracted form mines[12]. It has been used widely in jewelry and decoration from ancient times. Gold has a melting point of 1064.63 C and a boiling point of 2807 C. Besides its common applications, during recent decades gold has found its way in electronics and medical applications. Gold is known for its high heat and electrical conductivity while being inert and stable in most mediums[13].

Colloidal gold is a micro-sized or Nano-sized suspension of gold particles in a solution. Colloidal gold is known for a long time and have been vastly used in making Ruby glass back in time from fifth century[6]. Nowadays gold nanoparticles are synthesized in different shapes and sizes, according to desired application. Colloidal gold suspension does have very unique optical characteristics. For example gold nanosphere suspension can have a dark, intense reddish color if the particles are less than 100 nm or purple/blue color for larger particles. Faraday was the first scientist who suggested that these colors are formed due to presence of suspended gold particles in the solution back in 1857[14]. He found out that a dark reddish solution can be made by reducing Chloroaurate ($Aucl4^-$) with CS_2. Later in 1951, Turkevich introduced a new method in which Chloroaurate is reduced by citric acid[15, 16]. Both of these techniques produce spherical gold

nanoparticles and the size of nanospheres can be tuned. As a result of rapid science development during recent decades, new applications has been found for metallic nanoparticles, especially gold. It has been found that the size of gold nanospheres has a significant effect on its physical, chemical, and optical properties[6]. This size-dependent properties of gold nanospheres encouraged many scientists to study size and property dependence relation. They tried to develop reliable and reproducible techniques in making different sizes of gold nanospheres and introducing new characterization techniques. During Gold nanospheres synthesis, some other nanoparticle shapes like rods or cubes can be observed as by products[17]. These non-spherical nanoparticles were found interesting due to their outstanding physical and optical properties. These properties are caused not just by size but mainly due to topological shape aspects. Other shapes of gold nanoparticles can be formed by introducing new chemical agents or changing reaction conditions [6, 17, 18]. Hundreds of publications and papers on synthesis and characterization of gold nanosphere[14, 15], nanorods[19-22], nanocubes[23, 24], and nanowires[25, 26] can be found in the literature.

Among all the shapes, nanorods have been highlighted since they can be formed by a simple, high-yield synthesis technique[22]. Wet chemistry, short reaction time, and having control over aspect ratio of gold nanorods makes this technique favorable. This technique first introduced by Catherine Murphy [21, 22, 27-31] and later developed by Nikoobakht and Al-Seyyed [19, 20, 32]. Previously some other techniques like lithography or deposition has been used to make well defined gold nanorods [33, 34]. These techniques haven't been successful since they were expensive and time consuming which made them not feasible in large scale.

1.3 Project Objectives

The main objective of this research is to develop a new method to perform selective photo activation of adsorbed photo cleavable oligomers on the surface of nanoparticles. This method enables us to form chemically active sites on desired facets of nanoparticles while they are in suspension. Further surface chemistry is possible on targeted parts of nanoparticles. In this research we will try to form a dumbbell shape assembly of gold nanorods and nanospheres. This assembly can be used for near infrared imaging in Vivo.

1.4 Literature Review

There are thousands of papers and hundreds of books published on nanotechnology and specifically on nanoparticles synthesis and their probable practical applications during recent decades. In this part of my thesis, the most relevant and important papers interesting regarding metallic nanoparticles especially gold nanoparticles in different shapes, are reviewed.

1.4.1 Gold Nanospheres

Faraday was the first researcher who published a scientific paper in 1857 regarding gold colloidal suspension and light-material interaction, 'The Bakerian Lecture: Experimental relations of Gold (and other metals) to Light'[14]. Faraday was a pioneer in introducing new areas in nanotechnology and specifically colloidal gold suspensions. He used phosphorous to reduce gold chloride to gold nanospheres and was the very first scientist to recognize that the ruby color of colloidal gold is as a result of fine gold nanoparticles in the solution. As we said before, gold has been used to make ruby glass for thousands years but no one had any idea about the possible mechanism. Zsigmondy was the next scientist who developed a different synthesis technique based on what Faraday did[35]. He received Noble prize regarding his work on colloids and developing ultra-microscope[36]. His technique basically was a two-step procedure called "nuclear method" those days. This method further called Seed-mediated synthesis. Svedberg made important contributions in synthesis of gold nanoparticles and utilized his own invented ultracentrifuge to effectively separate nanoparticles [37-39]. Gustav Mie focused on colloidal gold color variation with nanospheres size based on developing theory of light scattering and absorption by nanoparticles[40]. Mie researched on influence of ellipsoidal shape on gold suspension optical properties[41].

Considering all efforts made to establish a reliable synthesis technique to produce spherical gold nanoparticles, maybe Turkevich can be named as the first scientist whose technique was widely used and well developed in 1951. In this method, hot chloroauric acid is reduced by small amount of sodium citrate solution. The final result will be a monodisperse colloidal gold 10-20 nm nanosphere suspension. Gold nanospheres were stable in suspension since citrate acts as a reducing agent and capping agent simultaneously. To produce larger particles, less amount of citrate should be used which leads to loss of monodispersity[15].

Back in early1990's, Brust and Schiffrin introduced a new method which gold nanoparticles were made in an organic solvent rather than water[42, 43]. In this technique, chloroauric acid in TOAB (tetraoctylamonium bromide) solution is reduced by means of $NaBH_4$ (sodium borohydride) in toluene solution. Sodium borohydride is a strong reducing agent while TOAB is a reaction catalyst and capping agent. TOAB physisorbs on the surface of gold nanoparticles. This weak interaction between surfactant and the surface causes aggregation of gold nanoparticles after a couple weeks.

Among all above techniques, Turkevich's method is still the most practical and preferred technique. Monodispersity, short-time preparation, high yield, nanosphere size tunability are the key features of this method. The size of nanospheres is controlled by citrate/gold solution ratio. The most limiting parameter in this synthesis technique is just the fact the only water can be used as the solvent[44]. The size of gold nanospheres synthesized using this method can be tuned from 2-200 nm. **Figure 1.1** shows a typical TEM (transmission electron microscopy) image of gold nanospheres synthesized by citrate reduction.

.

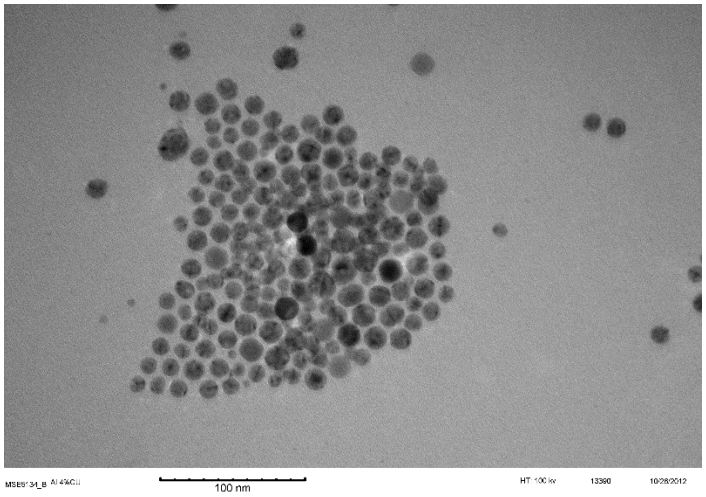

Figure 1.1 Typical TEM image of citrate coated gold nanospheres

Other methods have been developed during recent years for gold nanosphere synthesis. Most of these techniques are based on using different reductants and ligands rather than citrate [45-47]. Some other researchers worked on introducing new Templates or stabilizers within gold nanosphere synthesis [48-51].

Block copolymers can be used to produce stable gold nanospheres which can be made biocompatible. This block copolymer can form a steric barrier around gold nanosphere surface and make it stable in different environment based on the desired application[52].

The size and shape of the gold nanospheres can be tuned by changing synthesis parameters like gold to reducing agent ratio, temperature and etc. Typically, gold nanospheres display a sharp single UV-VIS absorption peak between 520 nm and 540 nm which is in the visible spectroscopy range (**Figure 1.2**).

This peak is weakly size dependent and shifts to a longer wavelength with increasing the size of nanospheres. The size distribution of nanospheres has a significant effect on the width of the peak. Wider peak represents wider size distribution of nanoparticles.

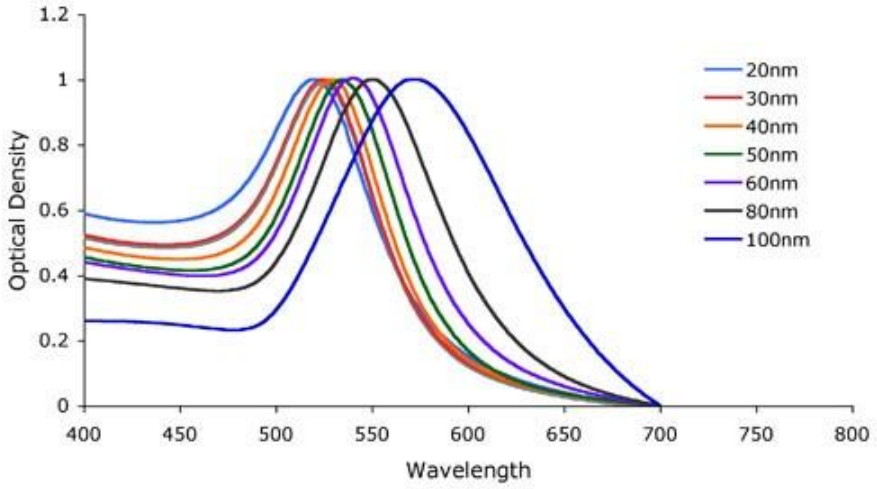

Figure 1.2 Typical UV-VIS absorbance graph of gold nanospheres with different sizes[53] 'used under fair use,2013'

1.4.2 Gold Nanorods

1.4.2.1Gold Nanorods Synthesis Methods

There are a numerous synthesis techniques in literature regarding gold nanorods. Hereby, we review most successful and well defined synthesis methods that are relevant to this research.

1.4.2.1.1 Template Method

This technique is a kind of fabrication synthesis and introduced by Hornyak et al. [54]. An alumina template is fabricated electrochemically from bare aluminum. Gold nanorods are formed by electrochemical deposition of gold in Nanopores of this alumina template. The pore sizes in this study was 50 nm in diameter and 500 nm deep. Silver (Ag) or copper (Cu) is first deposited on the alumina to form a conductive layer (film) for further deposition of gold. Later gold ions are electrochemically reduced and grow on this conductive layer within nanopores of template forming gold nanorods. Template and conductive layer are dissolved consecutively while an appropriate polymeric stabilizer is used within dissolution stage in order to form a steric barrier

and prevent nanorods from aggregation. The size and aspect ratio of gold nanorods can be tuned by controlling the size of template's nanopores. The length of nanorods can be controlled through concentration of gold ion in solution. Higher concentration of gold ion, more deposition rate, and longer rods. Yield was the main problem with this method[55]. Low amount of synthesized gold nanorods in comparison with spent time and cost made an unsuitable choice out of this method. But good control over size and aspect ratio of gold nanorods within this technique should not be neglected. This fabrication technique is schematically shown in

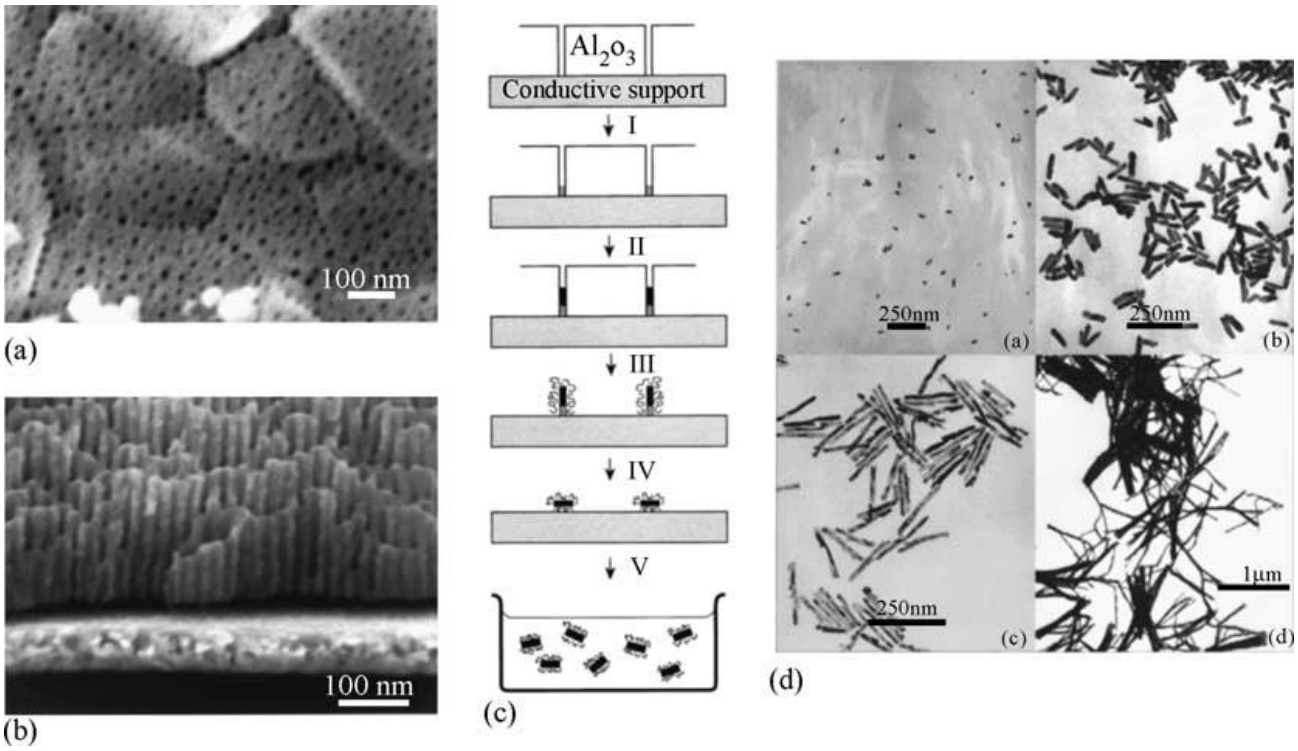

Figure 1.3 (a and b) Field emission gun-scanning electron microscopes images of an alumina membrane. (c) Schematic representation of the successive stages during formation of gold nanorods via the template method. (d) TEM micrographs of gold nanorods obtained by template technique [55] 'used under fair use,2013'

1.4.2.1.2 Electrochemical Method

This technique was introduced by Y.Y. Ying et al. in 1997 [56]. Gold nanorods are formed by means of a double electrode reduction cell. A sacrificial gold plate is used as an anode and a same size platinum plate is used as cathode[55, 56]. A solution of CTAB (cetylmethylamunium bromide) and TCAB (tetradodecylamonium bromide) is prepared and the electrodes are put in it. CTAB is a cationic surfactant while TCAB is pretty the same but more hydrophobic and serves as a co-surfactant. Acetone and cyclohexane are added to the solution and the cell is located in a bath sonicator at 36ºC temperature. Acetone loosens up CTAB micelles letting TCAB incorporation while cyclohexane as a nonpolar solvent improves elongated cylindrical TCAB micelles formations[55, 57]. This technique is schematically shown in **Figure 1.4**.

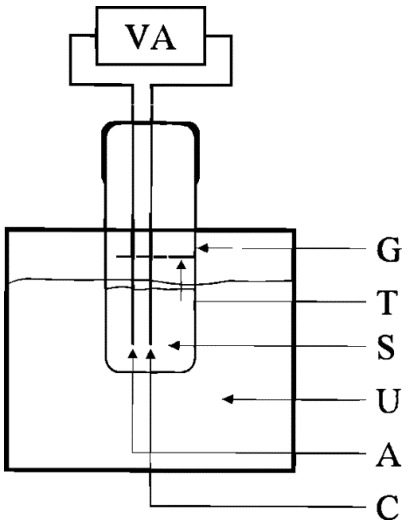

Figure 1.4 Schematic diagram of the setup for preparation of Au nanorods. The electrochemical system contains the following: VA, power supply; G, glassware electrochemical cell; T, Teflon spacer and the electrode holder; S, electrolytic solution; U, ultrasonic cleaner; A, anode (Au); C, cathode (Pt)[58] 'used under fair use,2013'.

2 mA current is applied to the cell for 30 min. Anodic gold plate dissolves gradually forming $AuBr_4^-$. This anionic group, complexes with cationic surfactants present in the solution

and reduces on the cathodic platinum plate. The aspect ratio of gold nanorods are controlled by a silver (Ag) plate located close to cathode electrode," We found that the amount of the silver ions and the speed of their release could efficiently affect the control of, mainly, the major-axis length of the nanorod" [58].

1.4.2.1.3 Seed-Mediated Growth Method

As we addressed before, using a two-stage gold nanoparticles synthesis is a well-known technique used in early 19^{th} century. But the interesting point is that after synthesis a significant amount of other nonspherical nanoparticles was observed. For example Brown et.al in 2000 reported 5-10% of other shapes, especially gold nanorods during their seed-mediated synthesis of gold nanospheres [59].

Murphy's group investigated this synthesis technique more, and probed the reducing agent role by testing different reducing agents under different reaction conditions[28, 29].

Murphy and coworkers used these results and for the very first time introduced a high yield gold nanorods synthesis methods. They reduced gold ions by a strong reducing agent, sodium borohydride ($NaBH_4$), and formed 3 nm seeds. After that gold seeds were grown in another solution by means of a mild reducing agent, Ascorbic acid. Ascorbic acid was chosen since it can prohibit nucleation of new seeds and assures that just primary seeds grow[31]. Applying silver nitrate, $AgNO_3$, as a shaping agent helped gold seeds to grow in 1D and form gold nanorods[17, 18, 21, 22, 27, 29, 31].

This synthesis technique is vastly used during recent decade and developed. High-yield, wet-chemistry approach, simple, and fast are the main characteristics of this technique which make it favorable rather than other techniques.

Since we used this technique to prepare our gold nanorods, in this part we mainly focus on this technique. Most recent reported developments and modifications will be discussed in details and compared together.

1.4.2.2 Wet- Chemistry Seed-Mediated Gold Nanorod Synthesis Mechanism

Busbee addressed in his paper, "wet chemical synthesis of gold nanorods involves surfactant-directed growth of nanorods from nanoseeds"[21]. It has been found that the most important factor in this synthesis is selective adsorption of surfactant and shaping agent to some specific crystal facets.

Figure 1.5 shows a typical shape of gold nanorod including its different facets.

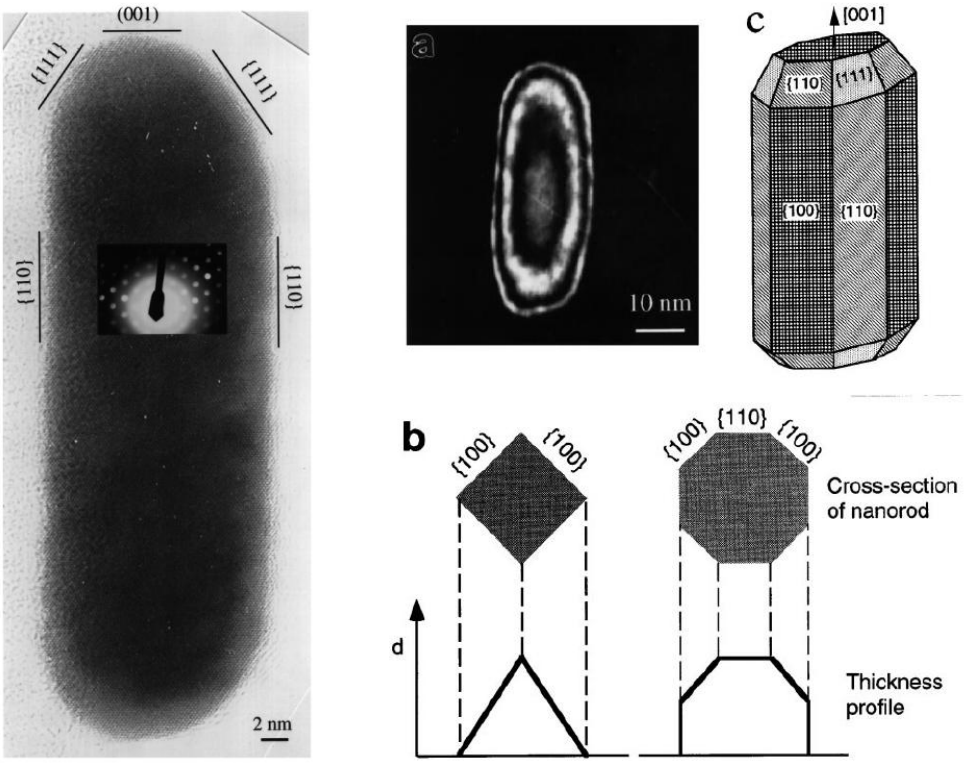

Figure 1.5 High resolution TEM of a gold nanorod oriented along the [110] direction and cross section area[60] 'used under fair use,2013'

It has been proposed that CTAB (cetyltrimethyl ammonium bromide) as the surfactant and Ag ion as the directing-agent prefer to adsorb to side facets like [100] and [110]. On the other hand tip facets are more favorable for ascorbic acid and ascorbate[60]. Highly selective ascorbate adsorption on [111] and [110] tip facets enhances reduction of Au III to atomic Au and crystal growth at the tips[21]. This mechanism helps gold nanorods to grow rapidly in [001] direction which is longitudinal axis of gold nanorods in comparison with transverse axis. Increasing concentration of surfactant (here CTAB) and directing agent (Ag) can significantly push the system toward forming higher aspect ratio gold nanorods. Besides increasing concentration, increasing PH is another technique to form longer gold nanorods. Ascorbate is a stronger reducing agent than ascorbic acid. Ascorbic acid's pk_a is 4.1. Therefore at PH higher than 4.1, most of ascorbic acid turn into ascorbate. More ascorbate in the solution means faster reduction of gold ion to atomic gold on the tip facets. Generally having a PH higher than 4.1 favors forming longer gold nanorods[21].

Initially gold salt is reduced using a strong reducing agent like sodium borohydride. Gold reduction forms a faceted gold nanosphere with an average diameter of 3 nm. In the next step, these faceted spherical seeds are placed in a gold salt solution in the presence of a mild reducing agent like ascorbic acid to grow. As mentioned before, surfactant (capping agent) and Ag (shape directing agent) selectively adsorb on the side facets. For example

CTAB as a cationic surfactant forms a micellar bi-layer around side facets of gold nanorods[32]. This bilayer formation blocks and slows down the growth of side facets in the transvers axis while tip facets are not covered and can grow rapidly in the longitudinal axis. **Figure 1.6** schematically shows gold nanorods formation using seed-mediated technique [61].

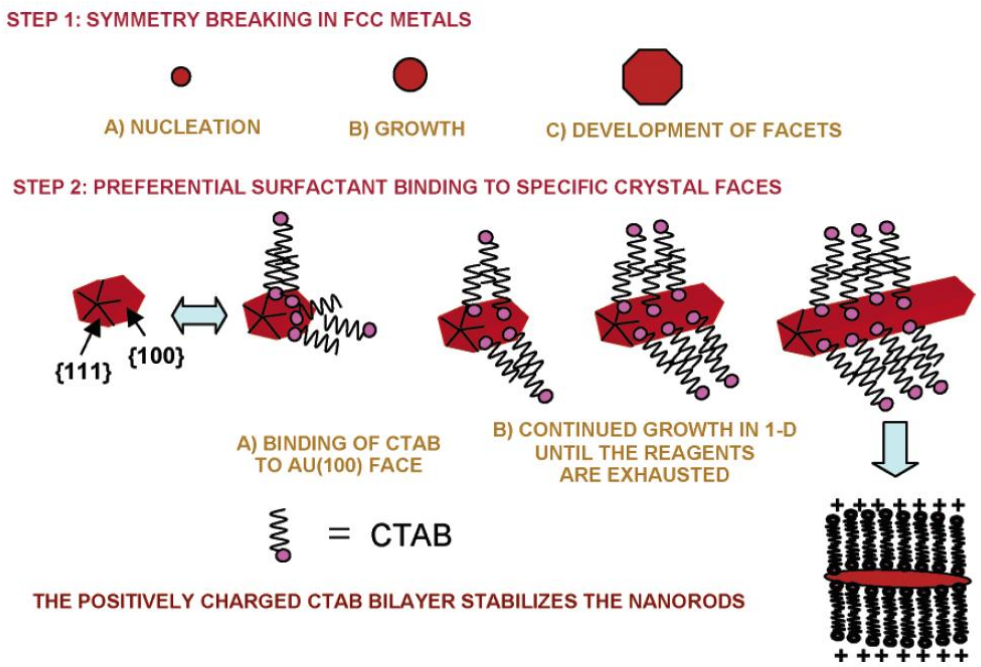

Figure 1.6 Gold nanorods formation mechanism by seed-mediated technique[61] 'used under fair use,2013'

This mechanism shows how flexible and tunable this synthesis method is. The size and aspect ratio of gold nanorods can be easily changed by changing surfactant type, concentration or even concentration of directing agent.

Figure 1.7 shows TEM images and UV-VIS absorbance graphs of different gold nanorods with different aspect ratios. Gold nanorods with higher aspect ratios do have a bigger longitudinal absorbance peaks (second peak) and the ratio of the second peak height over first peak height is larger. This proves that longer gold nanorods absorbance are bigger and the absorbance peak occurs in larger wavelength. Therefore size and aspect ratio of gold nanorods can be tuned according to the desired application.

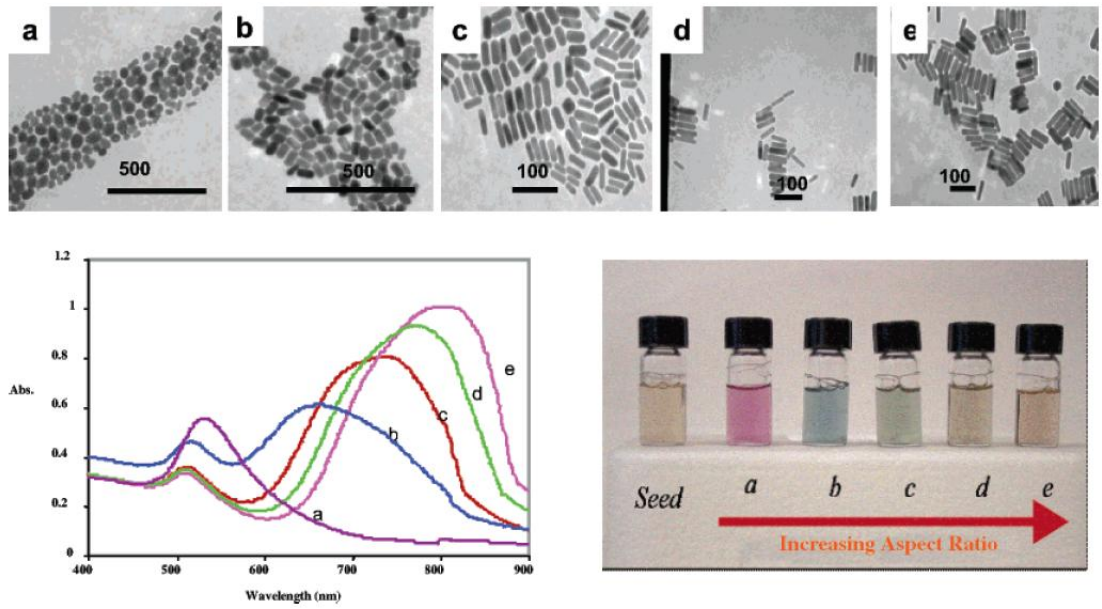

Figure 1.7 Transmission electron micrographs (top), optical spectra (left), and photographs of (right) aqueous solutions of gold nanorods of various aspect ratios. Seed sample: aspect ratio 1; sample a, aspect ratio 1.35 (0.32; sample b, aspect ratio 1.95 (0.34; sample c, aspect ratio 3.06 (0.28; sample d, aspect ratio 3.50 (0.29; sample e, aspect ratio 4.42 (0.23. Scale bars: 500 nm for a and b, 100 nm for c, d, e. [61] 'used under fair use,2013'

1.4.3 Gold Nanospheres and Nanorods Surface Plasmon Resonance

By changing the size of material from bulk to nanoparticles, its electronic related properties also change [62]. Electronic properties are a function of density of state and spatial length which both can be significantly affected by reducing size[63, 64]. As we addressed before, light absorption by metallic nanoparticles is known for a long time. This light absorption happens due to coherent oscillation of conduction band surface electrons with exposed electromagnetic field[62]. These surface electrons oscillation with electromagnetic field is called surface plasmon resonance. Interestingly this kind of behavior is not observed in atoms or bulk materials.

This plasmon absorbance is totally size dependent, and Mie's theory has formulated this relation[65]. **Figure 1.8** compares surface plasmon resonance in an elongated shape nanoparticle with a spherical particle.

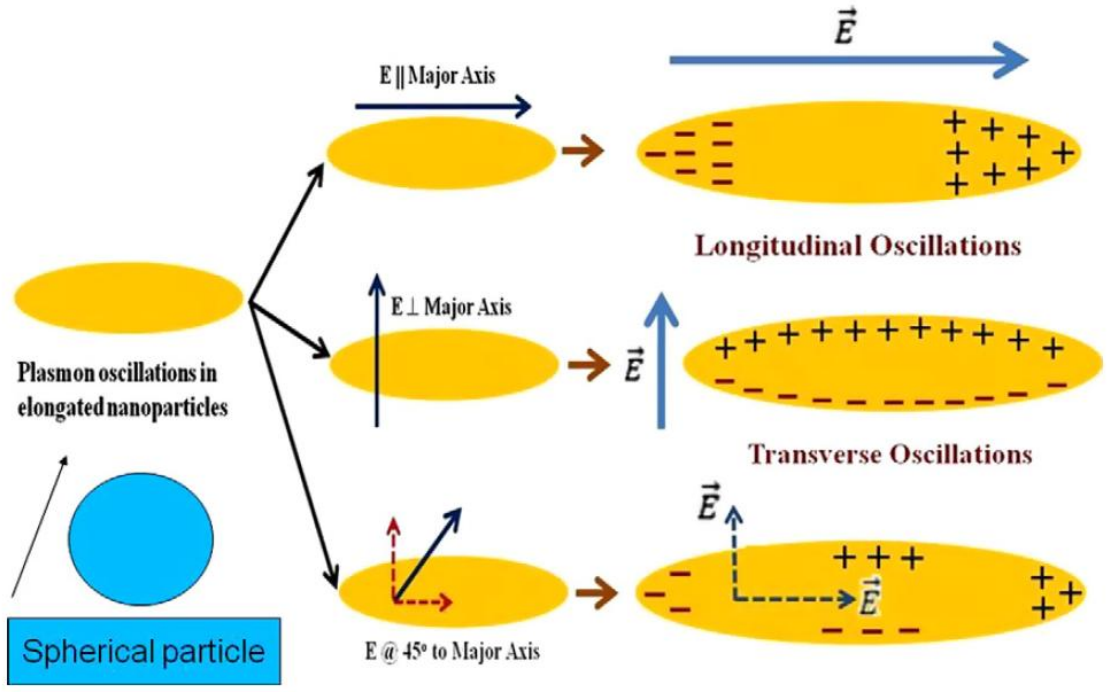

Figure 1.8 Schematic showing the transverse and longitudinal mode of oscillations of plasmons depending on the direction of electric vector of incident light[66] 'used under fair use,2013'

As we can see in **Figure 1.8**, spherical particles only do have one oscillation axis which is parallel to the field vector. On the other hand, elongated shape nanoparticles possess 2 oscillation axis's which one of them is in the direction of diameter of nanoparticle called transverse oscillation and the other along length of nanoparticle called longitudinal oscillation[66]. This phenomenon illustrates why we observe 1 peak in UV-VIS absorbance graph for spherical nanoparticles but 2 peaks are detected for elongated shape nanoparticles.

In **Figure 1.8** a very high accumulation of surface charges can be seen around tips during oscillation. This high concentration of surface electrons at the tips suggests that there should be a high energy absorbance at the tips of gold nanorods. On the other word, a high field intensity absorbance can be seen during surface Plasmon resonance. The maximum absorbance happens when the incident light and surface Plasmon absorbance have the same wavelength. **Figure 1.9** shows the ratio of electric field around different parts of gold nanorod over incident electric field intensity[67].

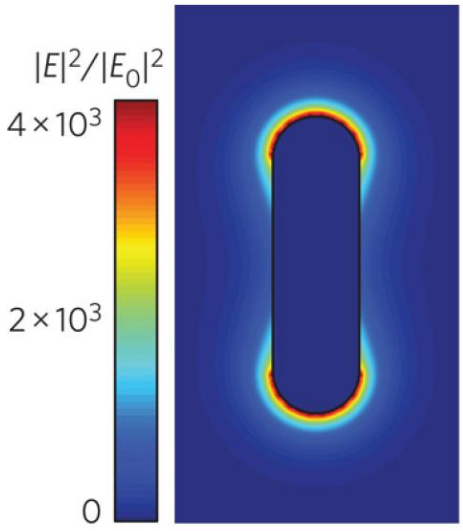

Figure 1.9 Calculation in the discrete dipole approximation of the electric field intensity around a gold nanorod, evaluated on resonance with its longitudinal SPR[67] 'used under fair use,2013'

Chapter 2: Silver Nanospheres

2.1 Introduction

In this chapter, the synthesis of silver nanospheres with targeted size of 20 nm is described. These nanoparticles were coated with oleylamine and efforts were made to find a conditions and a suspending fluid medium suitable for keeping them stable and dispersed long enough to use them and to deposit them as mostly single particle onto a hydrophobic glass or silicon substrate for further surface modifications

Figure 2.1 (a-b). Deposited silver nanospheres are reacted with a new photo cleavable oligomer. This new oligomer will replace current surface coating, oleylamine. Afterwards silver nanospheres are exposed to a polarized light which cleaves oligomer at poles of nanospheres. Further surface chemistry will be possible at photo activated poles, like attaching oppositely charged nanoparticles to form a dumbbell shape assembly of nanoparticles, **Figure 2.1** (c).

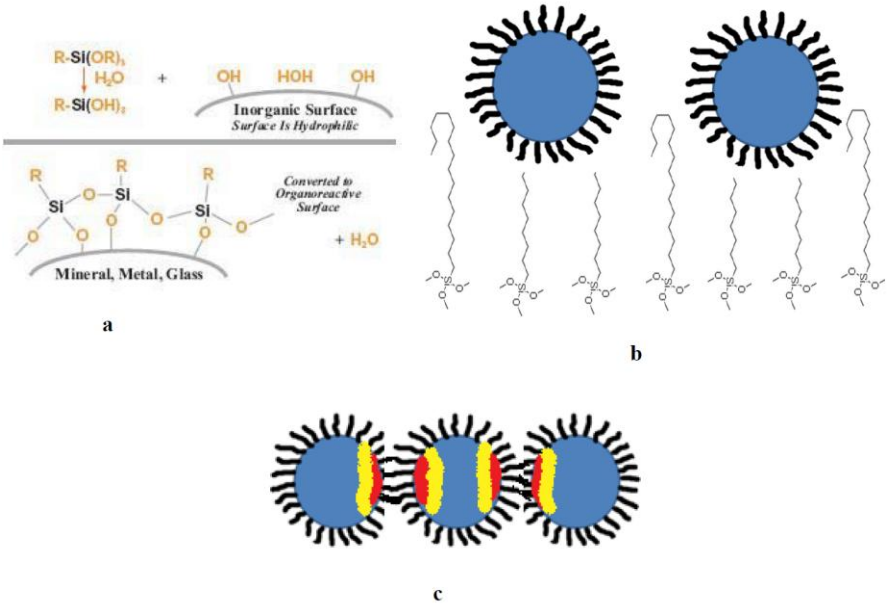

Figure 2.1 Schematic description of Ag nanospheres assembly formation steps a) hydrophobic silicone substrate formation b) seating Ag nanospheres separately on top of substrate c) changing surface coating, phtoactivation, and dumbbell shape assembly formation

2.2 Silver Nanospheres Synthesis

Silver nanospheres were synthesized using a technique developed by Hiramatsu et.al. in 2004 [47]. This method is based on reducing silver or gold ions with oleylamine in a reflux solvent for 8-24 hours. This production technique is fast, simple, and cheap. Only three materials are used, which are silver or gold salts, oleylamine, and a solvent. This technique can be modified for production of different metallic nanospheres which is beyond the scope of my research. In this chapter we focus on modifying this technique to produce ~20 nm silver nanospheres with UV-VIS absorbance peak at ~ 421 nm. Oleylamine simultaneously acts as a reducing agent and capping agent to prevent nanospheres from aggregation. It was used due to its low cost and availability [47]. Oleylamine is a clear slightly yellowish liquid and is an alkene amine coming from the fatty oleic acid family which is commercially available in different grades. However, the most common grades are ≥%70 purity. Therefore, choosing the oleylamine with the lowest possible impurity level is important for using it as a dispersant for nanoparticles. The reducing group in oleylamine molecule is an amine group which can undergo metal ion-induced oxidation.

Figure 2.2 shows the molecular structure of oleylamine with emphasis on head groups and carbon double bond. The double bond in oleylamine does not play any significant role in reaction.

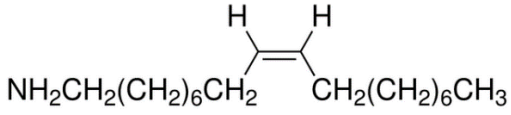

Figure 2.2 Oleylamine molecule

The key part in this synthesis is that it should be performed under nitrogen (N_2). The carbon double bond in oleylamine molecule (**Figure 2.2**) is sensitive to oxygen, particularly at high temperatures like 181 C. It can be easily oxidized and deactivated. My experiments show that it is impossible to do this synthesis without keeping it away from oxygen using a nitrogen blanket.

The size of nanoparticles is controlled with the solvent (growth temperature) and reaction time. The following solvents can be used to prepare silver nanospheres in different sizes.

Table 2.1 Solvents that have been used to synthesize silver nanospheres with different sizes

Solvent	Boiling temperature (C)	Silver Nanosphere size (nm)
Hexane	69	8.5
Toluene	110	12.7
1-2 dichlorobenzene	181	32.3

During synthesis, solvent is always under reflux which assures that the synthesis temperature is fixed. As table-1 suggests, the size of nanospheres is directly related to the solvent boiling temperature. Higher boiling temperatures lead to larger silver nanospheres. Due to our targeted size of silver nanospheres, larger than 20 nm, 1-2 dichlorobenzene was chosen as the solvent. Another parameter for controlling the size is time. Increasing the time of reaction increases particles size. In order to achieve silver nanospheres with 20 nm diameter, the reaction was conducted for 8 hours plus an additional half hour for cooling.

2.2.1 Materials

Silver acetate ($AgC_2H_3O_2$), 1-2 dichlorobenzene ($C_6H_4Cl_2$), and oleylamine ($C_{18}H_{37}N$) were purchased from Sigma-Aldrich Company and used as received. Oleylamine is oxygen sensitive, therefore, it should be stored in a sealed container under nitrogen and stored in the dark and at ~ 4C in a refrigerator.

2.2.2 20 Synthesis Method

All reagent solutions were made fresh for each synthesis described below. As an example of the synthesis of 20 nm silver nanospheres, the following steps were used.

Step 1: Dissolution of 50 mg silver acetate in 2.5 ml oleylamine

According to paper [47], this step can be easily done at room temperature (25 C), and the final result will be a uniform solution. We found that silver acetate barely dissolves in oleylamine at room temperature. Silver acetate forms a two-phase solid-liquid cloudy solution. Heating up the mixture to 40 C, gentle stirring, and bath sonication did not make a significant change in solubility of silver acetate in oleylamine. In order to dissolve silver acetate in oleylamine, using a cosolvent seemed essential. Since oleylamine and silver acetate both dissolve pretty well in 1-2 dichlorobenzene, that solvent was considered the best choice as cosolvent. Therefore, initially silver acetate was dissolved in 2.5 ml dichlorobenzene and later 2.5 ml oleylamine is added to the mixture. The solution was shaken well for 2 min which formed a uniform clear solution.

Step 2: Heating solvent (1-2 dichlorobenzene) to the boiling point, keeping it under reflux

1-2 Dichlorobenzene is a clear polar solvent and its boiling point is 181 C. An electrical mantle heater was used to heat the solvent to boiling point. Since 50 mls solvent was needed in this synthesis, we used a 250 ml two bottle neck Pyrex flask. One of the necks was tightly sealed by a precision seal septa which was used for nitrogen injection. The other neck was connected to a Pyrex condenser where cold water was used for cooling. The top of the condenser was tightly sealed using a precision seal septa. A needle was placed in the top of the condenser to purge the excess nitrogen in the system.

Nitrogen was fed to the glassware using a pure nitrogen capsule. The capsule's nitrogen outlet was passed through a drier to make sure no water entered the system. The nitrogen was fed using a needle at the bottom of the glassware and was purged through the top of the condenser.

This approach ensured that there was always a nitrogen blanket over the solution with a positive pressure difference in comparison with the surrounding.

In order to distribute heat uniformly to the solution, the mantle heater was half filled with sand and a 250 double neck flask was buried in that sand bed. A thermometer was placed in the sand bed. The mantle output was adjusted such a way that assured solvent remained in reflux.

Step 3: Rapid injection of silver acetate and oleylamine to 1-2 dichlorobenzene

The mixture prepared in step 1 should be rapidly injected to 1-2 dichlorobenzene while it is under reflux. A 20 ml Pyrex syringe with a long needle was used to make this injection through the septa as fast as possible. After injection, it was important to make sure there was no leak in the system and all reactants were under nitrogen. Immediately after injection, the solution color changed to light brown which showed that the initial nucleation had started. The system was left undisturbed for 8 hours. To produce larger nanoparticles, more growth time should be applied. After 8 hours, the mantle was turned off and the apparatus was allowed to cool down for 30 minutes. The flask was then purged with nitrogen for 10 minutes to make sure no oxygen was trapped in the flask and then it was sealed thoroughly.

Step 4: Changing suspension solvent (1-2 dichlorobenzene to hexane)

1-2 dichlorobenzene is not a suitable solvent for further surface modification. Thus, we decided to extract the silver nanospheres and to disperse them in hexane which was better suited for the step of depositing the nanospheres onto a hydrophobized glass surface. The following procedure was used to exchange the solvent for the suspended silver nanospheres.

- Centrifugation at 10,000 rcf (relative centrifugal force) for 30 min
- Removing supernatant solvent as much as possible (about 95-98%)
- Resuspending the sediment in pure n-Hexane with the same volume as that of the discarded 1-2 dichlorobenzene
- Filtering the suspension using 100 nm hexane-compatible filters

2.2.3 Silver Nanospheres Characterization Results

Oleylamine coated silver nanospheres were originally suspended in 1-2 dichlorobenzene. After solvent exchange, these nanospheres were suspended in n-Hexane. The nanoparticles as synthesized were too concentrated and needed to be diluted for further characterization. TEM (transmission electron microscopy), DLS (Dynamic light scattering), and UV-VIS spectroscopy were the characterization techniques utilized.

2.2.3.1 UV-VIS Absorbance Graphs

Figure 2.3 shows oleylamine coated silver nanospheres suspended in 1-2 dichlorobenzene and **Figure 2.4** shows these nanoparticles in n-Hexane. The graphs suggest that the absorbance peak is at 421 nm for silver nanospheres in 1-2 dichlorobenzene and at 405 nm in n-Hexane. As we know, UV-VIS absorbance is solvent related and the place of peak changes as the solvent changes.

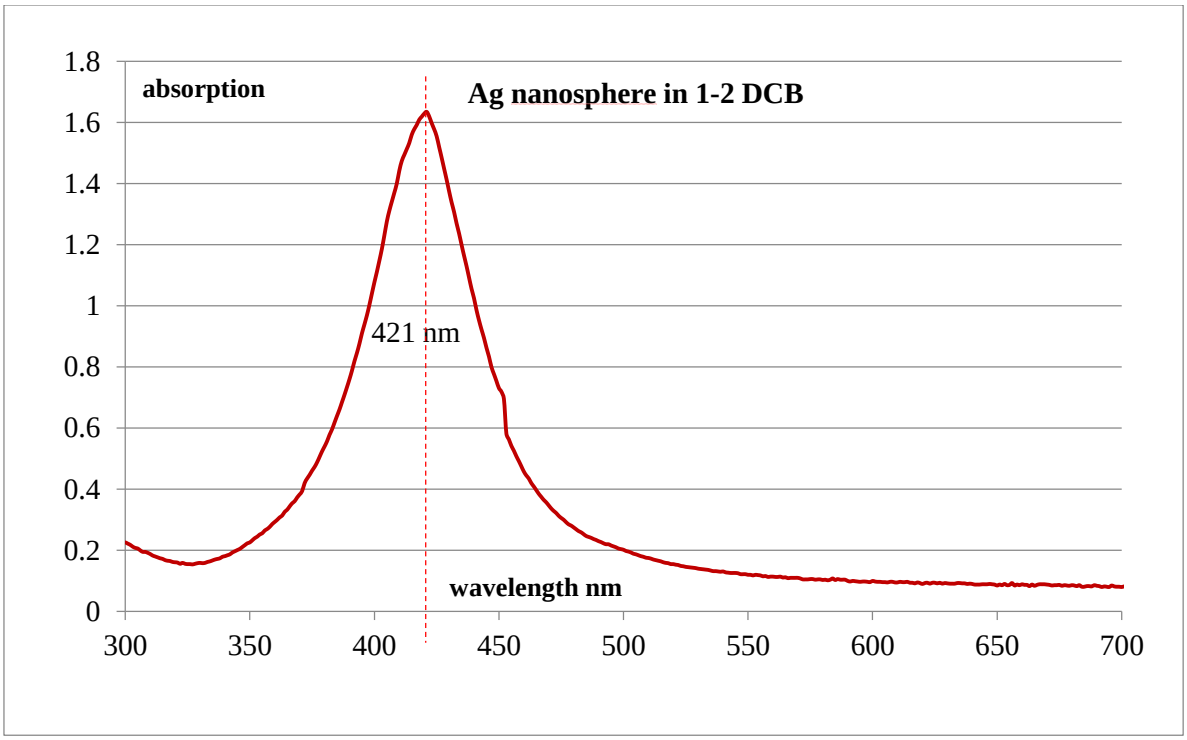

Figure 2.3 Silver nanospheres in 1-2 dichlorobenzene UV-VIS absorbance graph

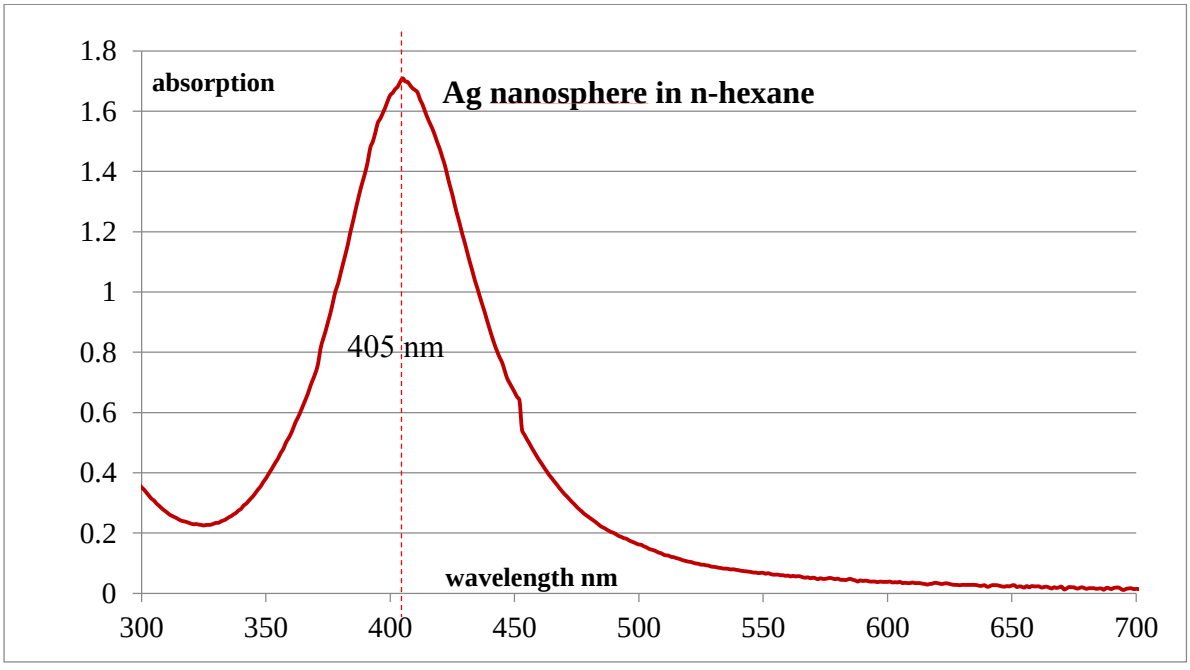

Figure 2.4 Silver nanospheres in n-Hexane UV-VIS absorbance graph

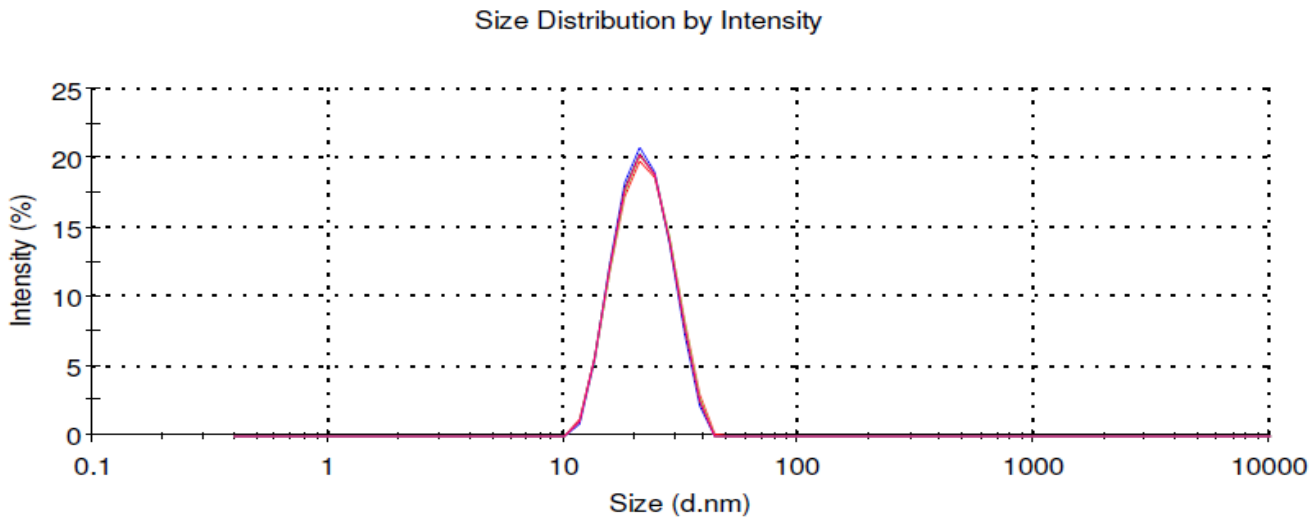

Figure 2.5 Dynamic light scattering size distribution by intensity of silver nanospheres in n-Hexane

2.2.3.2 Dynamic Light Scattering (DLS) Size Distribution

Dynamic light scattering is a size characterization technique. **Figure 2.5** shows the typical DLS size distribution graph by intensity of this sample. The size distribution by intensity shows a sharp narrow peak at approximately 23 nm for particles diameter. PDI (polydispersity index) for this sample is 0.045 which is a good indication of narrow size distribution and size monodispersity of synthesized silver nanospheres.

2.2.3.3 TEM (Transmission Electron Microscopy) Images

A Philips EM420 TEM was used to take images of silver nanospheres. TEM samples were prepared using a drop cast technique on a 200 mesh copper grid coated with a thick carbon layer. A very dilute drop of silver nanospheres (10 µl) was placed on the top of the copper grid and left to dry for 24 hours. TEM images were taken at 100 kv with different magnifications

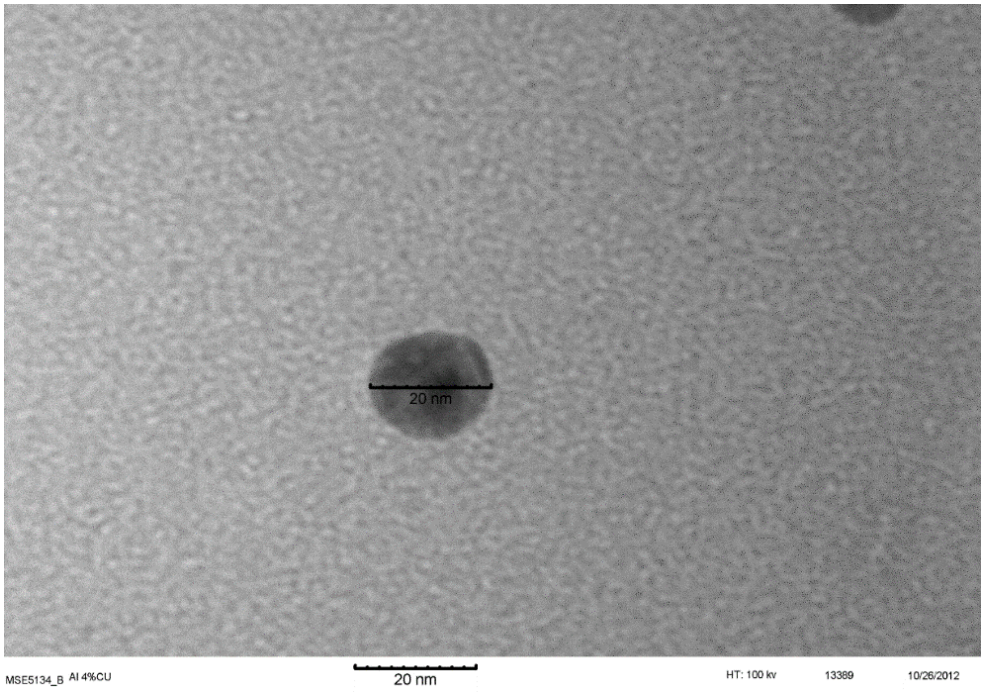

Figure 2.6 TEM image of silver nanospheres

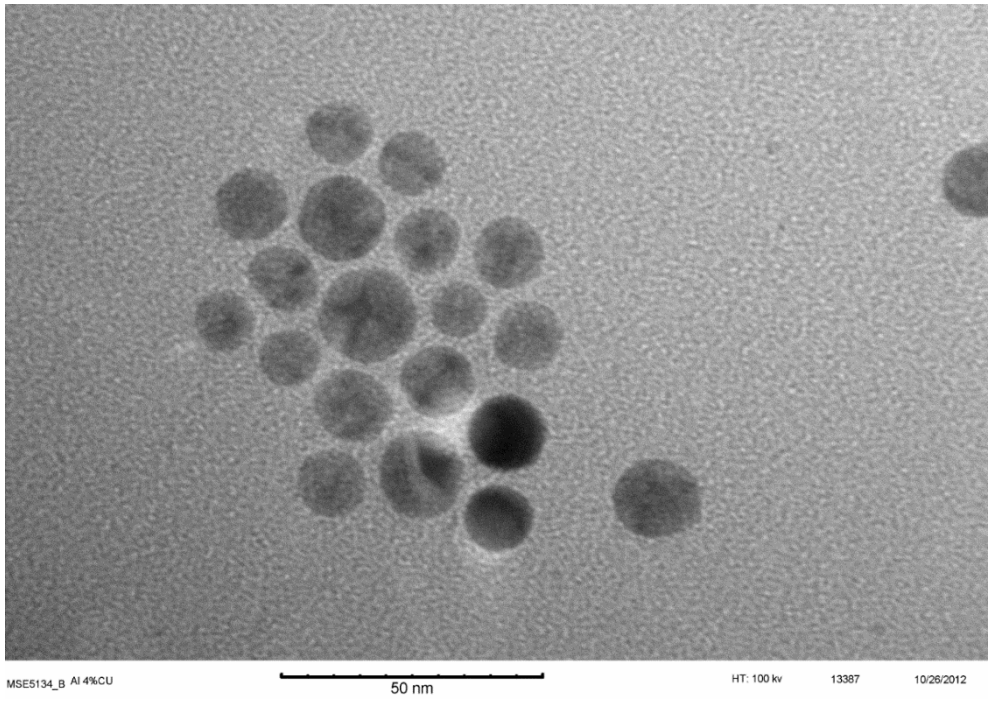

Figure 2.7 TEM image of silver nanospheres

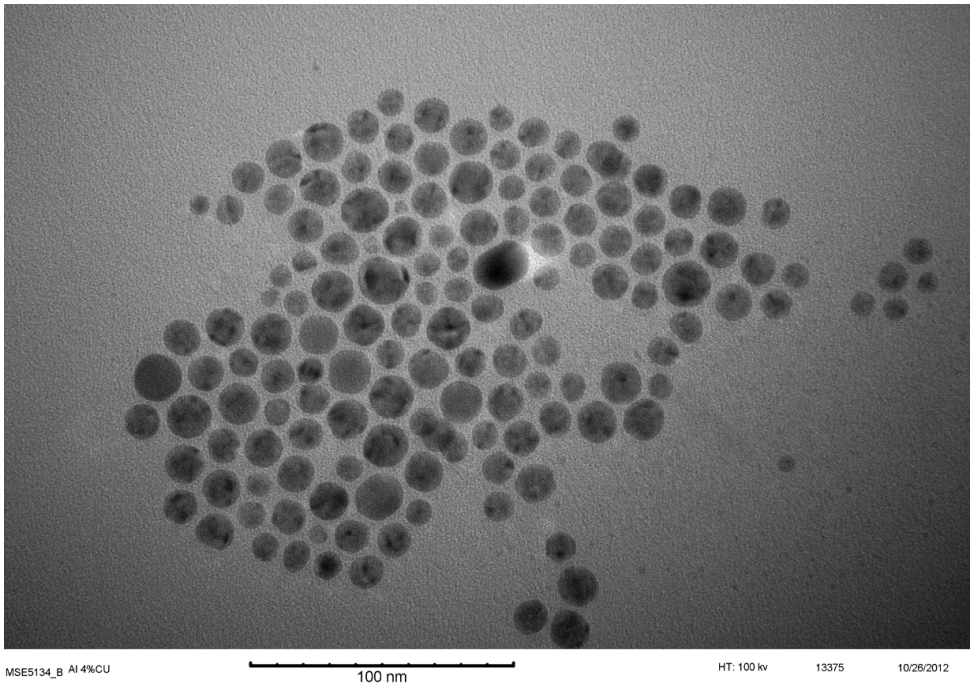

Figure 2.8 TEM image of silver nanosphere

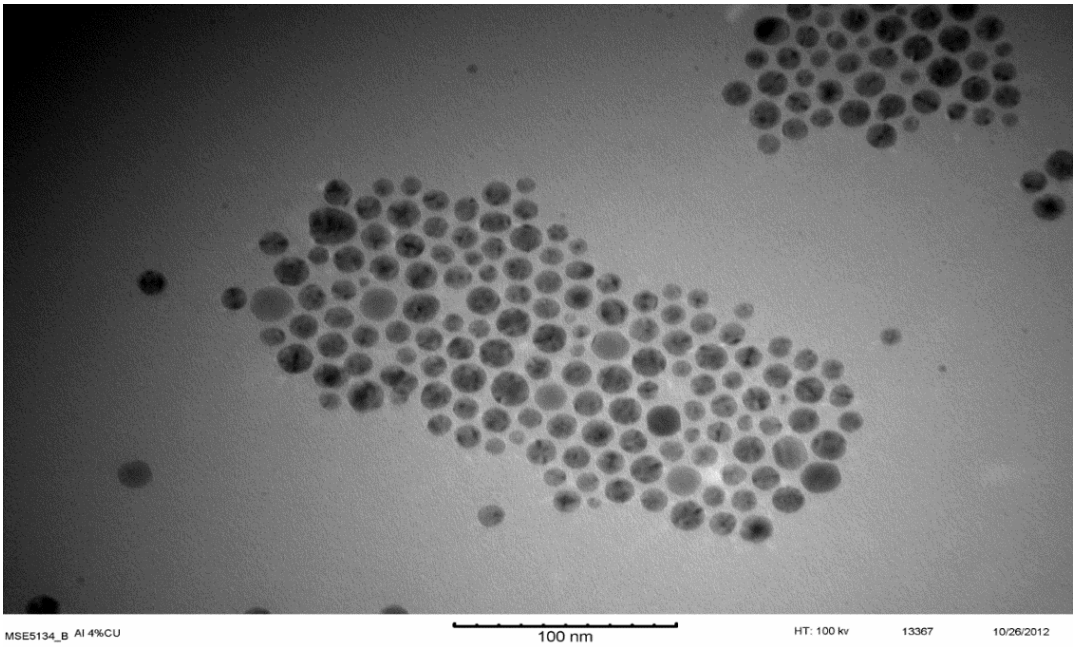

Figure 2.9 TEM image of silver nanosphere

TEM images shows a uniform average size distribution of 22 nm which is in good agreement with the DLS results. Interestingly, the silver nanospheres were stable both in 1-2 dichlorobenzene and n-Hexane for several months (**Figure 2.6**, **Figure 2.7**, **Figure 2.8**, **Figure 2.9**).

2.3. Deposition of Dispersed Silver Nanospheres on a Hydrophobic Substrate

This project aims to deposit dispersed silver nanospheres onto a hydrophobic substrate. The separation between deposited, adjacent particles should be enough to make possible further surface modification and attachment of other particles. In order to achieve such an assembly, a hydrophobic silicon substrate was prepared using the following procedure.

a. Clean the silicon substrates in RCA-1 (ammonium hydroxide: hydrogen peroxide: water 1:1:5 at 75-80 C for 15 minutes)

b. Rinse carefully with high purity water

c. Dry in oven at 140 C for 1 hour.

d. After drying, place the substrates without delay in a 5 mM solution of dodecyltriethoxysilane or hexadecyltrimethoxysilane in anhydrous heptane or anhydrous toluene.
    a. (Here we used hexadecyltrimethoxysilane and anhydrous toluene)

e. Incubate for 24 hours under a parafilm cover (to prevent water infiltration)

f. Rinse carefully with pure heptane or toluene.

g. Heat treat for 1 hour at 70 C.

h. Rinse with acetone to remove unreacted silane, followed by an isopropanol rinse. Drying with a stream of dry nitrogen gas.

i. If not planning to use the substrates the same day, then store them in anhydrous alcohol.

It is possible to reduce the incubation time by increasing the silane concentration. Using the pure liquid, 20 minutes of exposure should be sufficient. If the surface is insufficiently hydrophobic upon completion of the protocol, increasing either the incubation time or the silane concentration is a good approach.

After preparing the hydrophobic silicon substrate, the silver nanospheres were deposited on top of the substrate. The drop cast technique is not a good approach since we are looking to achieve uniform distribution of nanoparticles on the surface. The drop cast technique usually forces nanoparticles to stick together during evaporation of the solution. Therefore, we had to develop a new technique to form a uniform and well separated surface distribution of silver nanospheres. We know that silver nanospheres are coated with oleylamine which is nonpolar. The nanoparticles were suspended in n-hexane which is a nonpolar solvent that was compatible with the coating on the nanoparticles, thus making it favorable for the nanospheres to stay suspended. The combination of the above conditions did not make the hydrophobic surface a better place for silver nanospheres rather than suspending in solution. Therefore we tried to make the solution an unfavorable place for silver nanospheres by gradually adding a polar solvent like methanol to the system.

A 100 ml volume of a dilute suspension of silver nanospheres in n-hexane was placed on top of a stirring plate. The suspension was stirred vigorously at 600 rpm at room temperature. A hydrophobic silane coated silicone substrate was submerged in the solution by holding it there with a pair of tweezers. Methanol was added dropwise gradually up to 200 µl using a micropipette. The substrate was left undisturbed under stirring in the suspension of silver nanospheres for 15 min. After that, the substrate was removed and dried with a dry nitrogen gas stream. **Figure 2.10**, **Figure 2.11**, and **Figure 2.12** show FESEM micrographs of representative coated substrates.

FESEM micrographs represent a good deposition of silver nanospheres on the top of hydrophobic silicone substrate. These images suggest there are plenty of separately seated Ag nanospheres which are suitable for further surface modification and photo activation. Still some big aggregations of nanoparticles can be seen. These aggregations formation is unavoidable due to drying step in this technique. But the number of existing aggregation islands are less than separated nanoparticles which make it possible to perform next steps whithout any interuptions.

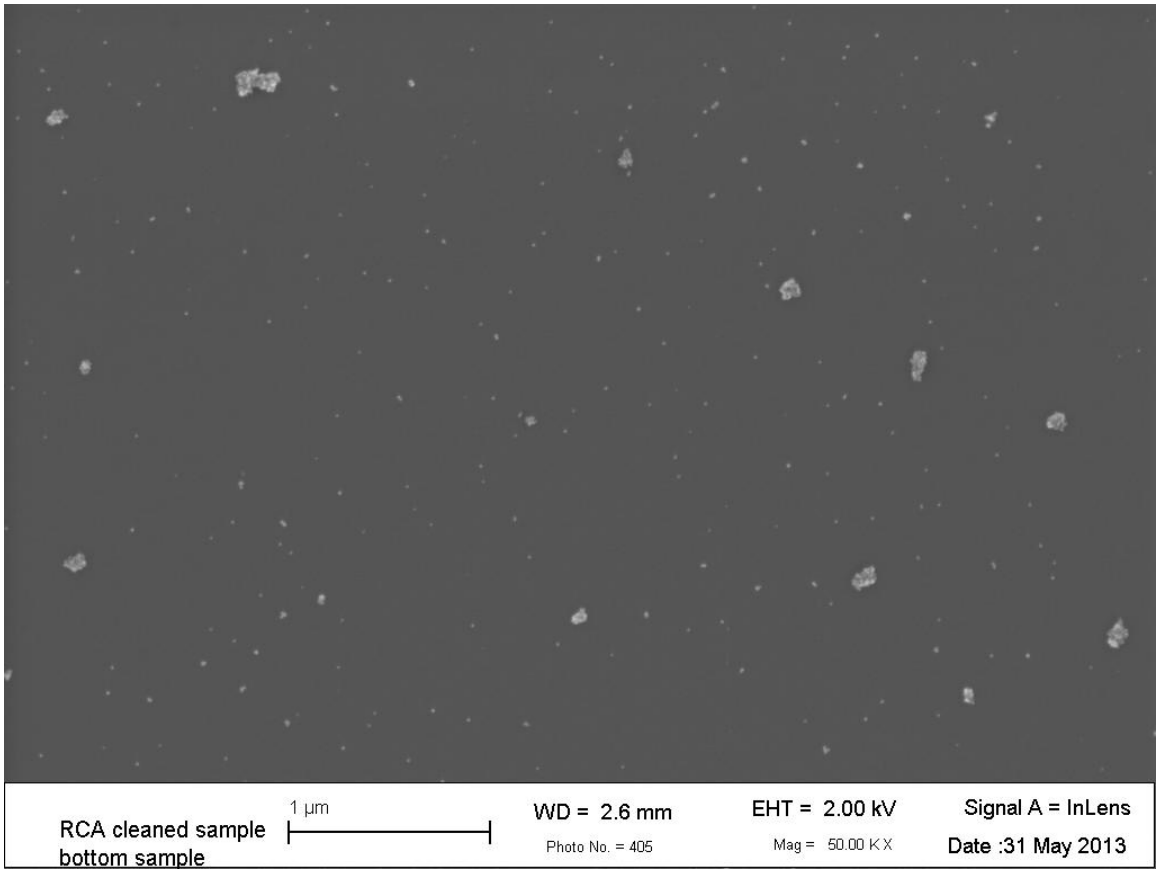

Figure 2.10 FESEM image of seated silver nanospheres on top of hydrophobic silicone substrate

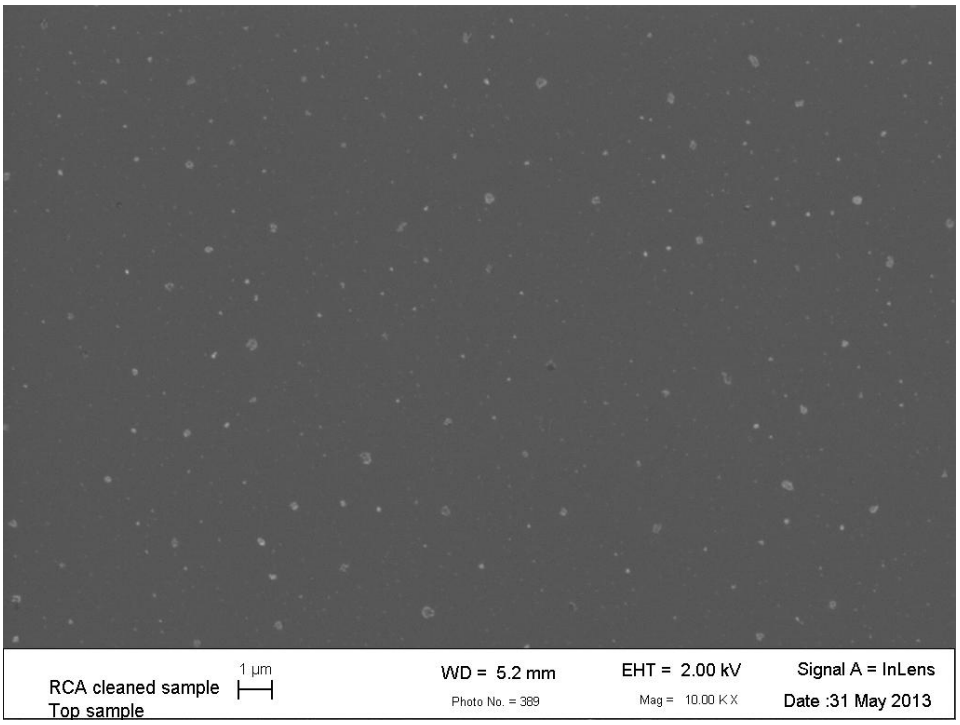

Figure 2.11 FESEM image of seated silver nanospheres on top of hydrophobic silicone substrate

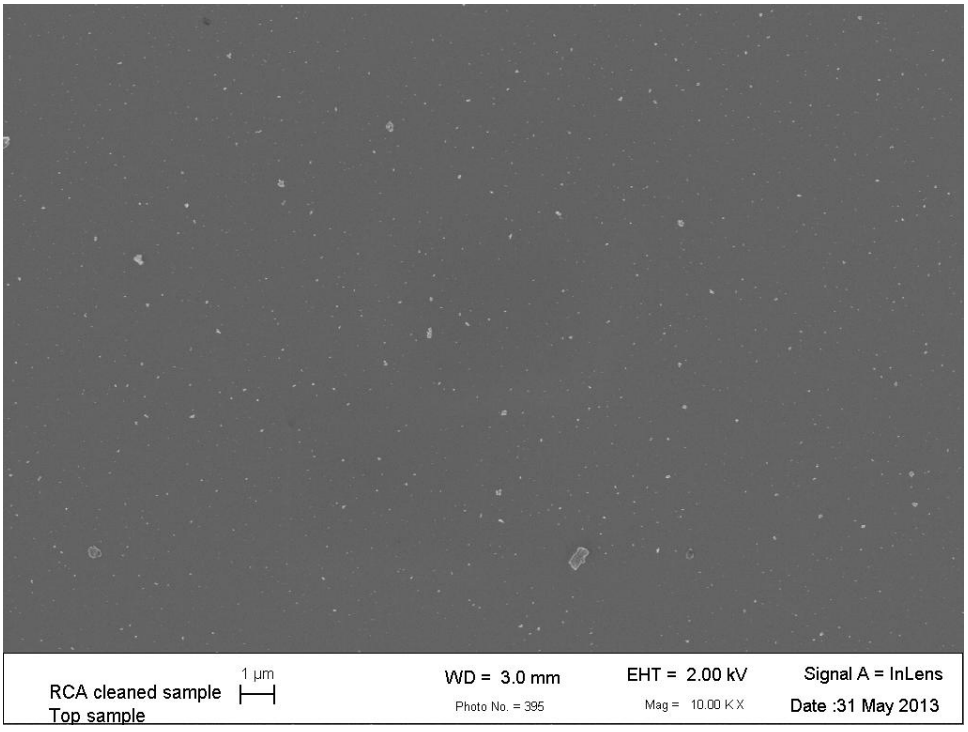

Figure 2.12 FESEM image of seated silver nanospheres on top of hydrophobic silicone substrate

2.4. Summary and Conclusion

We synthesized uniform sized silver nanospheres with a unimodal size distribution and a hydrophobic oleylamine coating. The targeted size for these nanoparticles was 20 nm which has a UV-Vis absorbance peak at 405 nm. We then coated these nanospheres onto a hydrophobic silicon substrate. The silver nanospheres were originally suspended in 1-2 dichlorobenzene, the solvent in which they were synthesized, but this was not a suitable solvent for conducting further surface chemistry. Thus, the silver nanospheres were extracted from 1-2 dichlorobenzene, and redispersed in n-Hexane. A new technique was introduced to effectively force oleylamine coated silver nanospheres to deposit onto a hydrophobic (silane coated) silicon substrate. The desired surface distribution and spacing of silver nanospheres was achieved by tuning concentration and other parameters involved in this method.

Chapter 3: Gold Nanorods Synthesis, Surface Modification, and Surface Photo Activation

3.1 Introduction

Gold nanoparticles have found many industrial and medical applications during recent decades. Gold nanorods are particularly interesting due to their shape-related optical properties which make gold nanorods good candidates for surface photo activation studies. In this research, we developed a technique to photo activate molecules and oligomers on the surface of gold nanorods while there are in suspension. Gold nanorods were first synthesized using a two-step seed mediated technique. The initial coating with a lower molecular weight surfactant was then exchanged with an oligomer that could be photocleaved using UV light. The cleavage efficiency and combinations of various surface active species were probed using several characterization techniques.

3.2 Gold Nanorod Synthesis

In this research we used silver-assisted seed mediated method [68] with slightly modification. This method has been used for more than a century in synthesis of well-defined nanospheres but B. Nikoobakht [19], and CJ. Murphy [18] were the first scientists who applied and modified this method for elongated shapes like gold nanorods.

3.2.1 Materials

All the materials were purchased from Sigma-Aldrich Inc. and were used as received. These include $AuCl_4$+$3H_2O$ or Gold(Iii) Chloride Trihydrate (99.9+% M&, Gold(Iii) Chloride Trihydrate, 99.9+% (Catalogue No. 520918-1G)) (←nomenclature in yellow seems wrong); $AgNO_3$ or Silver Nitrate (99.9999% Metals Basis (Catalogue No. 204390-10G)); CTAB or

Hexadecyltrimethylammonium Bromide (Biox (Catalogue No. h9151-25g)); L-Ascorbic acid (Bioultra, >= 99.5 % RT (catalogue No. 95209-50G)); NaBH4 or Sodium Borohydride (Granules, 99.99% ME (Catalogue No. 480886-25G)); HCl (1.0 Mol Hydrochloric Acid Fixanal (Catalogue No. 38282-1EA)). DI water with resistivity of 18.2 (MΩ) was used for glassware washing and preparing the solutions. A Millipore UV-synergy water purification system was used to produce the DI water. The structures of the main reagents are shown below.

CTAB (cetyltrimethylammonium): cationic micelle-forming surfactant, soft template

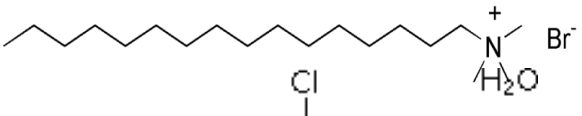

HAucl4.3H2O (Chloroauric acid)

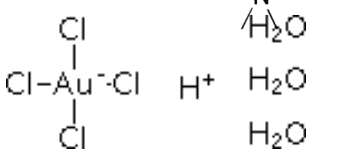

AgNO3 (silver nitrate): shape-directing agent

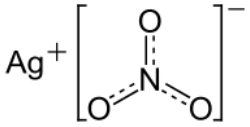

L-Ascorbic Acid: mild reducing agent

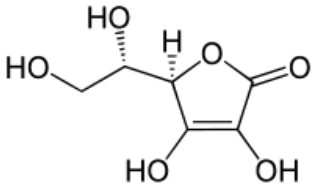

NaBH4 (sodium borohydride): strong reducing agent

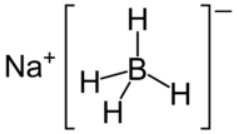

3.2.2 Glassware Cleaning Procedure

Nanoparticles synthesis can be strongly affected if any impurities or contamination exists in the system. Besides using high purity reagents and ultrapure DI water, having clean glassware is essential. In this research, the following procedure was applied to clean the glassware.

a. Washing glassware using appropriate detergent
b. Rinsing glassware with DI water
c. Leaving glassware to dry (in emergency nitrogen gas can be used for immediate drying)
d. Using plasma etcher, cleaner and asher (SPI Plasma-Prep™ II Plasma Etcher) for 30 min to clean the glassware surface
e. Capping top of glassware with parafilm and keeping them in a clean place.

3.2.3 Gold and Silver Salt Solutions Preparation

Gold and silver salt solutions - chloroauric acid and silver nitrate, respectively - are light sensitive. They should be prepared in the dark and after preparation should be kept covered with aluminum foil. We found that the gold salt solutions were more stable than silver solutions. For example, chloroauric acid solutions were still usable and stable after one month but we had to make fresh silver nitrate solutions every other week. Representative procedures for preparing these solutions are shown below.

0.03939(gr) $AuCl_4$+3H_2O + 10(ml) H_2O →10(ml), 10(mM) gold solution

0.01699(gr) $AgNO_3$ + 10(ml) H_2O → 10(ml), 10(mM) silver solution

Other solutions can be prepared in light and under a well-ventilated hood such as the following.

0.91113(gr) CTAB + 25(ml) H_2O → 25(ml), 0.1(M) CTAB

0.17612(gr) L-Ascorbic acid+ 10(ml) H_2O → 10(ml), 0.1(M) L-Ascorbic acid

0.00378(gr) $NaBH_4$ + 10(ml) H_2O → 10(ml), 10(mM) NaBH4

0.2 (ml), 1.0(M) HCl

$NaBH_4$ is a strong reducing agent. Sodium borohydride is so strong that even reacts with water and produces hydrogen. $NaBH_4$ solutions should be prepared freshly for each synthesis. Preparing $NaBH_4$ solutions 10-15 minutes prior to synthesis and keeping it cooled with ice is the best way to use it for this synthesis [19].

3.2.4 Seed-Mediated, Silver-Assisted Growth Method

As the name implies, this method is based upon formation of nanorods from nanoseeds grown in a water-based solution. Nanoseeds are formed separately in another step and then added to the main solution [68]. It should be noted that all synthesis reactions are done in darkness to prevent visible light disturbance. The main two steps in this technique are mentioned below.

Step-1: Preparation of Gold Seeds (In Darkness)

a. A 25 ml Erlenmeyer Flask is placed inside the warm water bath
b. Water bath temperature is kept at 28 C using a hot plate stirrer
c. 250 µl of 10 mM $HAuCl_4$ is mixed with 10 ml of 0.1 M CTAB under vigorous stirring in the flask (600 rpm)
d. Immediately, 600 µl of 10 mM $NaBH_4$ is added (should be fresh and Iced cooled)
e. The solution is stirred for at least 5 minutes while kept at 28 C.

The main chemical oxidation and reduction reactions are:

Oxidation reaction:

$$BH_4^- + 3H_2O \rightarrow B(OH)_3 + 7H^+ + 8e^-$$

Reduction reaction:

$$AuCl_4^- + 3e^- \rightarrow Au\ (0) + 4Cl^-$$

The final result will be a light brownish color solution which contains gold nano seeds approximately 2-3 nm in size (**Figure 3.1**). After preparation, this solution can be kept in light and can be used for 24 hours [19].

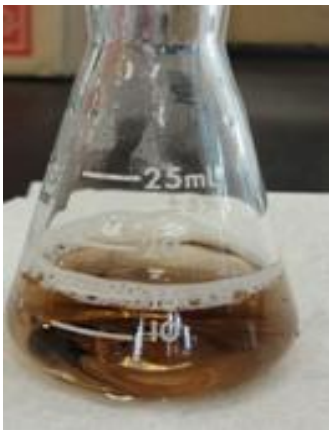

Figure 3.1 Suspension of gold nanoseeds

Step-2: Synthesis of Gold Nanorods (In Darkness)

a. A 25 ml Erlenmeyer Flask is placed inside the warm water bath
b. Water bath temperature is kept at 28 C using a hot plate stirrer
c. 500 µl of 10 mM $HAuCl_4$ is mixed with 10 ml of 0.1 M CTAB and 100 µl of 10 mM $AgNO_3$ solution in a 25 ml Erlenmeyer flask.
d. 200 µl of 1.0 M HCl and 80 µl of 0.1 M L-Ascorbic acid is added after one minute.
e. 24 µl of gold seeds (described in step 1) is added to the final solution
f. The solution should be kept under gentle stirring(80 rpm) at 28 C for 3 hours

The main chemical oxidation and reduction reactions are:

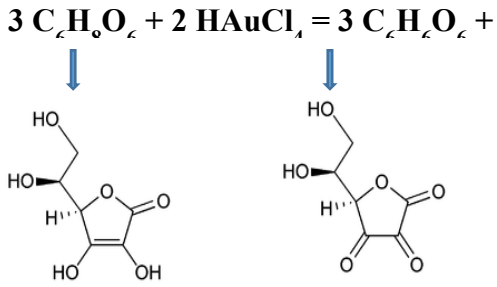

The final result will be a dark reddish color solution containing gold nanorods (**Figure 3.2**). These nanorods are 15-20 nm in diameter and 60-80 nm long. After preparation, this solution can be kept in light at room temperature and remain stable for over 6 months.

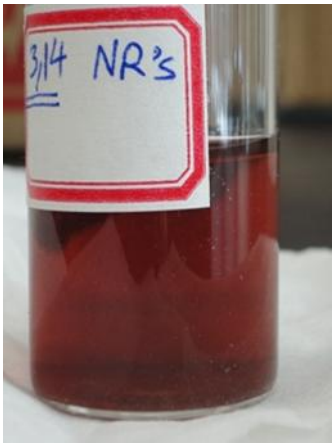

Figure 3.2 Suspension of synthesized CTAB coated gold nanorads

3.2.5 Gold Nanorods Characterization Techniques

After the gold nanorods were synthesized, the size and shape of the particle were studied. There all a lot techniques to probe chemical and physical properties of nanoparticles. Among all these techniques we chose the following four techniques:

1. DLS (dynamic light scattering)
2. TEM (transmission electron microscopy)
3. UV-VIS absorbance spectroscopy
4. NTA (Nanoparticle tracking analysis)

Each of these techniques will be discussed in details, and the characterization results will be showed separately.

3.2.5.1 DLS (Dynamic Light Scattering)

Dynamic light scattering (DLS) is a technique suitable to characterize particles, emulsions, and molecules suspended or dissolved in a solution. A laser beam is passed through the sample, and the Brownian motion of particles forms scattered light with different intensities. A detector detects this scattered light and its intensity fluctuations due to Brownian motions. These intensity fluctuations are then converted to an effective diffusion coefficient and the particle size is can calculated using the Stokes-Einstein equation [69].

Figure 3.3 shows a typical DLS output graph. This graph shows the intensity-average size distribution of gold nanorods in suspension (gold nanorads are synthesized following procedure mentioned in **Section 3.2.4**).

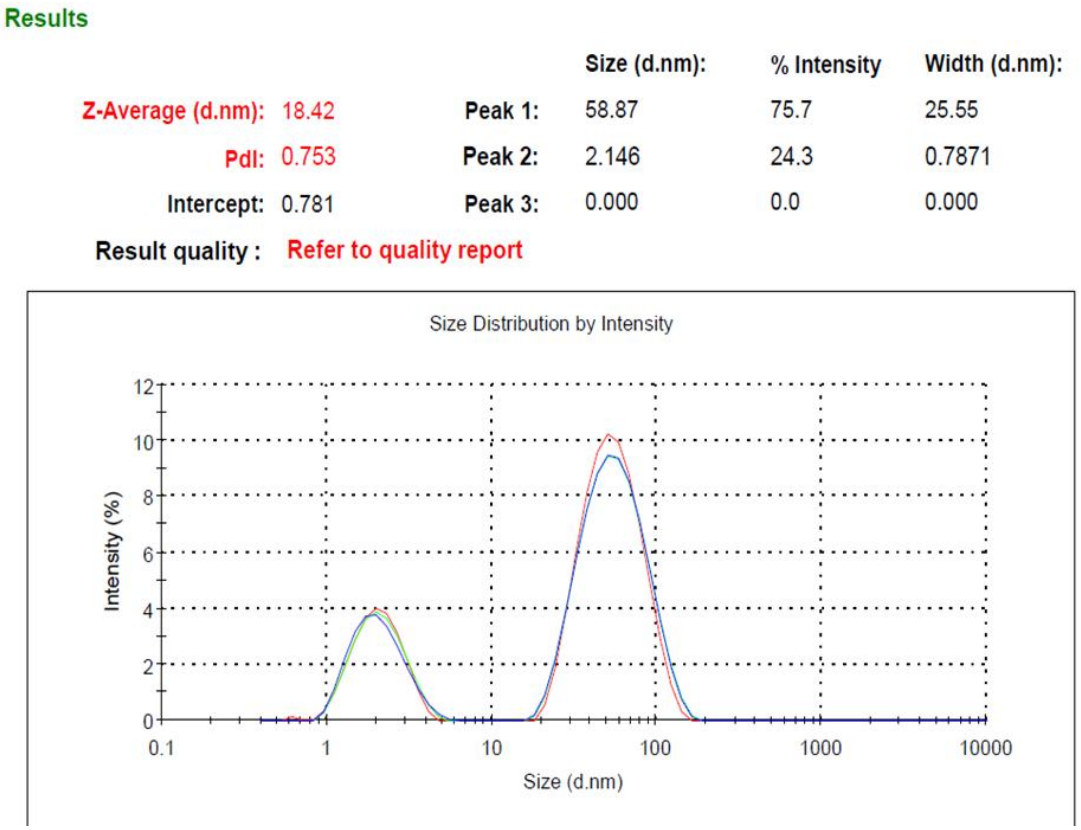

Figure 3.3 Dynamic light scattering size distribution of gold nanorods by intensity

It should be noted that, in dynamic light scattering, the reported particle size is typically based on spherical particles [70]. If the particles are nonspherical, for example elongated particles like gold nanorods, then this technique will report the equivalent spherical particle size distribution which have the same diffusion coefficients as the elongated nanoparticles of interest. This suggests that the sizes of gold nanorods measured by DLS is not the actual size of nanorods. For elongated gold nanorods, two separate peaks can usually be distinguished in the size distribution by intensity output. According to Malvern instruments, "The plot shows the relative percentage of light scattered by particles (on the Y-axis) in various size classes (on the X-axis)"[70]. Therefore if we suppose that diameter as X-axis, and Length as Y-axis for typical gold nanorods, then two peaks represents these axes. The peak at 2.14 nm in **Figure 3.3** most likely corresponds to spherical gold particles characteristics (diameter) in the suspension. The peak at 58.9 nm corresponds to the length of the gold nanorods converted to an equivalent spherical size. Interestingly, this peak is relatively close to the actual real length of the gold nanorods, 60 nm, as measured by TEM images. However, we do not have any proof to conclude that this second peak always corresponds to the gold nanorod length, and modeling these data is beyond the scope of this project.

The main advantage in using DLS to characterize gold nanorods is this technique is totally noninvasive and fast [69]. It enables us within a few minutes to probe gold nanorods formation and do aggregation studies.

3.2.5.2 UV-VIS Absorbance Spectroscopy

UV-VIS absorbance spectroscopy is one of the most well-known and accepted techniques regarding characterization of nanoparticles [71]. In this technique, light with different wavelengths is passed through the sample and its incident and transmitted intensities are measured. By applying

the Beer-Lambert law, the absorbance of sample (A) is measured at any wavelength in terms of the incident and transmitted light intensities, I_0 and I, respectively according to [72]:

$$A = \log_{10}(I_0/I) = \varepsilon CL$$

ε is the extinction coefficient (a function of the particle and its surrounding sample medium), C is the concentration of nanoparticles or molecule of interest, and L is the length that light passes through the sample

The Beer-Lambert law suggests that samples with higher concentrations have higher absorbance values. Changing the medium (solvent) of the sample changes the absorbance peak and can change the wavelength at which the peak occurs. The extinction coefficient ε correlates with the absorption of light by a specific chemical species at a given wavelength. L is the optical path length and is usually fixed by the internal diameter of the cuvette in which the liquid sample is place. The interesting point about UV-VIS absorbance is that the peak wavelength is only a function of the medium (solvent), particle material, and particle aspect ratio. Therefore, when the solvent and particles composition (gold, in the present case) are kept fixed, the peak wavelength will be only a function of the nanoparticle aspect ratio. The aspect ratio in a rod-like particle is defined as the ratio of (length/diameter). Higher aspect ratio nanoparticles have absorbance peaks at longer wavelengths.

For the purpose of this project, gold nanorods and gold nanospheres were synthesized. Each particle had its own specific size and aspect ratio. The UV-VIS absorbance of these particles were studied by varying the incident wavelength from the UV part of the spectrum (200-400 nm) to the infrared spectrum range (700-1100 nm).

Figure 3.4 shows a typical gold nanosphere UV-VIS absorbance graph with only one peak at 520 nm. This peak usually occurs between 520-540 nm depending on the diameter of gold nanospheres, and occurs at longer wavelengths for larger gold nanorods and nanospheres [73]. Changing the concentration of gold nanoparticles just changes the absorbance magnitude (peak height) but not the wavelength of the peak.

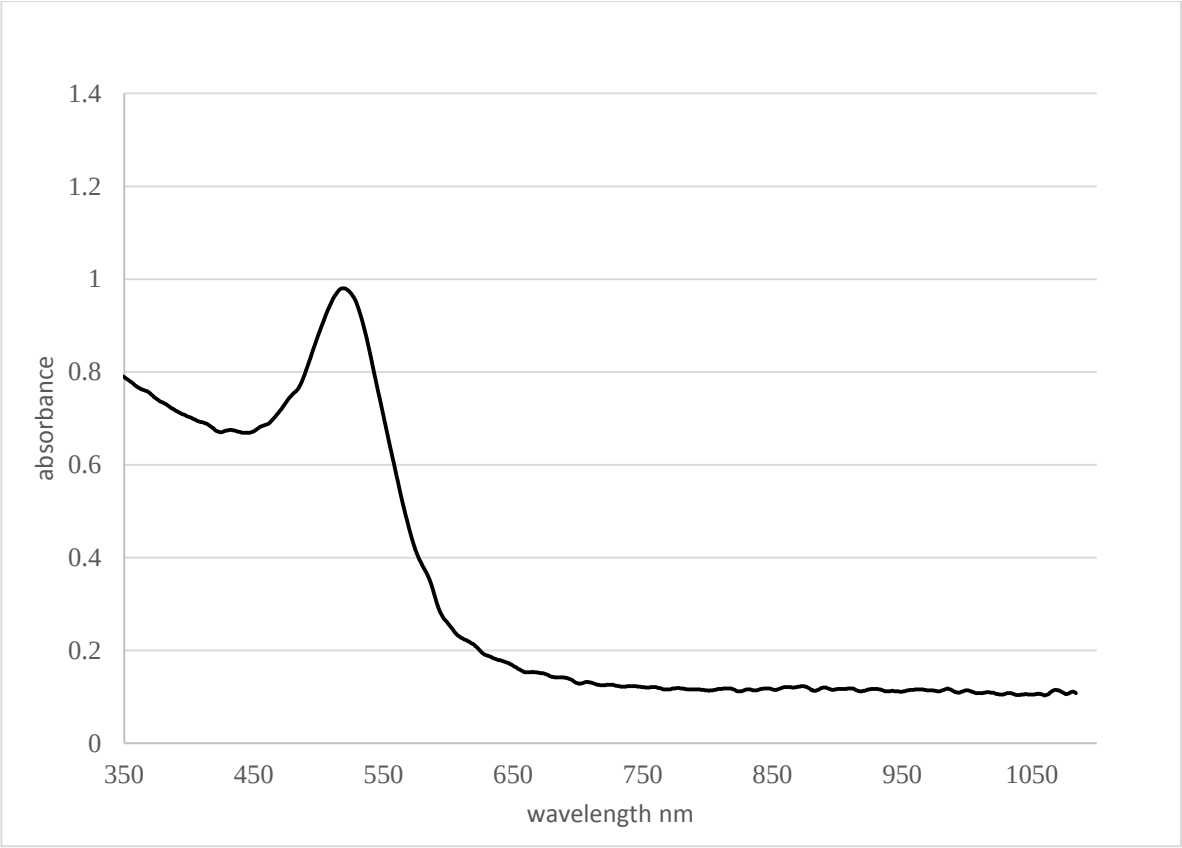

Figure 3.4 UV-Vis absorbance graph of gold nanospheres in water

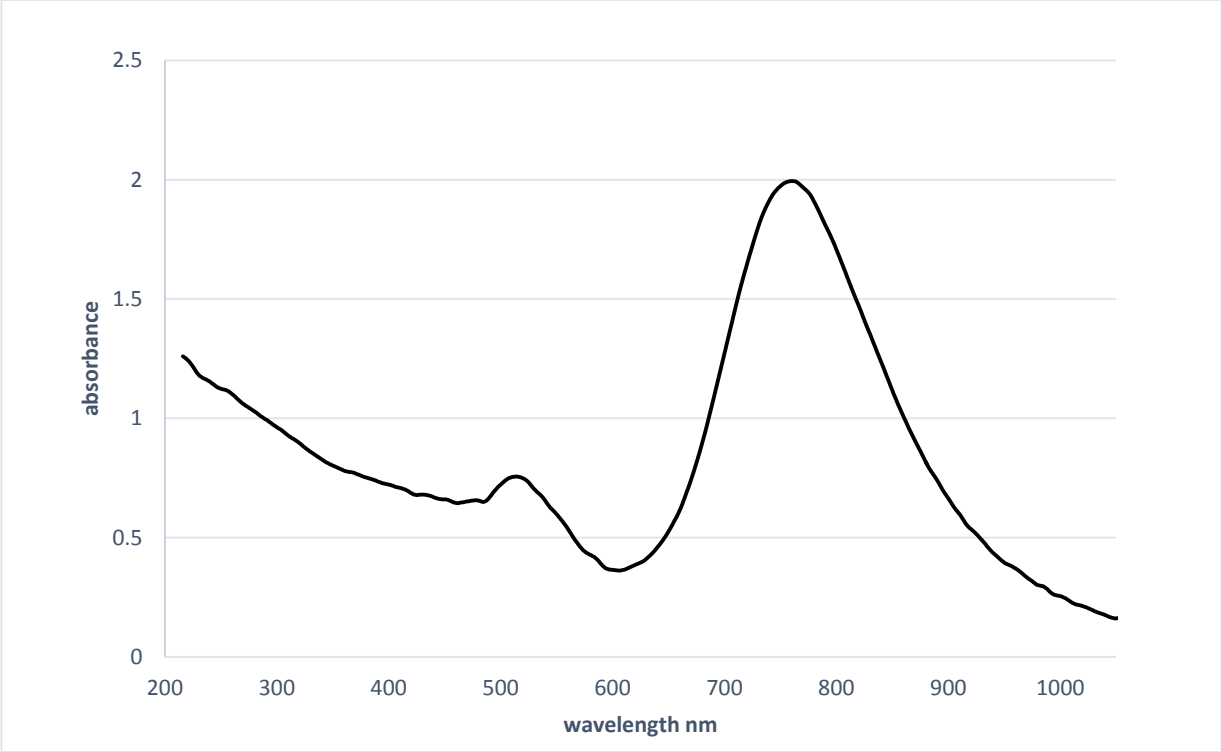

Figure 3.5 UV-Vis absorbance of gold nanorods in water

Figure 3.5 shows a typical UV-VIS absorbance graph for gold nanorods synthesized using the same synthesis procedure described in this chapter.

The UV-VIS absorbance graph of a typical gold nanorod suspension typically shows two peaks whereas only one peak occurs for gold nanospheres. The smallest peak for nanorods usually occurs between 520-540 and occurs at longer wavelengths for larger gold nanorods and nanospheres [73]. The second peak which only can be seen in elongated or rodlike gold nanoparticles represents the aspect ratio (length over diameter) of nanoparticle. Each of these peaks have their own specific name. The first peak (at the lower wavelength) is called the transverse band and the second peak (at the longer wavelength) is called the longitudinal band. The longitudinal band is a function of the gold nanorod aspect ratio and the wavelength at which it occurs increases with the aspect ratio.

3.2.5.3 TEM (Transmission Electron Microscopy) Imaging Characterization

TEM is the one of the most popular characterization techniques for nanoparticles [60]. In this technique, a real image of nanoparticles is taken. Different magnifications can be used to see a more detailed or general shape of nanoparticles. These images contain a lot of information regarding shape and size distribution, and even crystallographic structure and characteristics of nanoparticles. In this project, images are taken using a conventional Philips EM420 TEM at the Nano characterization Facilities Laboratory (NCFL) at Virginia Tech. All samples were prepared using the drop cast technique. A 200 mesh thick carbon film coated copper grid was used as a substrate. Approximately 10-15 µl of dilute sample was left as a drop on top of the grid and left for at least 24 hours undisturbed in the hood to dry. A pair of tweezers was used to hold and manipulate the grids which were then transferred to a grid holder for further imaging.

Figure 3.6, **Figure 3.7**, **Figure 3.8**, and **Figure 3.9** show TEM images taken from synthesized gold nanorods. These images suggests that during synthesis, other shapes like spheres, prisms, and cubes are formed too. The majority of nanoparticles are gold nanorods which represents high yield of this synthesis technique. On the other hand the second population belongs to big gold nanospheres. Nanocubes and nanoprisms are very rare and hard to find. Drop cast technique leads to aggregation and consequently formation of big aggregate islands on the top of grid. But still separately seated gold nanoparticles can be found. According to TEM images, average length of gold nanorods is approximately 60 nm and aspect ratio is 3.5. Size distribution of gold nanorods show that most of synthesized gold nanorods have the same size and aspect ratio.

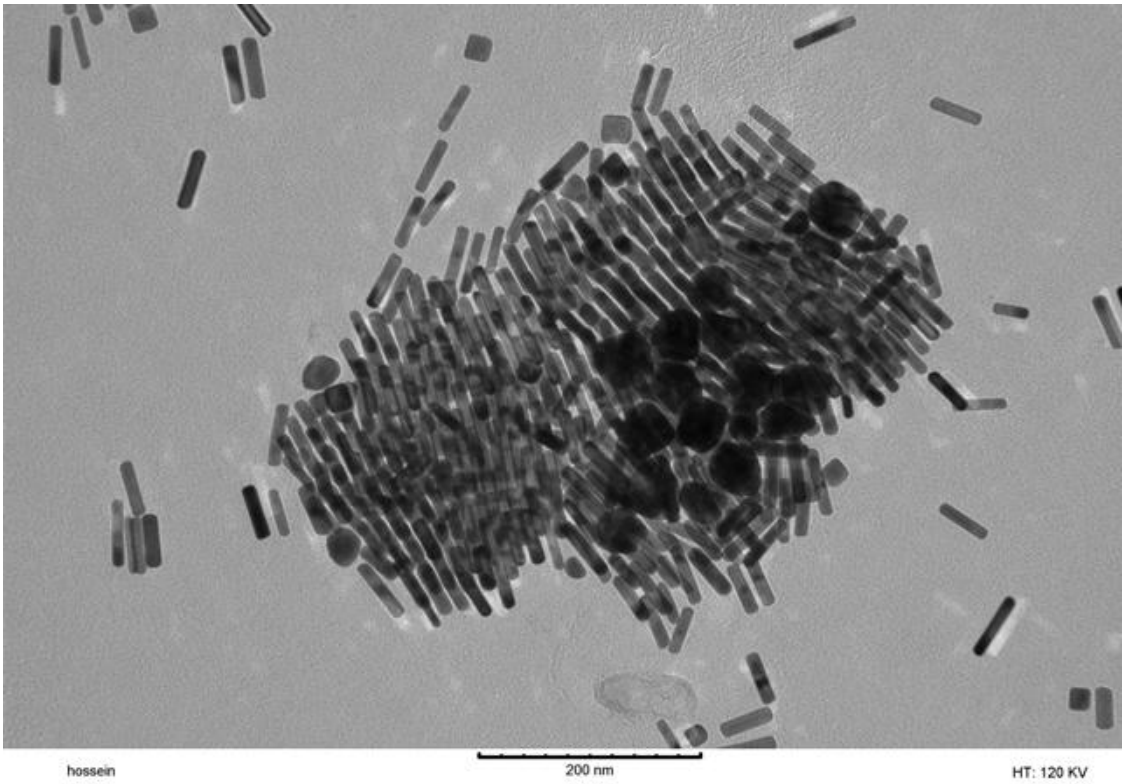

Figure 3.6 TEM image of synthesized gold nanorods using two-step technique

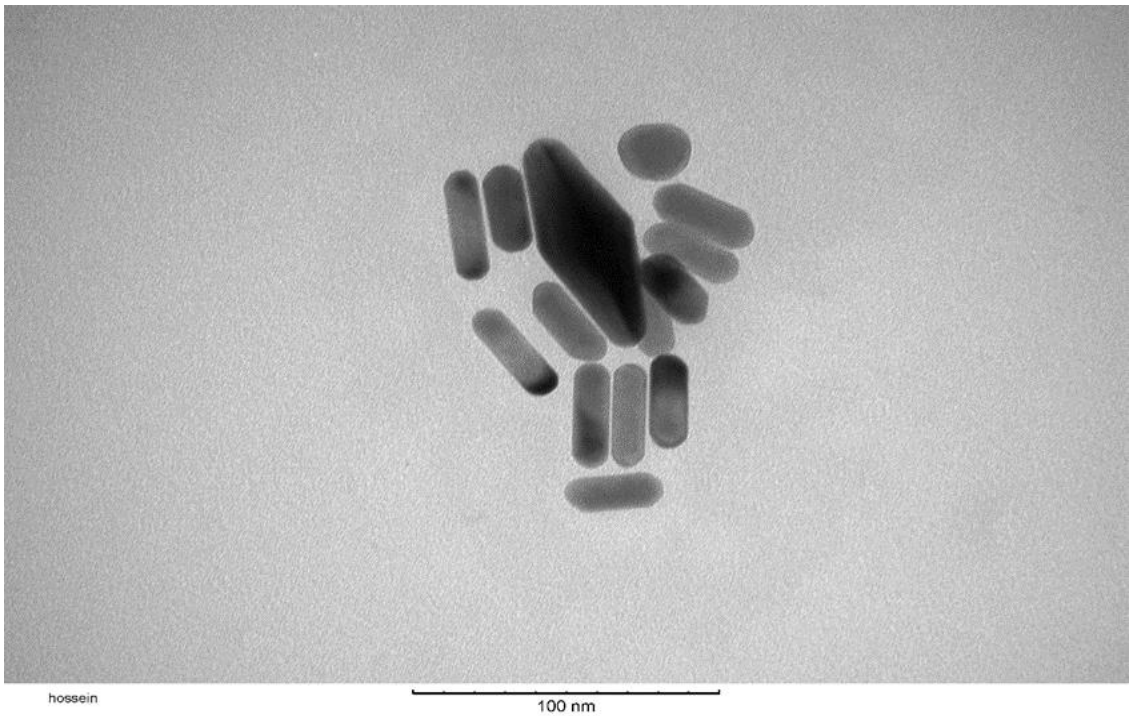

Figure 3.7 TEM image of synthesized gold nanorods using two-step technique

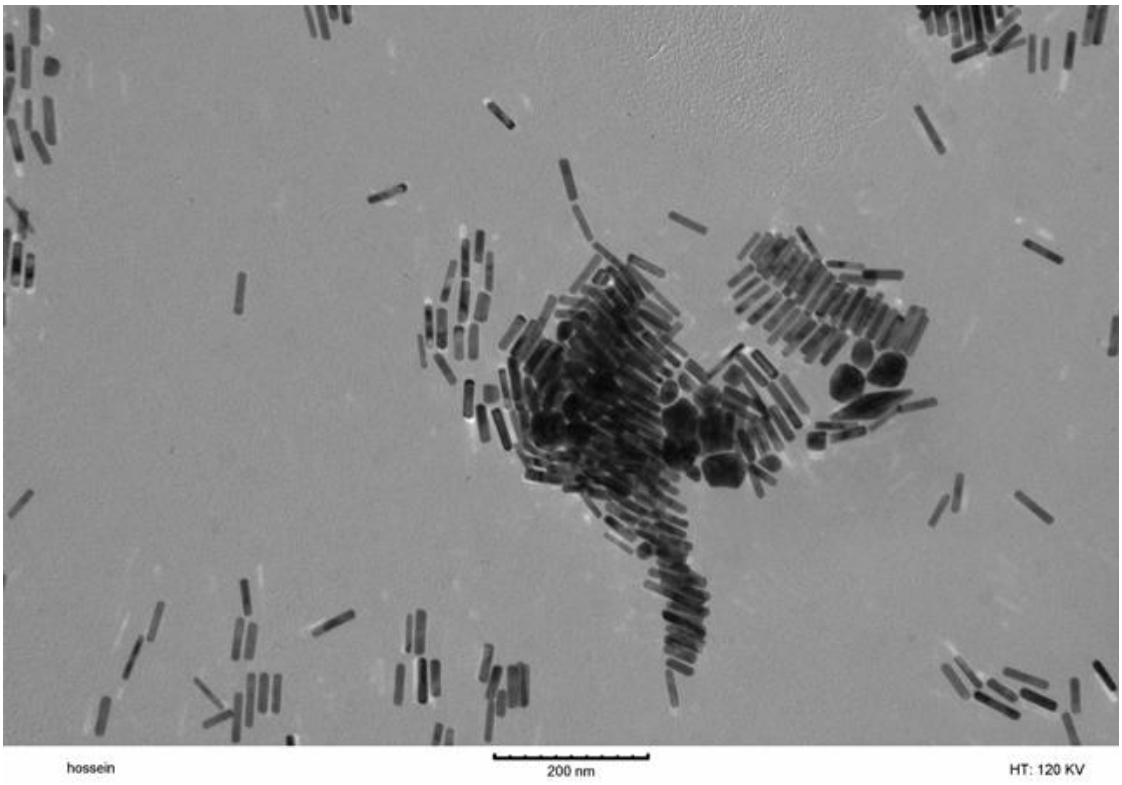

Figure 3.8 TEM image of synthesized gold nanorods using two-step technique

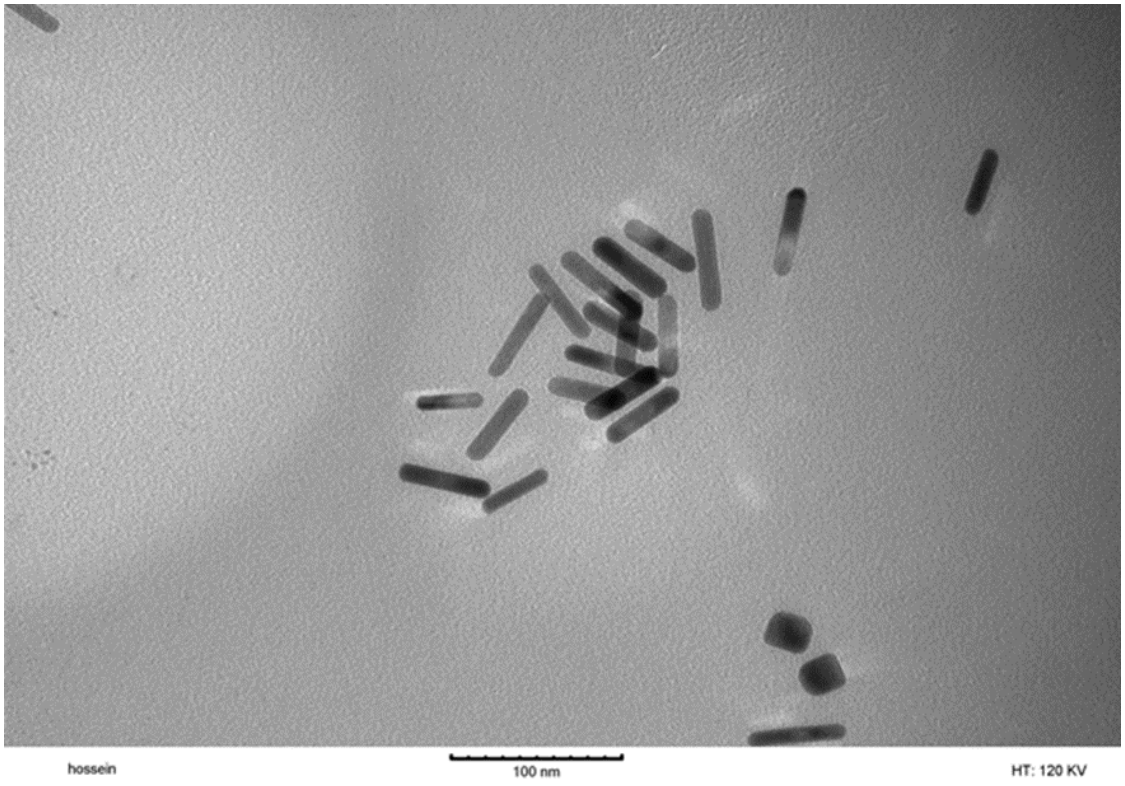

Figure 3.9 TEM image of synthesized gold nanorods using two-step technique

3.2.6 Shape Separation of Gold Nanorods

During gold nanorods synthesis, other shapes of gold nanoparticles such as nanocubes and nanoprisms are formed[44, 74].

Figure 3.6 shows nanocubes and **Figure 3.7** shows nanoprisms formed during gold nanorods synthesis. Thus, there was a need to separate, even crudely, the nanoparticles based on shape.

There are several papers introducing shape separation based on centrifugation of gold nanorods suspension [28, 44, 74]. Shape separation centrifugation technique is based on different settling time of nanoparticles with different shapes. It should be noted that settling velocity is shape and size related. Therefore, different nanoparticles with different shapes behave differently under the same centrifugal force[75]. **Figure 3.10** describes how this separation takes place.

Figure 3.10 Shape distribution of gold nanoparticles with different size and aspect ratio[74] 'used under fair use,2013'

There are two general rules in this separation technique: (1) larger nanoparticles sediment more rapidly, and (2) nanoparticles with higher aspect ratios sediment more slowly than nanoparticles with the same length but with lower aspect ratio [74, 75]. Interestingly none of the centrifugation times and relative centrifugal force (RCF) values suggested in prior literature worked for the size and aspect ratio range of our project interest and so we had to develop our own

centrifugation technique. As mentioned before, in this project we targeted to synthesis of 60 nm gold nanorods with an aspect ratio of 3.5. By trial-and-error, we found the following procedure gives the optimum separation for such gold nanorods. By optimum, we mean separating other shapes and lower aspect ratio gold nanoparticles without losing the nanorods with the desired aspect ratio. In brief, the procedure consisted of several steps:

a. Transferring recently synthesized gold nanoparticles suspension to centrifugation tube as is (No washing or other treatment was needed)
b. Centrifugation at 2000 RCF for 10 min
c. Removing 95% of the supernatant as an enriched gold nanorod suspension
d. Removing the remaining 5% and sediment as gold nanospheres and low aspect ratio particles.

The results of this separation technique were investigated using different characterization techniques. **Figure 3.11** shows UV-Vis absorbance graphs of unseparated gold nanoparticles suspension, supernatant suspension, and sediment suspension after centrifugation. Starting from the left-hand side of the graph, the first peak at 530 nm is due to a mixture of nanospheres and low aspect ratio gold nanorods. The peak of the separated (sedimented sample) shifted from 530 nm to 550 nm (red shifted) while the second peak (due to the longitudinal band) decreased significantly, shifting from 885 nm to 865 nm (blue shifted). This graph shows that most of the particles in the sediment are spheres or have a low aspect ratio and an elongated shape. The left-most peak in the curved labelled “nanorods” showed a significant blue shift from 530 nm to less than 520 nm. The ratio of the first peak height with the second peak height in the “nanorods” curve significantly decreased which implies a high concentration of high aspect ratio gold nanorods.

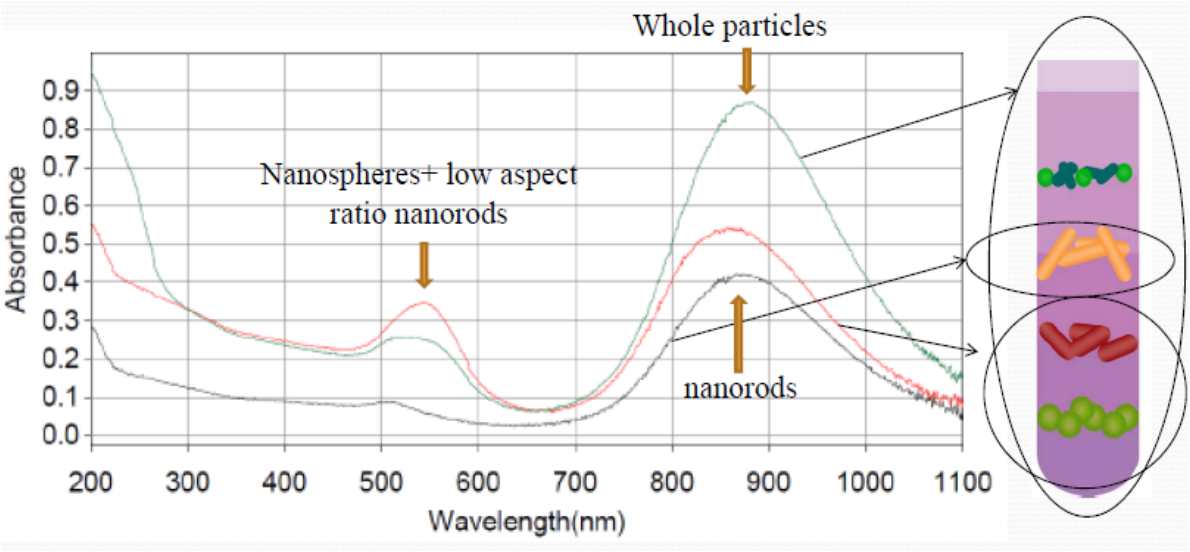

Figure 3.11 UV-Vis absorbance graphs of supernatant and sediment suspension for centrifugal separation of gold nanorods

Figure 3.12 and **Figure 3.13** show TEM images of separated supernatant suspension during this centrifugal separation technique. Most of the separated gold nanorods have the same aspect ratio and size with few, if any, other shape that can be seen.

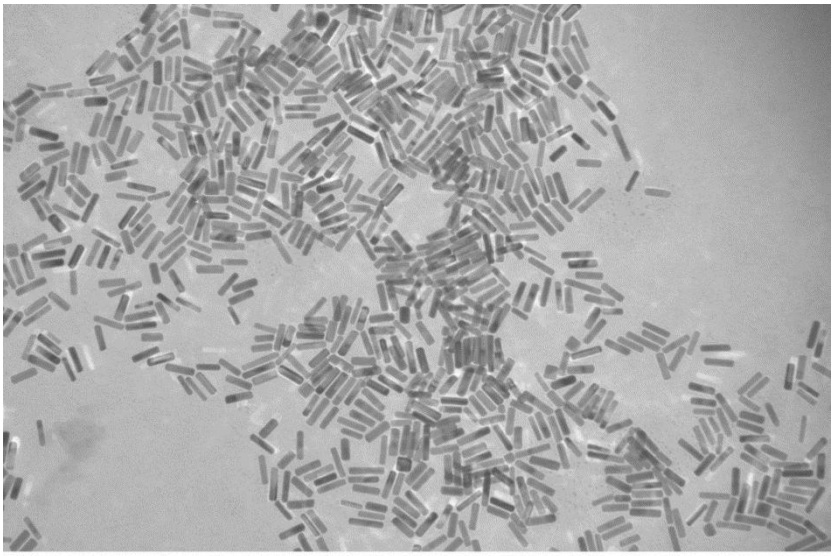

Figure 3.12 TEM image of separated supernatant suspension of gold nanorods

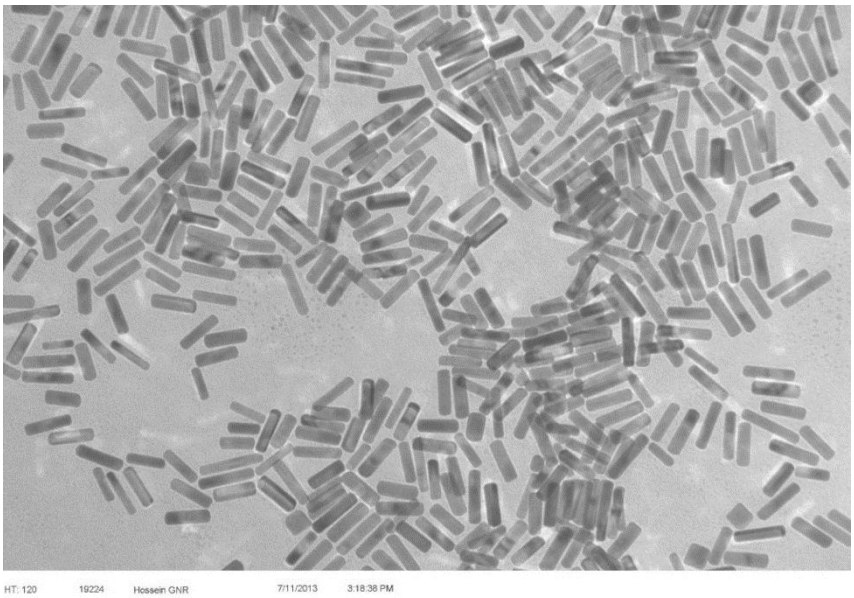

Figure 3.13 TEM image of separated supernatant suspension of gold nanorods

Figure 3.14 and **Figure 3.15** show TEM images of the sediment suspension for the same sample. It can be seen that most spherical nanoparticles and other shapes are separated. Low concentrations of gold nanorods in **Figure 3.14** and **Figure 3.15** represents a high yield separation.

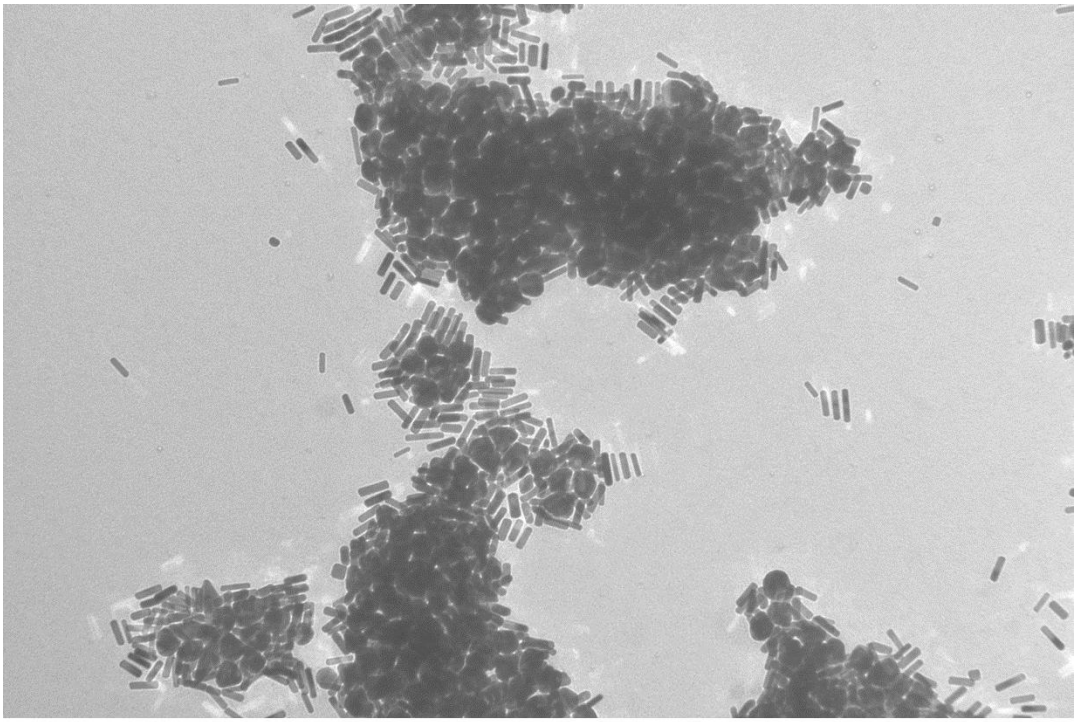

Figure 3.14 TEM image of separated sediment suspension of gold nanorods

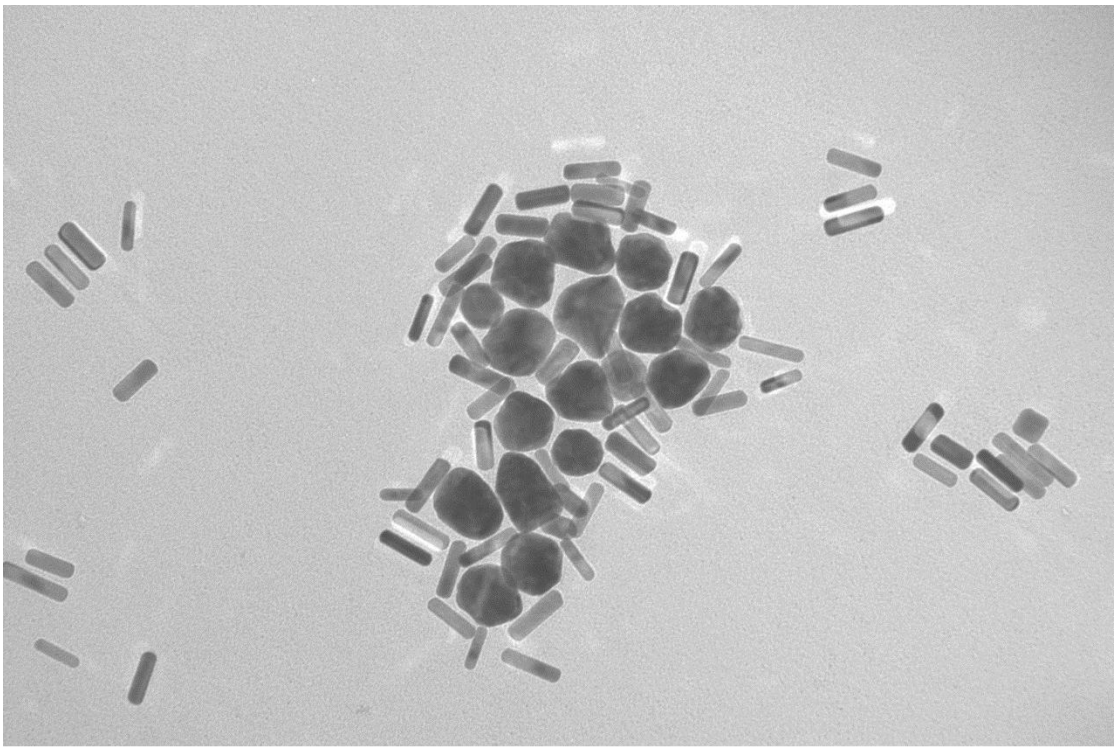

Figure 3.15 TEM image of separated sediment suspension of gold nanorods

3.2.7 Tuning Size and Aspect Ratio of Gold Nanorods

The size and aspect ratio of synthesized gold nanorods can be adjusted by varying the ratio of added reagents, specifically the ratio of CTAB (capping agent) and $AgNO_3$ (shape directing agent)[17, 18, 21, 22, 27-31, 61]. Increasing CTAB concentration or even using a co-surfactant like DTAB can form longer surfactant micelles. Longer micelles can lead to longer gold nanorods formation (aspect ratios up to 20). On the other hand, it has been shown that changing silver nitrate concentration can change the aspect ratio of gold nanorods. It is believed that silver ion has a high affinity for the bromide ion in the CTAB molecule. Since CTAB prefers side facets of gold nanorods rather than tip facets, it is believed that silver interacts with the bromide ion in the CTAB micelle around the side facets and makes the whole combination more stable. The final result is a denser micelle around the gold nanorod which inhibits the crystal growth through the side facets. This mechanism can used for fine tuning the gold nanorod aspect ratio without increasing the size polydispersity [18].

In this project we decided to keep all concentrations and physical conditions during synthesis fixed, and just change amount of added $AgNO_3$ slightly to probe its effect on the gold nanorods aspect ratio. We targeted a specific size and aspect ratio of gold nanorod (length: 60 nm and aspect ratio: 3.5) which has a longitudinal absorbance peak at 740 nm.

Figure 3.16 and **Table 3.1** summarize the relation between longitudinal absorbance peaks (representative of aspect ratio) of gold nanorods to the initial amounts of added $AgNO_3$. The set of experiments here show that aspect ratio of gold nanorod is directly related to and can be tuned by amount of added silver nitrate [18, 29, 61].

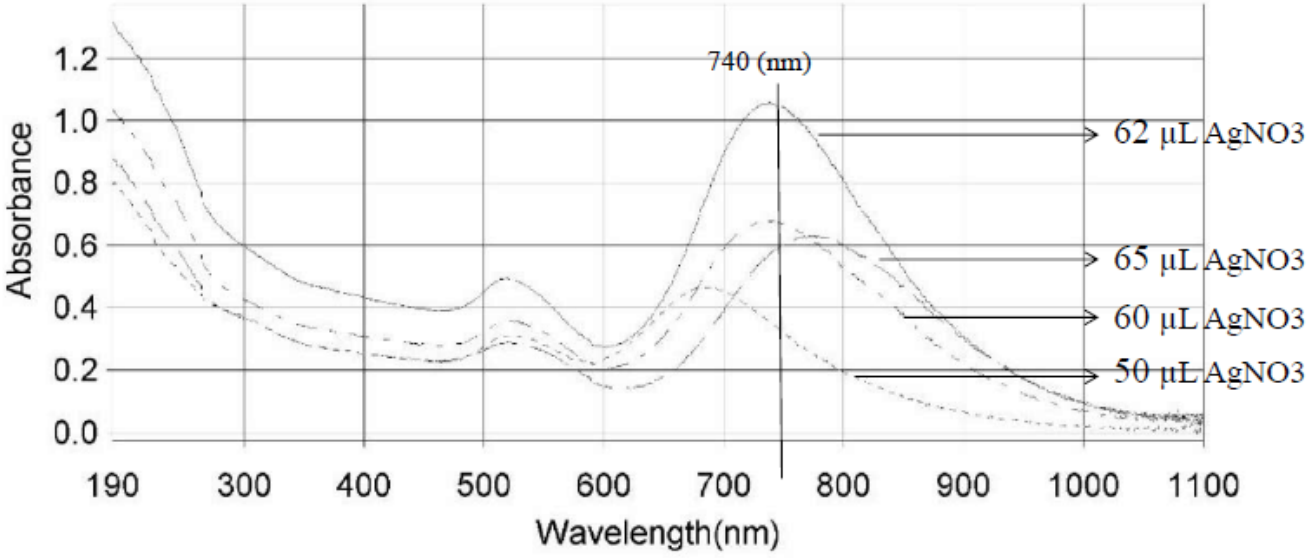

Figure 3.16 UV-Vis absorbance graphs for synthesized gold nanorods by varying amount of $AgNO_3$ in the synthesis

Table 3.1 Effect of concentration of added $AgNO_3$ on gold nanorod aspect ratios (longitudinal peak in UV-Vis absorbance)

Added AgNO3 (µL)	50	60	62	65
Longitudinal absorbance peak nm	685	735	740	780

3.3 Surface Modification (Coating Exchange) Of Gold Nanorods

CTAB has a key role in one-dimensional growth of gold nanorods. It simultaneously serves as a template for nanorods growth, while after synthesis prevents them from further aggregation [17, 18, 21, 27, 29]. Nikoobakht et al. showed that CTAB forms a bilayer micelle around gold nanorods [32]. This bilayer inhibits aggregation of nanorods by two mechanisms - steric and charge repulsion. CTAB forms a brush around gold nanorods and prevents them from getting close enough for strong Van der Waals interactions. On the other hand, CTAB is a cationic surfactant. CTAB's bilayer positive charge on a gold nanorod repels other nanorods with the same charge.

There are two main issues with CTAB stabilization of gold nanorods. The first problem is CTAB physisorbs on gold, i.e. there is no strong chemical interaction between CTAB and the gold surface. Therefore, physisorbed CTAB on the surface is always in equilibrium with excess CTAB in the solution. If the CTAB concentration in solution decreases, then CTAB will desorb which can result in gold nanorod aggregation. The second problem is that the excess CTAB in solution is cytotoxic. Thus, using CTAB coated gold nanorods in equilibrium with CTAB solution for medical applications is impossible. Therefore, many researchers have attempted to replace CTAB with more biocompatible coatings [76-78] including biocompatible polymers [79, 80]. All research up to now has been focused on producing biocompatible gold nanorods by forming a thick biocompatible, stable corona around nanorods. This thick corona has its own advantages but typically makes it impossible to do any further surface chemistry on the gold nanorods.

In this project, in contrast with prior work, we tried to do a selective surface modification on different facets of gold nanorods and to then to selectively photoactivate the gold nanorod tips. In order to achieve this goal, it was necessary to develop a novel oligomer to replace CTAB.

We were interested in knowing the minimum required length of oligomer to prevent aggregation. To answer this question, we developed a Matlab simulation code for calculating Van der Waals interaction between two identical parallel gold nanorods based on DLVO (Derjaguin, Landau, Verwey and Overbeek) theory. Size, aspect ratio of gold nanorods, and medium characteristics are inputs, and this code calculates Van der Waals interaction energy between two nanords versus their separation.

According to **Figure 3.17**, at over 2 nm separation the Van der Waals interaction energy between two parallel gold nanorods is less than 1kT. This suggests oligomers and polymers forming a brush longer than 1.5 nm on surface of gold nanorods can prevent further aggregation.

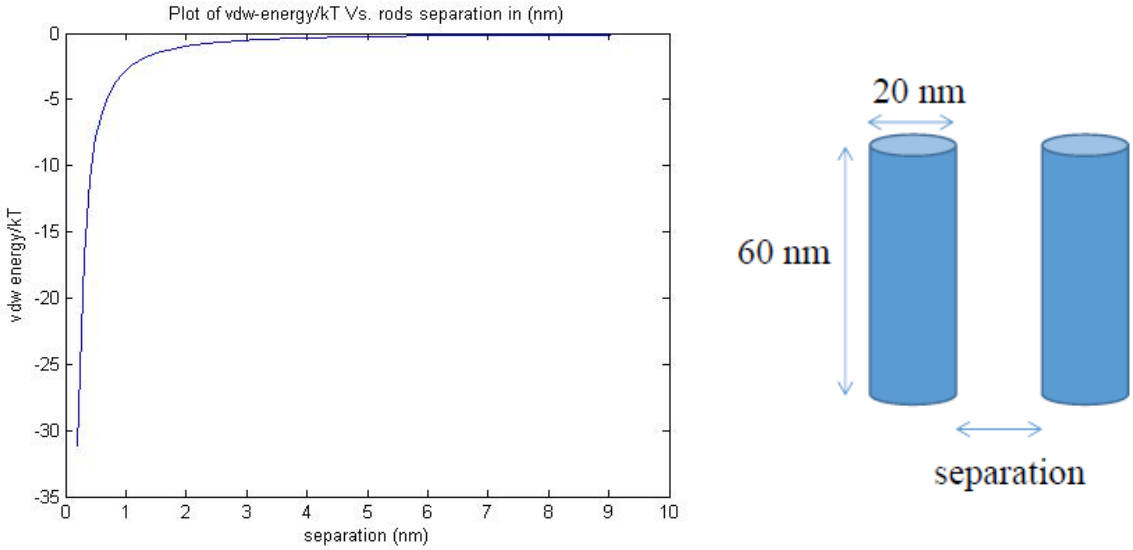

Figure 3.17 Van der Waals interaction energy versus separation of two parallel gold nanorods

3.3.1 Replacing CTAB

In order to replace CTAB efficiently, we needed first to wash the surface of gold nanorods. The gold nanorods surface was covered with a dense CTAB bilayer which is in equilibrium with excess CTAB in solution. Washing all excess CTAB led to fast desorption of CTAB on the surface and aggregation of gold nanorods. Therefore, we had to develop a procedure to remove CTAB from solution in such a way that did not lead to rapid aggregation. Centrifugal washing of gold nanorods is a fast, reliable technique and so we developed the following procedure:

a. Gold nanorods suspension was centrifuged at 15m000 RCF for 30 min.
b. 90% of the clear supernatant liquid was decanted.
c. DI water was added (equal in volume to that of the decanted supernatant)
d. The precipitate was resuspended in DI water by shaking
e. The gold nanorod solution was sonicated for 30 seconds in the sonication bath.

Our experiments show that gold nanorods can be washed for three successive washing without any sort of aggregation. A fourth washing led to irreversible aggregation which is not desirable in this project. The effect of the gold nanorod centrifugal washing is shown in the following tables and graphs.

Figure 3.18 and **Table 3.2** shows UV-Vis absorbance graphs for each washing step of CTAB coated gold nanorods. We assumed that the area under the curves was directly proportional to the concentration of gold nanorods in the suspension since all other parameters were fixed. After the third washing, the results in **Table 3.2** show that approximately 40% of the nanorods were lost during the washing procedure. Losing some gold nanoparticles during the washing procedure is unavoidable. In this research, losing 40% of the nanorods during the washing procedure was considered acceptable.

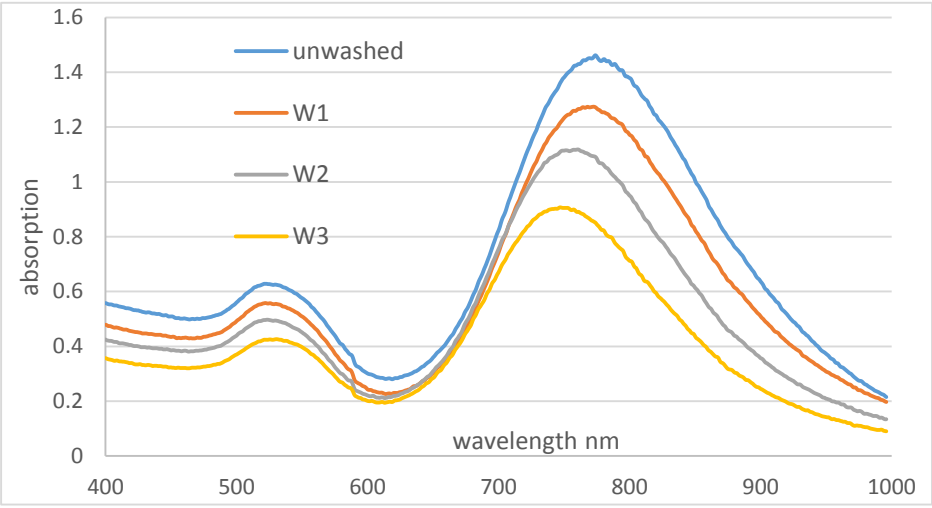

Figure 3.18 UV-Vis absorbance graphs for 3 successive CTAB coated gold nanorods washing

Table 3.2 Under curve surface area of UV-Vis absorbance graphs for each washing versus unwashed CTAB coated gold nanorods

	Unwashed GNR	Wash 1(W1)	Wash 2 (W2)	Wash 3 (W3)
Under curve area (absorbance*nm)	413.6265	355.037	303.5435	245.4305
Percentage ratio	100	85.83	73.38	59.33

3.3.1.1 First Generation of Oligomers

In view of the modeling of the Van der Waals interactions mentioned previously that suggested a steric barrier of 1.5 nm on the surface of the nanorods was needed to prevent aggregation, a new, surface-active oligomer was synthesized by Prof. Webster Santos's group in the Chemistry department at Virginia tech. The structure of this oligomer is shown in **Figure 3.19** and it will be designated henceforth as "Oligomer-1".

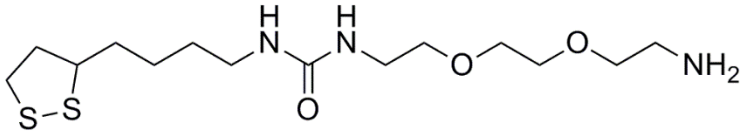

Figure 3.19 Molecular structure of Oligomer-1

This oligomer has a disulfide head group for binding to the gold and contains to ethylene oxide units. Gold-thiol chemistry is well known for a long time, and thiol-PEG (polyethylene oxide) has been widely used to replace CTAB as a biocompatible polymer [6, 76, 78, 81]. A primary amine with positive charge was used as a tail group in this oligomer to enhance its charge repulsion characteristics. Oligomer-1 is approximately 1.5 nm which according to DLVO Van der Waals interaction modeling should be long enough to inhibit aggregation of gold nanorods if it could be deposited onto the gold surface at densities high enough to form a dense monolayer. Thus, we developed a procedure to replace CTAB with Oligomer-1 as shown below:

a. 10 ml freshly synthesized gold nanorods were washed 3 times according to the washing procedure mentioned in **Section 3.3.1**.
b. 415 µl of 5mM solution of Oligomer-1 were added to 10 ml gold nanorods solution (final concentration of Oligomer-1 in the mixture is 0.2 mM)
c. The mixture was bath sonicated for 20 seconds
d. The mixture was then left undisturbed for 24 hours.

After this procedure, there was still some excess Oligomer-1 and CTAB in the solution. Thus, the washing procedure described in **Section 3.3.1** was used to remove excess, unreacted Oligomer-1 from the suspensions. Interestingly, after the first wash, a dense sediment of gold nanorods was formed at the bottom of tube.

This sediment required about 2 minutes bath sonication to resuspend. Two conclusions from these experiments are: (1) washed Oligomer-1 coated gold nanorods are stable for about 2 hours and after that significant aggregation occurs, and (2) centrifugal washing causes most of the particles to sediment but these sediments form only weak aggregates that can be resuspended reversibly.

The zeta potential for the CTAB-coated gold nanorod control sample was +58 mv, while it decreased to +41 mv for the Oligomer-1 coated gold nanorods. All zeta potential measurements were done using the Malvern Zetasizer Nano-ZS instrument. This change in zeta potential value and the instability of gold nanorods after replacement qualitatively shows this replacement has occurred. We know that CTAB forms a bilayer around gold nanorods with a thickness that has been estimated to be 3.5 nm [32] while Oligomer-1 is only 1.5 nm. Thus, the shorter length of Oligomer-1 and the lower zeta potential of the rods after replacement with Oligomer-1 accounts

for why the surface modification with Oligomer-1 failed to stabilize the gold nanorod. Therefore, another means of stabilization was needed.

3.3.1.2 Second Generation of Oligomers

As a second approach, Prof. Santos' group synthesized a new oligomer called Oligomer-2 which is similar to that of Oligomer-1 except it is longer as shown in **Figure 3.20**.

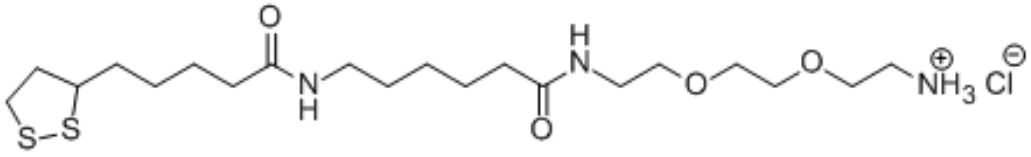

Figure 3.20 Molecular structure of Oligomer-2

Oligomer-2 is 2.5 nm which is 1 nm longer than Oligomer-1. The head and tail groups in this oligomer are the same as the previous version. Oligomer-1 was totally water soluble while Oligomer-2 was only partially water soluble which make replacement of the CTAB with Oligomer-2 more difficult. We found out that Oligomer-2 is soluble in methanol. Therefore we modified the replacement procedure. Instead of adding Oligomer-2 dissolved in water to the gold nanorod suspension, we first dissolved Oligomer-2 in methanol and added that to aqueous gold nanorod suspensions. The washing procedure was exactly the same as with Oligomer-1. However, the final result was very different. Oligomer-2 coated gold nanorods were stable against washing up to two successive washings. They were stable in DI water for slightly more than 24 hours. The zeta potential was + 32 mv for the Oligomer-2 coated gold nanorods while it was +58 mv for the CTAB-coated gold nanorod control sample. All results show that Oligomer-2 is a better choice

due its longer steric barrier formation around gold nanorods. But its poor solubility in water is the main problem here. These experiments show that we a longer version of Oligomer-2 was needed for better stability but, based on the finding with that oligomer, it was thought likely that a longer oligomer might be even less in water. Therefore, increasing the length of the oligomers was not considered to be a good approach and so a different approach was used involving a mixed coating of PEG and a photocleavable oligomer as described next.

3.3.1.3 Mixed Coating Of 5k (MW) Thiol-PEG and Photocleavable Oligomer

The main objective of this project is to do a selective photo-activation chemistry at the tips of gold nanorods. These primary photo-activated sites should be strongly positively charged to enable further chemical or physical attachment to the tips. For example, using negatively charged gold nanospheres of the same diameter, we can form a dumbbell shape assembly of nanoparticles. This dumbbell shape assembly possesses a very unique characteristic which is a very high magnitude of surface plasmon resonance at the gap narrow gap between the nanorod and nanosphere.

A brief review of publication in gold nanorods coatings shows several successful experiments involving mono-thiol PEG (polyethylene glycol) with a molecular weight of 5000 g/mole [76-78], henceforth referred to as "5k mS-PEG". Therefore, we changed strategy about surface coating of gold nanorods and developed a new technique for selective photoactivation surface chemistry. In this technique which is mainly based on our previous experiments, we used a mixed brush of PEG and a photocleavable oligomer instead of using a uniform long brush of photocleavable oligomer. This mixed brush is made up of lipoic acid based photocleavable oligomer synthesized by Prof. Santos' group, henceforth referred to as "LIP3", and 5k mS-PEG.

LIP3 has been extensively studied by Prof. Robinson's group in this project for modifying the surfaces of gold films. Its structure is shown in **Figure 3.21**. LIP3 cleaves when exposed to UV light at 365 nm. Cleavage happens between adjacent N and carboxyl group in the middle of oligomer. It is partially water soluble before cleavage but is totally water soluble after cleavage. After cleavage a short chain of carbon (approximately 1 nm) with a primary amine will be left on the

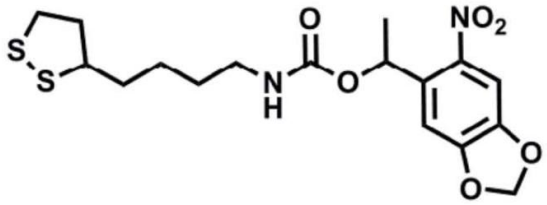

Figure 3.21 Lip3 molecular structure

surface gold nanorods. Our prior experiments suggest that this short chain by itself is not long enough to protect nanorods from aggregation. On the other hand, mixing this oligomer with 5k mS-PEG is problematic because the radius of gyration for 5k PEG is 5.5 nm whereas the total length of LIP3 is only 1 nm. Therefore, a mixed brush of LIP3 and 5k mS-PEG could leave the primary amine resulting from the photocleavage step inaccessible for further chemical or physical treatment after photoactivation. Thus, a different approach was taken to forming a mixed layer of LIP3 and 5k mS-PEG on the gold surface.

According to prior studies on the role of CTAB in the formation of gold nanorods and its capping characteristics, CTAB forms a very dense bilayer only along the side-walls of gold nanorods[19, 32]. **Figure 1.6** suggests that gold nanorods tips are not covered by CTAB and can be easily accessible for further surface chemistry. Based on these results, we developed a new two-step replacement procedure to replace CTAB with a separately located mixed brush. In this approach, first gold nanorods tips are exposed to LIP3 while side walls are protected by a dense bilayer of CTAB. After that the whole system is exposed to 5k mS-PEG solution. Since LIP3

chemically reacts with gold surface, it was hypothesized that 5k mS-PEG would mainly attach to the rod side walls so that the final result would be a gold nanorod covered with LIP3 at the tips and with 5k mS-PEG on the side walls.

3.3.1.3.1 Mixed Brush Replacement Procedure

The mixed brush replacement procedure is described below.

Step 1: Washing

Freshly synthesized gold nanorods were separated from other shapes using the low speed centrifugal technique described earlier in **Section 3.2.6**. Gold nanorods were washed twice using the washing procedure described in **Section 3.3.1**.

Step 2: Suspension of gold nanorods in a 60% water/ 40% ethanol CTAB solution

LIP3 is partially water soluble but is completely soluble in ethanol. On the other hand, CTAB has a very high critical micelle concentration (cmc) in ethanol which is 240 times more than in water. All these data imply that LIP3 replacement cannot be done in water, and CTAB-coated gold nanorods suspension will fail immediately in ethanol. In order to meet both these conditions, it was hypothesized that a mixed water/ethanol solvent could be a good solution. Using trial-and-error, we found that 0.66 mM CTAB in 60% water/40%ethanol is the best mixture to keep washed gold nanorods in suspension. Gold nanorods are stable for 1 day in this solution and it makes LIP3 replacement possible. The ethanol allows LIP3 to reach gold nanorods surface easily without forming micelles.

Besides, excess CTAB concentration in the solution assures that side walls are protected by CTAB and only tips are accessible for LIP3 attachment.

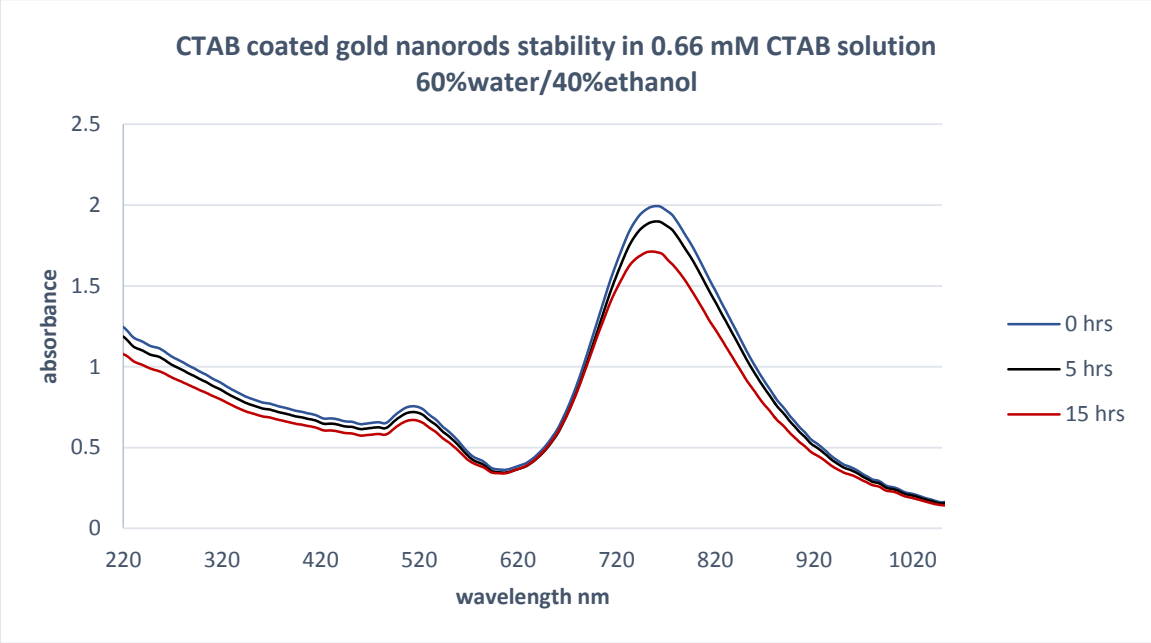

Figure 3.22 UV-Vis absorbance graphs of CTAB coated gold nanorods stability in 0.66 mM CTAB solution 60%water/40%ethanol in different times

Figure 3.22 shows a stability study on CTAB-coated gold nanorods in such a solution. After 15 hours, about 85% of gold nanorods were still in suspension and no significant aggregation could be observed. Having gold nanorods in suspension is a necessity for LIP3 replacement on the surface of gold nanorods.

Step 3: LIP3 addition

A 2 mM LIP3 solution was added to the washed and resuspended gold nanorods in 0.66 mM CTAB 60%water/40%ethanol solution. The LIP3 concentration in the mixture was 0.2 mM. The mixture was bath sonicated for 10 seconds and left undisturbed for 15 hours at room temperature. LIP3 is highly light sensitive and thus all these procedures were done in the dark.

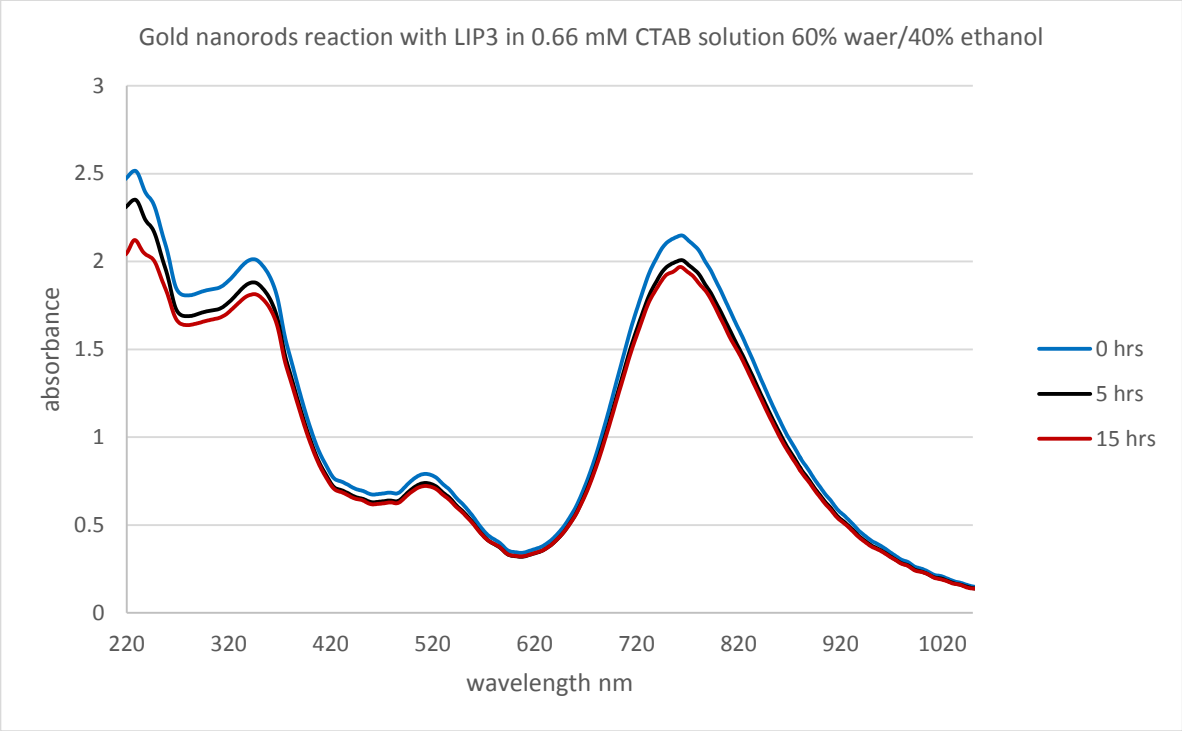

Figure 3.23 UV-Vis absorbance graphs of Gold nanorod's reaction with LIP3 in 0.66 mM CTAB solution 60%water/40%ethanol in different times

Figure 3.23 shows how LIP3 reacts with the gold nanorod surface versus time. In this figure an absorbance peak was observed at 350 nm which specifically belongs to LIP3. Interestingly, only LIP3 in solution shows this peak while reacted LIP3 on gold surface shows no peak. Thus, changes in this peak can be directly related to LIP3 concentration changes in the mixture. As **Figure 3.23** shows, the height of the absorbance peak at 350 nm decreases with time which demonstrates LIP3 is reacting with the gold surface and leaving the solution. Most of the LIP3 reaction with gold surface happens within the first 5 hours and the apparent rate of reaction decreases with time after that.

Step 4: 5k mS-PEG addition

A 2 mM 5k mS-PEG solution was added to the mixture. The PEG concentration in the mixture was 0.2 mM. The mixture was bath sonicated for 10 seconds and left undisturbed for 30 hours.

The 5k mS-PEG reaction with LIP3 coated gold nanorods is shown in **Figure 3.24**. After 30 hours gold nanorods were still stable in solution and no aggregation was observed. Bath sonication shows no significant difference in UV-Vis absorbance of gold nanorods, which shows good stability of gold nanorods after total 45 hours reaction with LIP3 and 5k mS-PEG. A drop in the absorbance peak at 350 nm can be seen after 30 hours which proves that LIP3 is still reacting with surface even in presence of 5k mS-PEG.

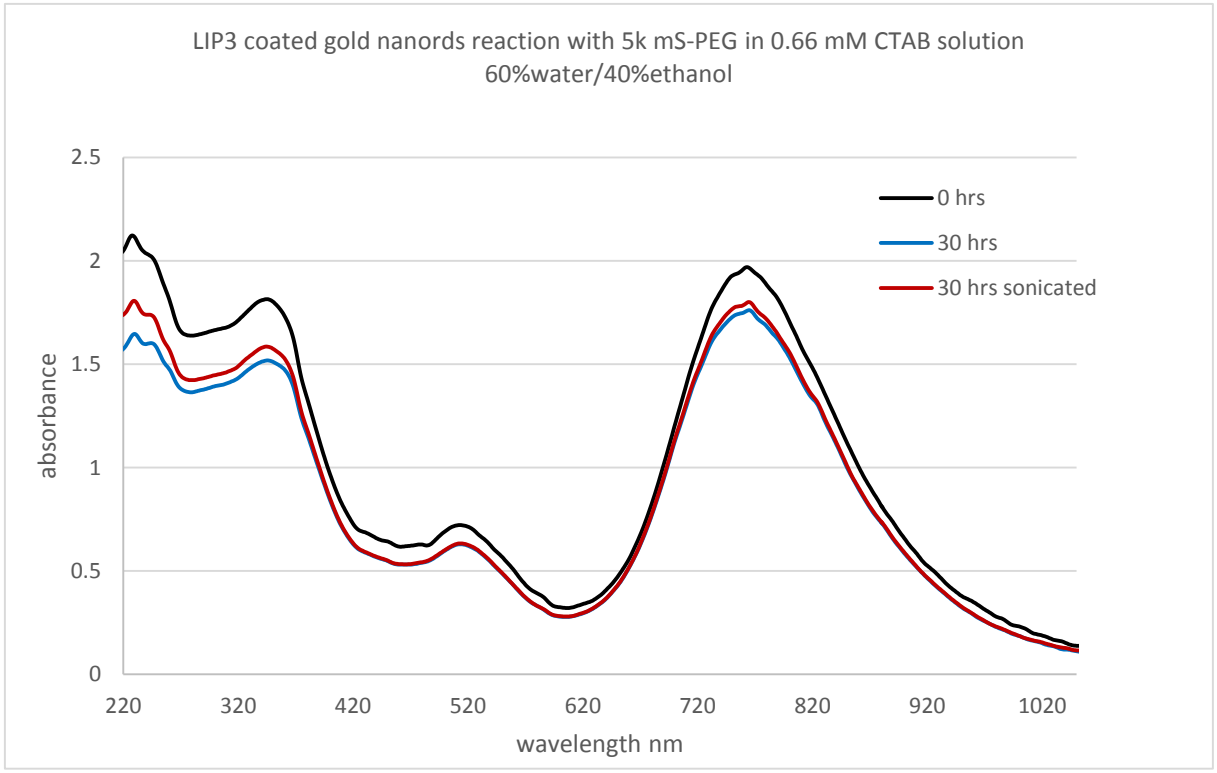

Figure 3.24 UV-Vis absorbance graphs of LIP3 coated gold nanorods reaction with 5k mS-PEG in 0.66 mM CTAB solution 60%water/40%ethanol in different times

Step 5: Washing

Mixed brush coated gold nanorods were washed twice using the same washing procedure in step 1. Instead of using DI water to resuspend gold nanorods, a mixed solvent of 60%water/40%ethanol was used.

The effect of two washings on the stability of LIP3-PEG and PEG-only coated gold nanorods (Control 1) is shown in **Figure 3.25**. Unfortunately, during the washing procedure, some PEG-coated gold nanorods were lost. The difference in height of longitudinal peaks in both graphs is approximately proportional to the amount of lost Pegylated gold nanorods. The wavelengths of the longitudinal peaks in both graphs were different which implies that PEG-coated gold nanorods and LIP3-PEG coated gold nanorods have different aspect ratios. PEG coated gold nanorods have slightly smaller longitudinal peak wavelengths and consequently a slightly lower aspect ratio.

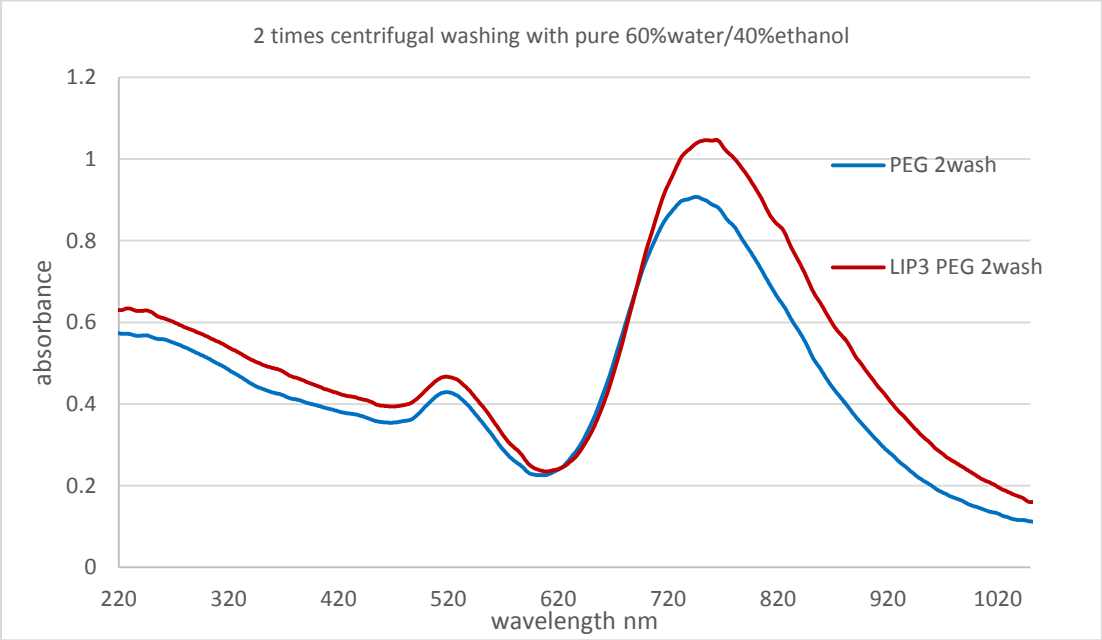

Figure 3.25 UV-VIS absorbance graphs of PEG coated gold nanorods and LIP3-PEG coated gold nanorods after 2 times washing with pure centrifugal washing with pure 60%water/40%ethanol

Step6: Photoactivation

A suspension of mixed brush coated gold nanorods was transferred to a crystallization disk and placed in a UV cross linker where they were exposed to UV light at 360 nm for 30 min.

To investigate this two-step replacement photo activation technique, two separate gold nanorod suspension controls were used.

a. Control 1: PEG coated gold nanorods - Only step 3 (LIP3 addition) is skipped for this control gold nanorods suspension (**Figure 3.26**)

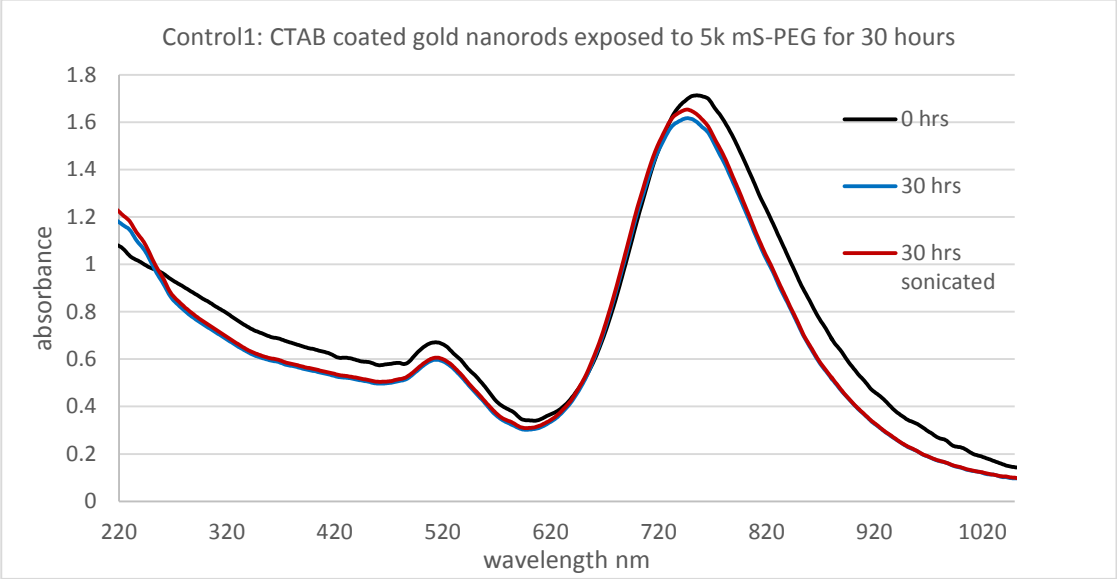

Figure 3.26 UV-Vis absorbance graphs of Control 1, PEG reaction with surface of CTAB coated gold nanorods suspended in 0.66 mM CTAB solution 60%water/40%ethanol in different times

b. Control 2: LIP3/PEG coated gold nanorods unexposed to UV - Only step 6 (UV photo activation) is skipped for this control gold nanorods suspension

Both controls were subjected to the same procedures used to process the other suspensions.

Step7: Washing

The UV exposed LIP3-PEG coated gold nanorods, unexposed LIP3-PEG coated gold nanorods (control 2), and the PEG coated gold nanorods (control 1) were washed twice using the same procedure described in step1 using DI water. **Figure 3.27** shows how the washing procedure affects the suspensions of gold nanorods. All three samples (UV exposed LIP3-PEG coating, unexposed LIP3-PEG coating, and PEG coating) of gold nanorods show a good stability against centrifugal washings with DI water. Unfortunately, both controls (unexposed LIP3-PEG coated, and PEG coated) have a high affinity to the side walls of the centrifugal tubes and during the second washing we lost ~50% of the nanoparticles.

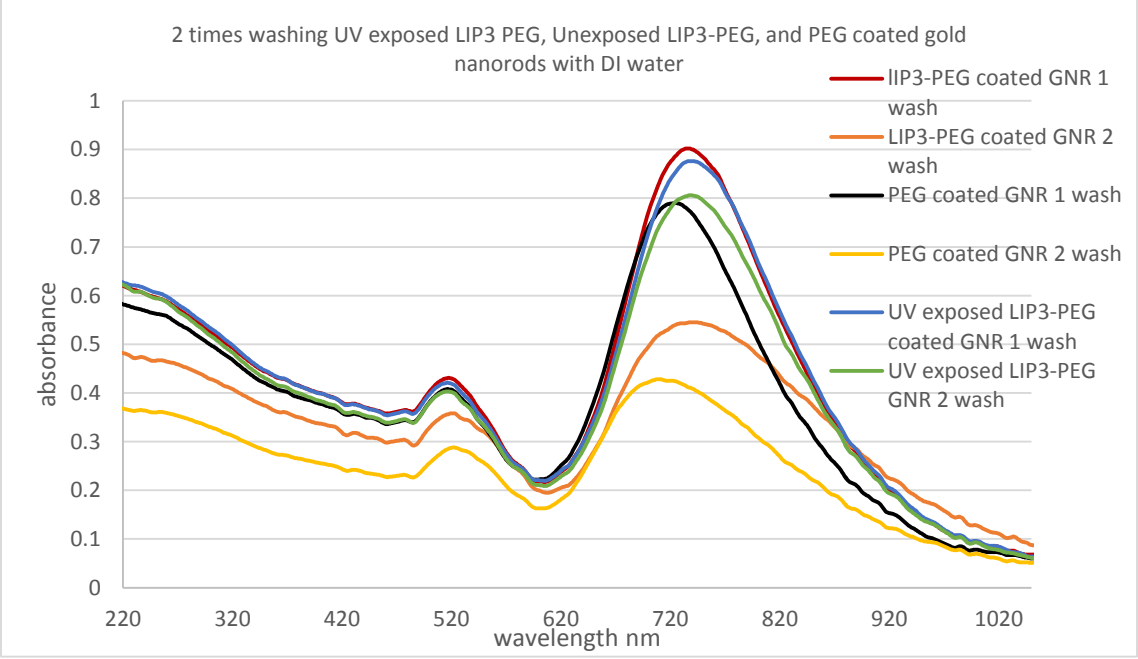

Figure 3.27 UV-Vis absorbance graphs of UV exposed LIP3-PEG, Unexposed LIP#-PEG, and PEG coated gold nanorods centrifugal washing with DI water

3.3.1.3.2 Zeta Potential Measurements

Zeta potential measurements for photoactivated LIP3-PEG coated gold nanorods, and both controls are shown in **Table 3.3**. All measurement were done after step 7 (two times washings of gold nanorods).

Table 3.3. Zeta potential values of gold nanorods (GNR) with different coatings measured in different liquid phases.

Zeta potential values	**mv**
3 Washed CTAB GNR	+58
PEG coated GNR (control1 in DI water)	+3
Unexposed LIP3-PEG GNR (control2 in DI water)	+1
UV exposed LIP3-PEG GNR (DI water)	+23
PEG coated GNR (control1 in 0.001 NaCl)	+1
Unexposed LIP3-PEG GNR (control2 in 0.001 NaCl)	+0.5
UV exposed LIP3-PEG GNR (0.001 NaCl)	+13.5

The Smoluchowski approximation was used to calculate the final value of the zeta potential based on the measured electrophoretic mobilities. According to the literature, there is not a fixed value of Henry's function in Henry's equation for measuring zeta potential. The Smoluchowski approximation uses 1.5 for Henry's constant while the Huckel approximation uses 1.0 [82]. We estimate the more realistic value for this constant is between 1.3-1.4. In this project we are only interested in zeta potential changes trend through different surface modifications on gold nanorods. Thus, the Smoluchwski approximation values were considered acceptable for assessing the effects of different surface modification.

The zeta potential values in **Table 3.3** for both controls (PEG coated GNR's and Unexposed LIP3-PEG coated GNR's) are close to zero. Based on these values, we believe that PEG and LIP3 have mostly replaced CTAB on surface of gold nanorods. PEG and inactivated LIP3 have no charged groups and, therefore, the stability of the Control 1 and Control 2 samples are mainly due to a steric barrier formed around the nanorods. The zeta potential value for UV exposed LIP3-PEG gold nanorods was +23 mv while the value for UV unexposed LIP3-PEG gold nanorods (Control 2) was +1 mv. We believe this significant difference is due to UV cleavage of LIP3 oligomer during UV photo activation. The following conclusions can be derived from the Zeta potential measurements:

a. CTAB was efficiently replaced by the thiol-EG polymers and oligomers.
b. UV photoactivation of LIP3 oligomers on the surface of gold nanorods was successfully achieved.
c. The very low zeta potential of the Control 1 and Control 2 samples implies that the stability of surface modified gold nanorods is due to steric barrier characteristic of 5k mS-PEG polymer.

3.4 Addition of Gold Nanospheres Suspension to Gold Nanorods Suspension

In the previous section, we showed results suggesting that LIP3 UV photoactivation on surface of gold nanorods successfully happened. In this section, we further investigated if this 2-step replacement procedure actually occurred as we supposed, i.e. if selective attachment of amine functional groups at the tips actually occurred. During the CTAB replacement procedure, we hypothesized that CTAB formed a dense bilayer around the side walls of gold nanorods while leaving the tips only lightly coated. We hypothesized that adding a suitable amount of LIP3 to CTAB coated gold nanorods led to selective adsorption of LIP3 to the tips of the nanorods. Since

the side walls were covered with positively charged CTAB, attachment of neutral semi-hydrophobic LIP3 oligomer to side walls was believed to be negligible. We further hypothesized that adding 5k mS-PEG to the mixture would result in attachment of the PEG to the CTAB-coated side walls while relatively little PEG would attach to the tips that were already coated with LIP3. Our hypothesis was that the final structure would be a gold nanorod whose tips were coated mainly by LIP3 and its side walls by PEG.

In order this hypothesis, we exposed positively charged UV photo activated gold nanorods to negatively charged citric coated gold nanospheres. If the nanospheres selectively attach to the tips of the gold nanorods, then our hypothesis would be proven. On the other hand if this attachment occurred randomly all over the gold nanorod surface, then it would suggest that LIP3 and PEG formed a more homogeneous coating on the nanorods.

Negatively charged citric coated gold nanospheres were synthesized using the Turkevich method [15] by Professor Robinson's research group. The intensity-average size distribution for these gold nanospheres by DLS (dynamic light scattering) shows a hydrodynamic diameter of 21 nm. The zeta potential value for the synthesized gold nanospheres was -41 mv. **Figure 3.28** shows the UV-Vis absorbance graph of the nanospheres. Unlike gold nanorods, nanospheres just have one absorbance peak and this peak happens in the range of 520-540 nm, depending on the size of gold nanospheres. Here, the transverse peak was located at 520 nm which is consistent with the nanosphere size.

Since we did not have an accurate, direct measurement of the number concentration of gold nanorods in suspension, we express concentration in terms of the elemental gold concentrations which was is approximately 27 mg/liter. Therefore, the gold nanosphere suspension was diluted to form a suspension with the same 27 mg/liter elemental gold concentration. The gold nanorods

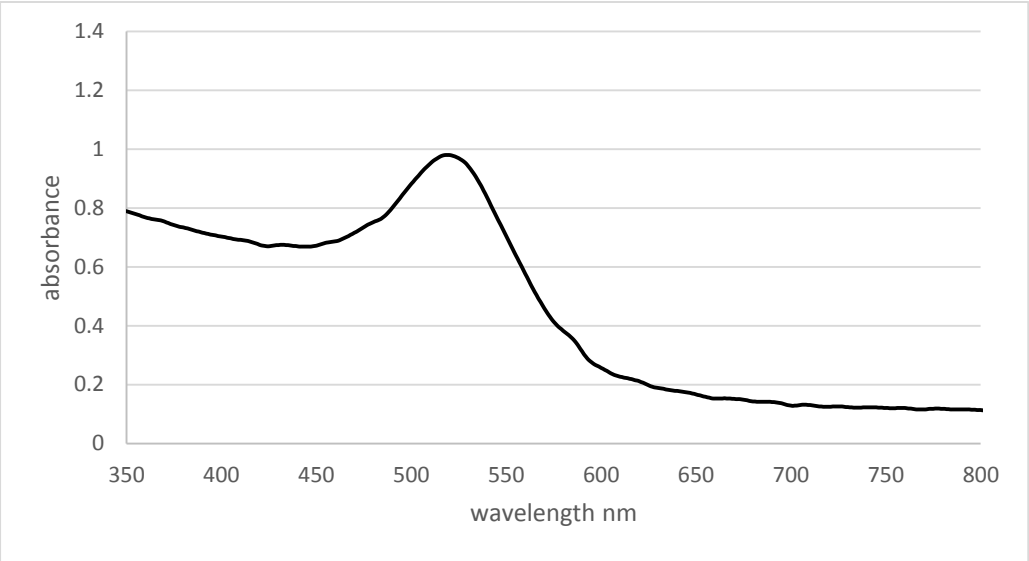

Figure 3.28 UV-Vis absorbance graph of citrate coated gold nanospheres

were mixed with the nanospheres in a 1mm wide quartz cuvette so that we could investigate attachment using UV-Vis absorbance spectrometry.

3.4.1 UV Unexposed PEG Coated Gold Nanorods (Control 1) and Citrate Coated Gold Nanospheres

Figure 3.29 shows the UV-Vis absorbance graphs of the Control 1 and citrate coated gold nanospheres at different times after mixing.

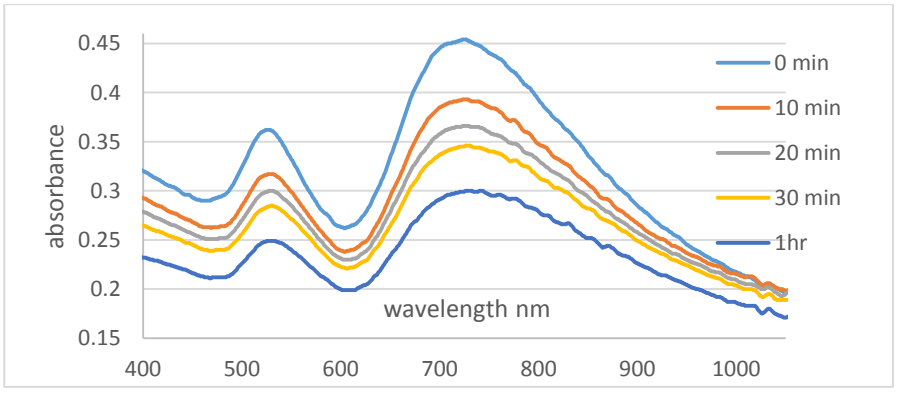

Figure 3.29 UV-Vis absorbance graphs of time stability study of PEG coated gold nanorods (control1) interaction with citrate coated gold nanospheres

PEG coated gold nanorods are well protected by PEG steric barrier around them while highly negatively charged citrate coated gold nanospheres are stable due to charge repulsion. After 1 hour still the place of both transverse and longitudinal peaks are fixed (not shifted) which indicates no regular assembly of nanoparticles has happened. Approximately 50% of gold nanorods have interacted with gold nanospheres after one hour. These aggregates leave the suspension as sediments.

TEM images were of the mixed suspensions of PEG-coated gold nanorods and citrate coated gold nanospheres. Ideally, cryo-TEM involving rapidly freezing the samples would have been best for characterizing these structures but that was not available. Preparing samples for conventional TEM and SEM images requires that the nanoparticles be deposited on top of a grid or substrate using the drop cast technique which often results in the formation of aggregates on the substrate as an artifact. **Figure 3.30** and **Figure 3.31** show how citrate-coated gold nanospheres attach all over PEG-coated gold nanorods. **Figure 3.32** shows a bigger area of the grid at a lower magnification in which considerable aggregation of the nanoparticles can be seen. However, individual gold nanorods and nanospheres can be seen in this image. PEG coated gold nanorods and citrate coated gold nanospheres follow no specific trend in attaching to each other.

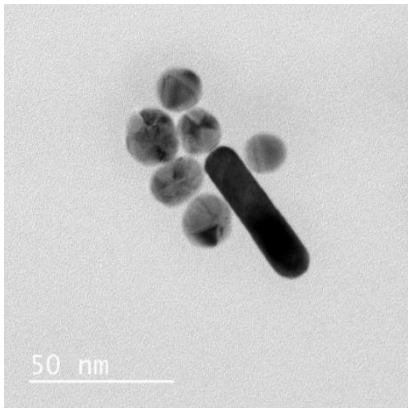

Figure 3.30 TEM image of PEG coated gold nanorod + citrate coated gold nanospheres

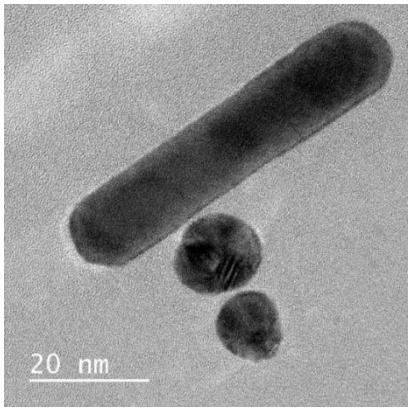

Figure 3.31 TEM image of PEG coated gold nanorads + citrate coated gold nanospheres

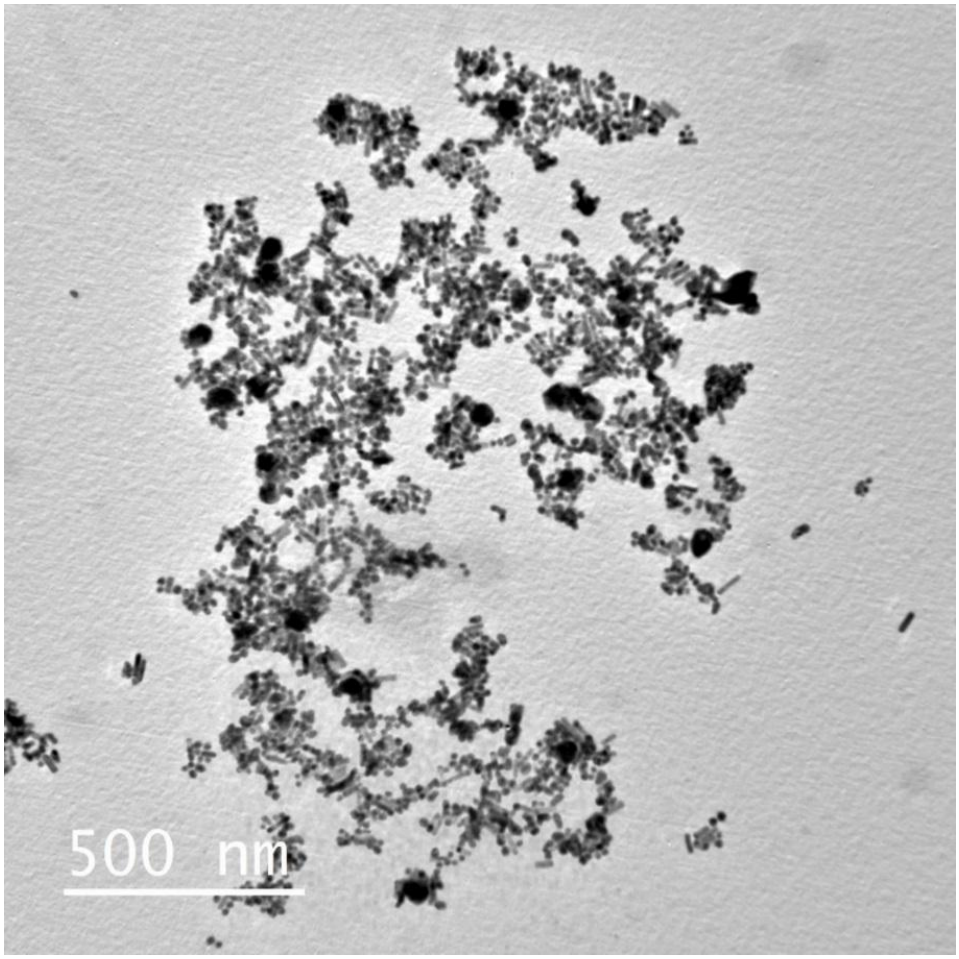

Figure 3.32 TEM image of PEG coated gold nanorod + citrate coated gold nanospheres

3.4.2 UV Unexposed LIP3-PEG Coated Gold Nanorods (Control 2) and Citrate Coated Gold Nanospheres

The results for the Control 2 sample were similar to those for Control 1. **Figure 3.33** shows how UV unexposed LIP3-PEG coated gold nanorods and citrate coated gold nanospheres interacted with each.

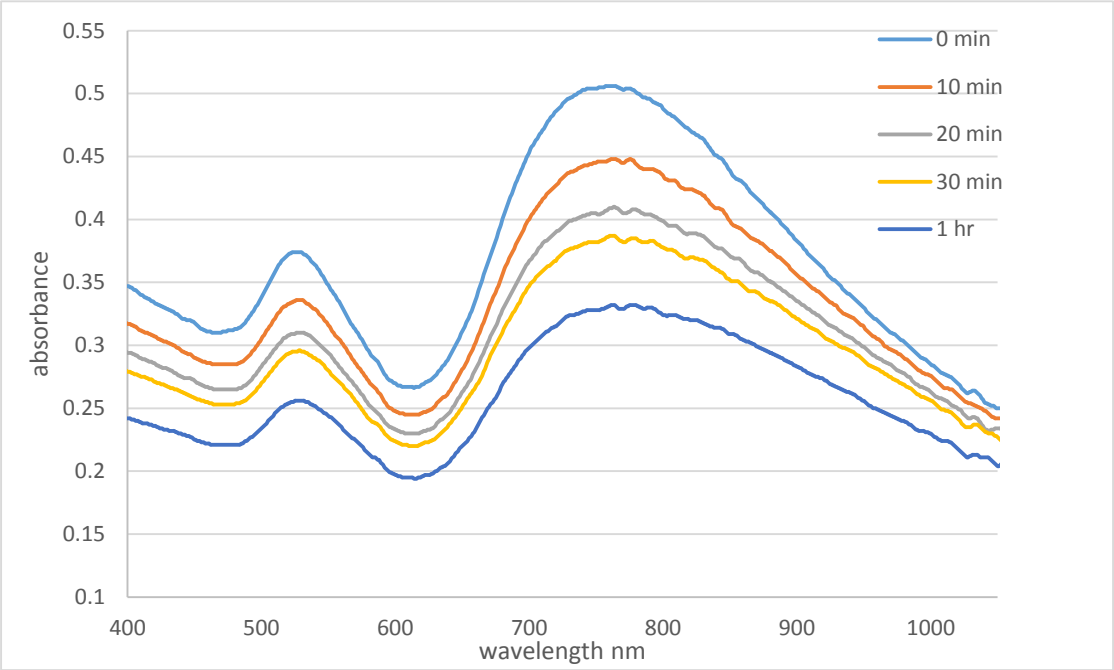

Figure 3.33 UV-Vis absorbance graphs of UV unexposed LIP3-PEG coated gold nanorods and citrate coated gold nanospheres in different times

Interestingly, Control 2 and Control 1 show the same behavior when interacting with citrate coated gold nanospheres. Transverse and longitudinal peaks remain in the same place (no shifting). The trend of aggregation in Control 2 is similar to that in Control 1 according to the UV-Vis absorbance graphs. After 1 hour, about 50% of the gold nanorods aggregated and sedimented. The following TEM images in **Figure 3.34**, **Figure 3.35**, **Figure 3.36** and **Figure 3.37** show how

Control 2 UV unexposed LIP3-PEG coated gold nanorods interacted with citrate coated gold nanospheres. Control 2 behaves very much like the Control 1 samples. It is interesting to note that the negatively charged gold nanospheres seem to prefer side walls rather than tips of gold nanorods. In PEG coated gold nanorods, no specific trend could be noticed while, in UV unexposed LIP3-PEG sample, a biased affinity to stick to side walls could be observed. The only difference between Control 1 and Control 2 is that in Control 2, the tips of the nanorods were coated with LIP3.

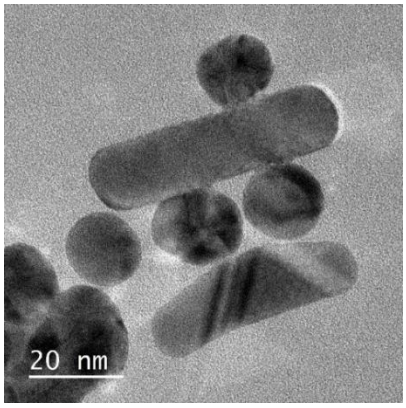

Figure 3.34 TEM image of UV unexposed LIP3-PEG coated gold nanorods and citrate coated gold nanospheres

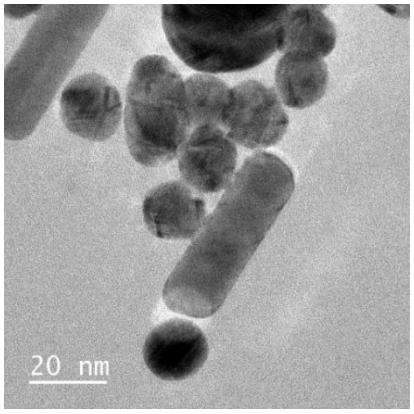

Figure 3.35 TEM image of UV unexposed LIP3-PEG coated gold nanorods and citrate coated gold nanospheres

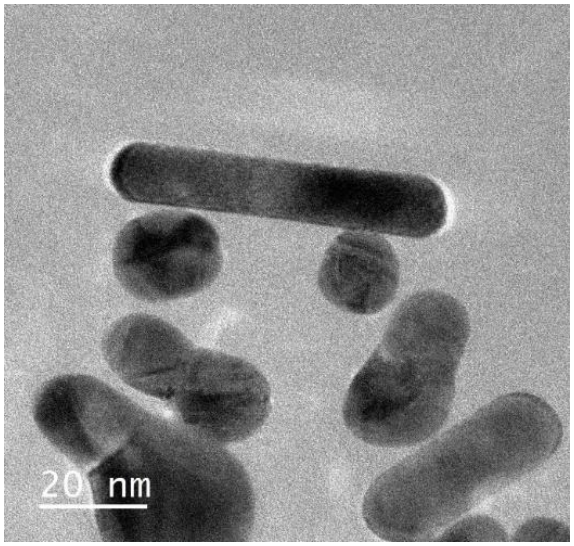

Figure 3.36 TEM image of UV unexposed LIP3-PEG coated gold nanorods and citrate coated gold nanospheres

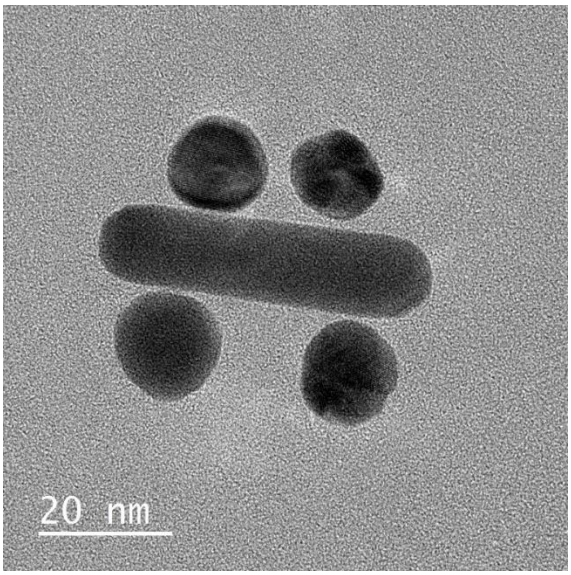

Figure 3.37 TEM image of UV unexposed LIP3-PEG coated gold nanorods and citrate coated gold nanospheres

3.4.3 UV Exposed LIP3-PEG Coated Gold Nanorods and Citrate Coated Gold Nanospheres

The same procedure that was used for the Control 1 and Control 2 samples was followed for the UV exposed LIP3-PEG coated gold nanorods and citrate coated gold nanospheres. **Figure 3.38** shows how these nanoparticles interacted with each other as a function of time.

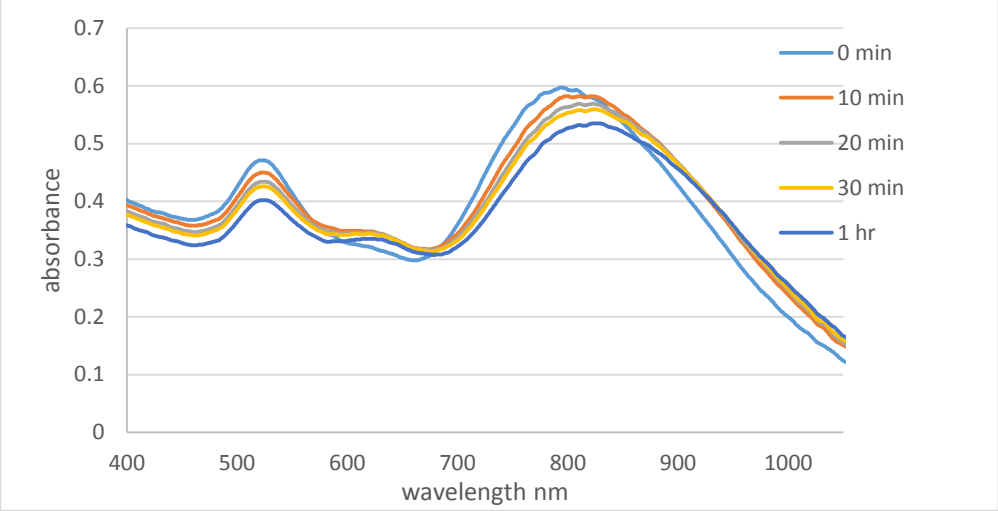

Figure 3.38 UV-Vis absorbance graphs of UV exposed LIP3-PEG gold nanorods and citrate coated gold nanospheres versus time

The UV-Vis absorbance graphs of UV exposed LIP3-PEG coated gold nanorod and gold nanospheres were very different from those of Control 1 and Control 2 where the peaks location was fixed with time. For the UV exposed sample, the wavelength of the longitudinal peak shifts to longer wavelengths (red shifts) as time increases. In addition, a third peak at 640 nm appears which was not present in Control 1 and Control 2. This time-dependent blue shifting of the longitudinal peak occurs because the total aspect ratio of the assembly of gold nanorods and nanospheres is increasing with time. The most plausible explanation is that gold nanospheres are sticking to the tips of the gold nanorods more than to the side walls. Therefore as time goes on, more gold nanospheres attach to the tips of gold nanorods to form dumbbell-shaped assemblies.

This dumbbell shape assembly has a higher aspect ratio and consequently a longitudinal absorbance peak at longer wavelengths.

We believe that the third absorbance peak at 640 nm represents nanoparticle assemblies which have a lower aspect ratio than those of the original synthesized gold nanorods. It is likely that these assemblies consist of gold nanospheres attached to side walls of the gold nanorods which decreases the aspect ratio. The height of the third peak is very small in comparison to that of the longitudinal peak which can be interpreted as a relatively low concentration of these low aspect ratio assemblies in comparison with that of the dumbbell shape assemblies.

The TEM images in **Figure 3.39**, **Figure 3.40**, **Figure 3.41**, **Figure 3.42** and **Figure 3.43** are consistent with the results from the UV-Vis absorbance measurements. According to these TEM images, negatively charged gold nanospheres strongly prefer to bind to the tips of the gold nanorods compared to the side walls. This strongly suggests that most of positive charge distribution is located at the tips where, according to our hypothesis, LIP3 has the highest concentration. Higher adsorption of LIP3 at the tips results in a high density of amine groups at the tips after UV photo activation. Meanwhile, the side walls are covered primarily with 5k PEG that forms a steric barrier against aggregation.

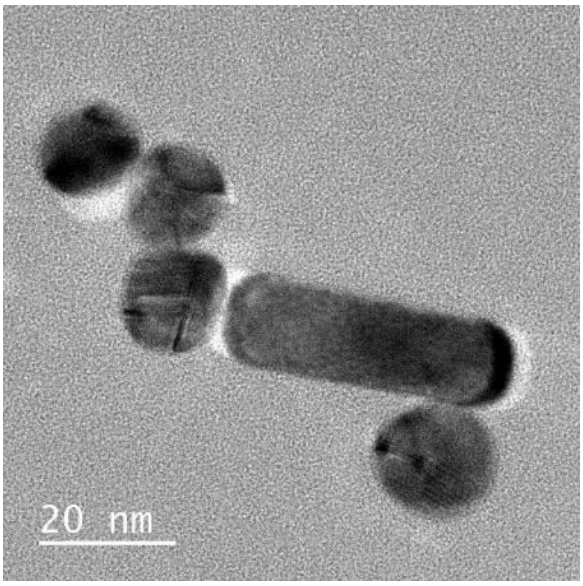

Figure 3.39 TEM image of UV exposed LIP3-PEG coated gold nanorods and citrate coated gold nanospheres

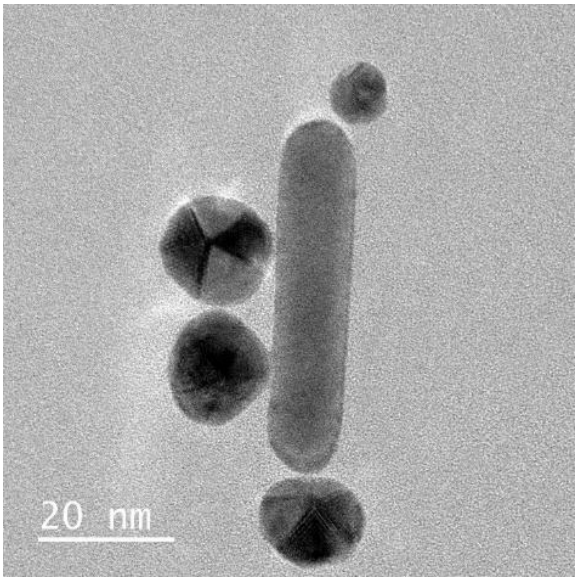

Figure 3.40 TEM image of UV exposed LIP3-PEG coated gold nanorods and citrate coated gold nanospheres

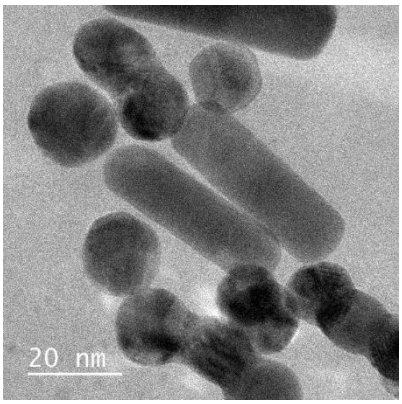

Figure 3.41 TEM image of UV exposed LIP3-PEG coated gold nanorods and citrate coated gold nanospheres

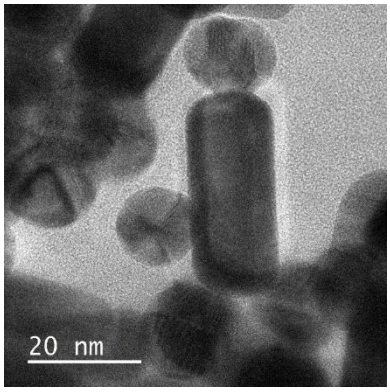

Figure 3.42 TEM image of UV exposed LIP3-PEG coated gold nanorods and citrate coated gold nanospheres

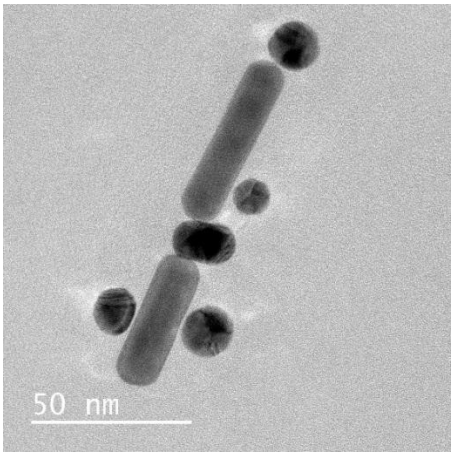

Figure 3.43 TEM image of UV exposed LIP3-PEG coated gold nanorods and citrate coated gold nanospheres

In summary, all three characterization techniques (zeta potential measurements, UV-Vis absorbance, and TEM images) suggest that the 2-step CTAB replacement technique results in selective attachment of LIP3 at the tips of gold nanorods while the side walls were then coated with 5k PEG. Photoactivation of the LIP3 finally results in a stable suspension of gold nanorods with amine groups preferentially located on the tips.

Chapter 4: Achievements and Future Work

4.1 Achievements

The main achievements in this work are summarized below:

1. Gold nanorods were successfully synthesized based on the seed-mediated growth method.
2. The gold nanorod aspect ratio was tuned by varying added amounts of silver nitrate.
3. A low speed centrifugal separation technique was introduced to efficiently separate gold nanorods from other shapes in suspension.
4. Different generations of surface-active, photocleavable oligomers were synthesized and applied on the surfaces of gold nanorods to replace CTAB.
5. A new 2-step coating replacement technique was introduced to selectively replace CTAB with coatings of a photocleavable oligomer at the nanorod tips and PEG on the side walls.
6. Selective UV photo activation was done at the tips of gold nanorods while nanoparticles were in suspension.
7. Dumbbell-shaped assemblies of gold nanorods and gold nanospheres were formed in suspension by exposing the tip-activated gold nanorods to oppositely charged gold nanospheres.

4.2 Future Work

In future work, the following is recommended:

1. New generations of photo cleavable oligomer should be synthesized to achieve even better functionalization based on results achieved in this work.
2. Different compositions of ethanol/water mixed solvents should be studied to optimize the coating replacement procedure.
3. The reaction times of the oligomer and PEG on the gold nanorod surface should studied further. This could be done using flat gold surfaces and a surface sensitive spectroscopic technique such as FTIR or XPS.
4. The final composition and surface density of the mixed coatings should be quantitated using thermogravimetric analysis, XPS, and FTIR to accurate measure the organic content of the samples.

5. Since only one UV exposure time was used in these experiments, the effect of varying the UV exposure time on photo activation efficiency and final zeta potential values should be studied.

References

1. Kuchibhatla, S.V., et al., *One dimensional nanostructured materials.* Progress in materials science, 2007. **52**(5): p. 699-913.
2. Suryanarayana, C., *The structure and properties of nanocrystalline materials: Issues and concerns.* JOM Journal of the Minerals, Metals and Materials Society, 2002. **54**(9): p. 24-27.
3. Suryanarayana, C., *Nanocrystalline materials.* International Materials Reviews, 1995. **40**(2): p. 41-64.
4. Suryanarayana, C., *Recent developments in nanostructured materials.* Advanced Engineering Materials, 2005. **7**(11): p. 983-992.
5. Gleiter, H., *Nanocrystalline solids.* Journal of applied crystallography, 1991. **24**(2): p. 79-90.
6. Daniel, M.-C. and D. Astruc, *Gold nanoparticles: assembly, supramolecular chemistry, quantum-size-related properties, and applications toward biology, catalysis, and nanotechnology.* Chemical reviews, 2004. **104**(1): p. 293-346.
7. Boisselier, E. and D. Astruc, *Gold nanoparticles in nanomedicine: preparations, imaging, diagnostics, therapies and toxicity.* Chemical Society Reviews, 2009. **38**(6): p. 1759-1782.
8. Panyam, J. and V. Labhasetwar, *Biodegradable nanoparticles for drug and gene delivery to cells and tissue.* Advanced drug delivery reviews, 2012.
9. Parkin, I.P. and R.G. Palgrave, *Self-cleaning coatings.* Journal of Materials Chemistry, 2005. **15**(17): p. 1689-1695.
10. Becheri, A., et al., *Synthesis and characterization of zinc oxide nanoparticles: application to textiles as UV-absorbers.* Journal of Nanoparticle Research, 2008. **10**(4): p. 679-689.
11. Fan, X., C. Xia, and R.C. Advincula, *Grafting of polymers from clay nanoparticles via in situ free radical surface-initiated polymerization: Monocationic versus bicationic initiators.* Langmuir, 2003. **19**(10): p. 4381-4389.
12. page, p.t.w.; Available from: http://periodictable.com/Elements/079/.
13. web.
14. Faraday, M., *The Bakerian lecture: experimental relations of gold (and other metals) to light.* Philosophical Transactions of the Royal Society of London, 1857. **147**: p. 145-181.
15. Turkevich, J., P.C. Stevenson, and J. Hillier, *A study of the nucleation and growth processes in the synthesis of colloidal gold.* Discussions of the Faraday Society, 1951. **11**: p. 55-75.
16. Enustun, B. and J. Turkevich, *Coagulation of colloidal gold.* Journal of the American chemical society, 1963. **85**(21): p. 3317-3328.
17. Sau, T.K. and C.J. Murphy, *Room temperature, high-yield synthesis of multiple shapes of gold nanoparticles in aqueous solution.* Journal of the American Chemical Society, 2004. **126**(28): p. 8648-8649.
18. Murphy, C.J., et al., *Gold nanorod crystal growth: from seed-mediated synthesis to nanoscale sculpting.* Current Opinion in Colloid & Interface Science, 2011. **16**(2): p. 128-134.
19. Nikoobakht, B. and M.A. El-Sayed, *Preparation and growth mechanism of gold nanorods (NRs) using seed-mediated growth method.* Chemistry of Materials, 2003. **15**(10): p. 1957-1962.

20. Nikoobakht, B., Z. Wang, and M. El-Sayed, *Self-assembly of gold nanorods.* The Journal of Physical Chemistry B, 2000. **104**(36): p. 8635-8640.
21. Busbee, B.D., S.O. Obare, and C.J. Murphy, *An Improved Synthesis of High-Aspect-Ratio Gold Nanorods.* Advanced Materials, 2003. **15**(5): p. 414-416.
22. Johnson, C.J., et al., *Growth and form of gold nanorods prepared by seed-mediated, surfactant-directed synthesis.* Journal of Materials Chemistry, 2002. **12**(6): p. 1765-1770.
23. Kundu, S., et al., *Anisotropic growth of gold clusters to gold nanocubes under UV irradiation.* Nanotechnology, 2007. **18**(7): p. 075712.
24. Huang, C.-J., et al., *Electrochemical synthesis of gold nanocubes.* Materials Letters, 2006. **60**(15): p. 1896-1900.
25. Wang, B., et al., *Novel structures and properties of gold nanowires.* Physical Review Letters, 2001. **86**(10): p. 2046.
26. Kondo, Y. and K. Takayanagi, *Synthesis and characterization of helical multi-shell gold nanowires.* Science, 2000. **289**(5479): p. 606-608.
27. Gao, J., C.M. Bender, and C.J. Murphy, *Dependence of the gold nanorod aspect ratio on the nature of the directing surfactant in aqueous solution.* Langmuir, 2003. **19**(21): p. 9065-9070.
28. Jana, N.R., L. Gearheart, and C.J. Murphy, *Wet chemical synthesis of high aspect ratio cylindrical gold nanorods.* The Journal of Physical Chemistry B, 2001. **105**(19): p. 4065-4067.
29. Jana, N.R., L. Gearheart, and C.J. Murphy, *Seed-mediated growth approach for shape-controlled synthesis of spheroidal and rod-like gold nanoparticles using a surfactant template.* Advanced Materials, 2001. **13**(18): p. 1389.
30. Jana, N.R., L. Gearheart, and C.J. Murphy, *Seeding growth for size control of 5-40 nm diameter gold nanoparticles.* Langmuir, 2001. **17**(22): p. 6782-6786.
31. Jana, N.R., L. Gearheart, and C.J. Murphy, *Evidence for seed-mediated nucleation in the chemical reduction of gold salts to gold nanoparticles.* Chemistry of Materials, 2001. **13**(7): p. 2313-2322.
32. Nikoobakht, B. and M.A. El-Sayed, *Evidence for bilayer assembly of cationic surfactants on the surface of gold nanorods.* Langmuir, 2001. **17**(20): p. 6368-6374.
33. Bouhelier, A., et al., *Surface plasmon characteristics of tunable photoluminescence in single gold nanorods.* Physical review letters, 2005. **95**(26): p. 267405.
34. Losic, D., et al., *Fabrication of gold nanorod arrays by templating from porous alumina.* Nanotechnology, 2005. **16**(10): p. 2275.
35. Siedentopf, H. and R. Zsigmondy, *Uber sichtbarmachung und größenbestimmung ultramikoskopischer teilchen, mit besonderer anwendung auf goldrubingläser.* Annalen der Physik, 1902. **315**(1): p. 1-39.
36. Zsigmondy, R., *Colloids and the Ultra Microscope.* Journal of the American Chemical Society, 1909. **31**(8): p. 951-952.
37. Svedberg, T. and K.O. Pedersen, *The Ultracentrifuge.* The Ultracentrifuge., 1940.
38. Svedberg, T. and H. Rinde, *THE DETERMINATION OF THE DISTRIBUTION OF SIZE OF PARTICLES IN DISPERSE SYSTEMS1.* Journal of the American Chemical Society, 1923. **45**(4): p. 943-954.
39. Svedberg, T. and H. Rinde, *The ultra-centrifuge, a new instrument for the determination of size and distribution of size of particle in amicroscopic colloids.* Journal of the American Chemical Society, 1924. **46**(12): p. 2677-2693.

40. Mie, G., *Contributions to the optics of turbid media, particularly of colloidal metal solutions.* Contributions to the optics of turbid media, particularly of colloidal metal solutions Transl. into ENGLISH from Ann. Phys.(Leipzig), v. 25, no. 3, 1908 p 377-445, 1976. **1**: p. 377-445.
41. Sinclair, D., *Light scattering by spherical particles.* JOSA, 1947. **37**(6): p. 475-479.
42. Brust, M., et al., *Synthesis and reactions of functionalised gold nanoparticles.* J. Chem. Soc., Chem. Commun., 1995(16): p. 1655-1656.
43. Brust, M., et al., *Synthesis of thiol-derivatised gold nanoparticles in a two-phase liquid–liquid system.* J. Chem. Soc., Chem. Commun., 1994(7): p. 801-802.
44. Sharma, V., K. Park, and M. Srinivasarao, *Colloidal dispersion of gold nanorods: Historical background, optical properties, seed-mediated synthesis, shape separation and self-assembly.* Materials Science and Engineering: R: Reports, 2009. **65**(1): p. 1-38.
45. Leff, D.V., L. Brandt, and J.R. Heath, *Synthesis and characterization of hydrophobic, organically-soluble gold nanocrystals functionalized with primary amines.* Langmuir, 1996. **12**(20): p. 4723-4730.
46. Weare, W.W., et al., *Improved synthesis of small (d core≈ 1.5 nm) phosphine-stabilized gold nanoparticles.* Journal of the American Chemical Society, 2000. **122**(51): p. 12890-12891.
47. Hiramatsu, H. and F.E. Osterloh, *A simple large-scale synthesis of nearly monodisperse gold and silver nanoparticles with adjustable sizes and with exchangeable surfactants.* Chemistry of Materials, 2004. **16**(13): p. 2509-2511.
48. Esumi, K., et al., *Preparation of gold colloids with UV irradiation using dendrimers as stabilizer.* Langmuir, 1998. **14**(12): p. 3157-3159.
49. Garcia, M.E., L.A. Baker, and R.M. Crooks, *Preparation and characterization of dendrimer-gold colloid nanocomposites.* Analytical chemistry, 1999. **71**(1): p. 256-258.
50. Manna, A., et al., *Synthesis of dendrimer-passivated noble metal nanoparticles in a polar medium: comparison of size between silver and gold particles.* Chemistry of materials, 2001. **13**(5): p. 1674-1681.
51. Kim, F., et al., *Platonic gold nanocrystals.* Angewandte Chemie, 2004. **116**(28): p. 3759-3763.
52. Sakai, T. and P. Alexandridis, *Mechanism of gold metal ion reduction, nanoparticle growth and size control in aqueous amphiphilic block copolymer solutions at ambient conditions.* The Journal of Physical Chemistry B, 2005. **109**(16): p. 7766-7777.
53. cytodiagnostics. Available from: http://www.cytodiagnostics.com/gold_nanoparticle_properties.php.
54. Hornyak, G.L., C.J. Patrissi, and C.R. Martin, *Fabrication, characterization, and optical properties of gold nanoparticle/porous alumina composites: the nonscattering Maxwell-Garnett limit.* The Journal of Physical Chemistry B, 1997. **101**(9): p. 1548-1555.
55. Perez-Juste, J., et al., *Gold nanorods: synthesis, characterization and applications.* Coordination Chemistry Reviews, 2005. **249**(17): p. 1870-1901.
56. Yu, Y.-Y., et al., *Gold nanorods: electrochemical synthesis and optical properties.* The Journal of Physical Chemistry B, 1997. **101**(34): p. 6661-6664.
57. Törnblom, M. and U. Henriksson, *Effect of solubilization of aliphatic hydrocarbons on size and shape of rodlike C16TABr micelles studied by 2H NMR relaxation.* The Journal of Physical Chemistry B, 1997. **101**(31): p. 6028-6035.

58. Chang, S.-S., et al., *The shape transition of gold nanorods.* Langmuir, 1999. **15**(3): p. 701-709.
59. Brown, K.R., D.G. Walter, and M.J. Natan, *Seeding of colloidal Au nanoparticle solutions. 2. Improved control of particle size and shape.* Chemistry of Materials, 2000. **12**(2): p. 306-313.
60. Wang, Z., et al., *Crystallographic facets and shapes of gold nanorods of different aspect ratios.* Surface science, 1999. **440**(1): p. L809-L814.
61. Murphy, C.J., et al., *Anisotropic metal nanoparticles: synthesis, assembly, and optical applications.* The Journal of Physical Chemistry B, 2005. **109**(29): p. 13857-13870.
62. Link, S. and M.A. El-Sayed, *Spectral properties and relaxation dynamics of surface plasmon electronic oscillations in gold and silver nanodots and nanorods.* The Journal of Physical Chemistry B, 1999. **103**(40): p. 8410-8426.
63. Henglein, A., *Physicochemical properties of small metal particles in solution:" microelectrode" reactions, chemisorption, composite metal particles, and the atom-to-metal transition.* The Journal of Physical Chemistry, 1993. **97**(21): p. 5457-5471.
64. Henglein, A., *Small-particle research: physicochemical properties of extremely small colloidal metal and semiconductor particles.* Chemical Reviews, 1989. **89**(8): p. 1861-1873.
65. Bohren, C.F. and D.R. Huffman, *Absorption and scattering of light by small particles*. 2008: Wiley. com.
66. Avasthi, D., et al., *Ion tracks in silica for engineering the embedded nanoparticles.* Nuclear Instruments and Methods in Physics Research Section B: Beam Interactions with Materials and Atoms, 2010. **268**(19): p. 3027-3034.
67. Zijlstra, P., P.M. Paulo, and M. Orrit, *Optical detection of single non-absorbing molecules using the surface plasmon resonance of a gold nanorod.* Nature Nanotechnology, 2012. **7**(6): p. 379-382.
68. Liu, M. and P. Guyot-Sionnest, *Mechanism of silver (I)-assisted growth of gold nanorods and bipyramids.* The Journal of Physical Chemistry B, 2005. **109**(47): p. 22192-22200.
69. instruments, m. *Dynamic Light Scattering DLS for particle size characterization of proteins, polymers and colloidal dispersions*. Available from: http://www.malvern.com/labeng/technology/dynamic_light_scattering/dynamic_light_scattering.htm.
70. instruments, m., *Characterisation of Colloidal Gold Using Dynamic Light Scattering*. 2007.
71. Link, S., M. Mohamed, and M. El-Sayed, *Simulation of the optical absorption spectra of gold nanorods as a function of their aspect ratio and the effect of the medium dielectric constant.* The Journal of Physical Chemistry B, 1999. **103**(16): p. 3073-3077.
72. Ricci, R.W., M. Ditzler, and L.P. Nestor, *Discovering the Beer-Lambert Law.* Journal of chemical Education, 1994. **71**(11): p. 983.
73. Haiss, W., et al., *Determination of size and concentration of gold nanoparticles from UV-vis spectra.* Analytical Chemistry, 2007. **79**(11): p. 4215-4221.
74. Sharma, V., K. Park, and M. Srinivasarao, *Shape separation of gold nanorods using centrifugation.* Proceedings of the National Academy of Sciences, 2009. **106**(13): p. 4981-4985.
75. Xiong, B., et al., *Separation of nanorods by density gradient centrifugation.* Journal of Chromatography A, 2011. **1218**(25): p. 3823-3829.

76. Niidome, T., et al., *PEG-modified gold nanorods with a stealth character for< i> in vivo</i> applications.* Journal of Controlled Release, 2006. **114**(3): p. 343-347.
77. Huang, X., et al., *Cancer cell imaging and photothermal therapy in the near-infrared region by using gold nanorods.* Journal of the American Chemical Society, 2006. **128**(6): p. 2115-2120.
78. Fu, W., et al. *Biomedical applications of gold nanoparticles functionalized using hetero-bifunctional poly (ethylene glycol) spacer*. in *Materials Research Society Symposium Proceedings*. 2005. Cambridge Univ Press.
79. Wilson, C.G., et al., *Polyelectrolyte-coated gold nanorods and their interactions with type I collagen.* Biomaterials, 2009. **30**(29): p. 5639-5648.
80. Durr, N.J., et al., *Two-photon luminescence imaging of cancer cells using molecularly targeted gold nanorods.* Nano letters, 2007. **7**(4): p. 941-945.
81. Kopwitthaya, A., et al., *Biocompatible PEGylated gold nanorods as colored contrast agents for targeted in vivo cancer applications.* Nanotechnology, 2010. **21**(31): p. 315101.
82. Sennett, P. and J. Olivier, *Colloidal dispersions, electrokinetic effects, and the concept of zeta potential.* Industrial & Engineering Chemistry, 1965. **57**(8): p. 32-50.